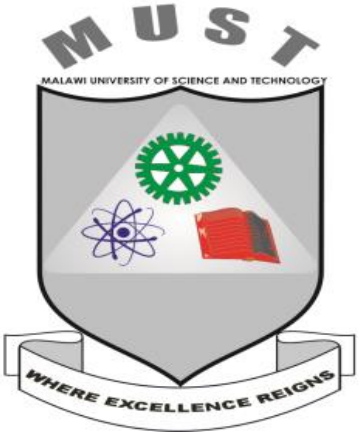


DESIGN OF PARABOLIC SOLAR COOKER

JOSEPH NYIRENDA

(SES-029-17)

Dissertation Submitted to Ndata School of Climate and Earth Sciences of The Malawi University of Science and Technology in Partial Fulfillment of The Requirements for The Award of The Bachelor of Science Degree in Sustainable Energy Systems.

DECLARATION

I Joseph Nyirenda declare that this research project represents my own work and that it has never been submitted to this institution or any other institution for any academic purpose. All sources of information have been appropriately acknowledged.

Date …… Signature……

CANDIDATE

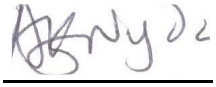
Date…… Name……

Signature……

SUPERVISOR

Date…… Name Mr. Austin K. Nyirenda

……

Signature: 

DEAN OF FACULTY

Date…… Name……

Signature……

DISCLAIMER.

This document describes work undertaken as part of a program of study at Ndata School of Climate and Earth Sciences of the Malawi University of Science and Technology. All views and opinions expressed therein remain the sole responsibility of the author(s), and do not necessarily represent those of the School.

COPYRIGHT STATEMENT:

This copy of the dissertation has been supplied on condition that anyone who consults it is understood to recognize that its copyright rests with its author and that no quotation from the dissertation and no information derived from it may be published without acknowledgement.

ABSTRACT.

Charcoal and firewood are today's most accessible sources of energy for the preparation of daily meals and heating water for bathing. However, due to the increase in population, there is also an increase in the rate of cutting down trees which leads to the problem of deforestation which is also directly proportional to soil erosion. Apart from deforestation, the use of charcoal and firewood also produces greenhouse gases such as carbon dioxide (CO_2) and methane (CH_4) which are major causes of global warming, climate change, and some health problems such as tuberculosis, lung cancer, asthma, and bronchitis in humans. Therefore, the main object of this research project was to design a parabolic solar cooker which will be the alternative to the use of charcoal and firewood, and the designed parabolic solar cooker have new physical features which increase the systems efficiency and good thermal storage. During the process, all factors such as material selection and design were considered accordingly in order to build finest parabolic solar cooker. The dimensions of the designed parabolic solar cooker were also determined according to other high performance parabolic solar cookers and the placement of pot stand was compared to the theoretical focal spot. And also, there was a task of finding relevant materials for heat storage. After investigation latent heat materials shows a better potential for this application, especially for their ability to store a lot of energy at constant temperature. The influence of solar tracking inaccuracy was also investigated as well, and shows that by choosing a large absorber, it was possible to both reduce the influence of these inaccuracies and of the solar angles. The design was then simulated using SOLIDWORKS and MATLAB. And the results produced was then compared with already existing parabolic solar cookers which has high performances, and from that comparison, the results conclude that a new design of parabolic solar cooker has proved its ability in terms of thermal performance and achieving high efficiency of 0.796.

Keywords: Solar cooking, Parabolic solar cooker, Solar cooker design, thermal performance, Energy, Malawi.

ACKNOWLEDGEMENTS

Firstly, I would like to thank the Malawi University of Science and Technology through the Ndata School of Climate and Earth sciences for funding this research study.

I also thank my supervisor Mr. Austin. k. Nyirenda and all supervisory committee for directing me the best approach to do this study.

I also thank all the classmates and other friends for different kinds of support.

Contents

DECLARATION i
DISCLAIMER. ii
COPYRIGHT STATEMENT: iii
ABSTRACT. iv
ACKNOWLEDGEMENTS v
Contents vi
1. INTRODUCTION 1
1.1. BACKGROUND 1
1.2. PROBLEM STATEMENT. 2
1.3. Literature review. 2
1.3.1. Introduction to solar cookers. 2
1.3.2. Solar energy. 2
1.3.3. Earth-sun geometric relationship. 4
1.3.4. Earth-sun angles. 6
1.4. History of solar cookers. 13
1.5. How solar cookers work. 14
1.6. Principle of solar cooking: 15
1.7. Types of solar cookers. 15
1.8. Sunshine in Malawi. 19
1.8.1. Available solar cookers in Malawi 21
1.8.2. Solar cookers are needed due to 23
1.8.3. Advantages of solar cookers. 23
1.8.4. Disadvantages of solar cookers. 23
1.9. Outline of thesis. 24
2. STUDY OBJECTIVES. 25
2.1. specific objectives: 25
3. THE THEORETICAL PART OF SOLAR COOKERS. 26
3.1. Dish theory: parabolic dish Geometry. 26
3.2. Solar Energy collection. 29
3.3. Geometric concentration Ratio (CR_g). 31
4. METHODOLOGY. 32

4.1. Introduction....32
4.2. Setting/study site. 32
4.3. Product specification....33
4.4. Conceptional Evaluation....34
5. EMBORDIMENT AND DETAILED DRAWINGS. 43
5.1. Introduction....43
5.2. Design calculations 43
5.3. Heat transfer in cooking section 47
Material Properties....53
5.4. Detailed Drawings 55
5.4.1. Final design....55
5.4.2. Parabolic dish. 58
5.4.3. Supporting stand. 59
59
5.4.4. Cooking stand. 60
5.4.5. Cooking area with thermal storage part. 61
5.4.6. Cooking plate 62
5.4.7. Dish adjusting support. 63
6. SIMULATION AND RESULTS. 64
6.1. SOLIDWORKS RESULTS. 65
Thermal analysis simulation 65
6.1.1. Model Information....65
Study Properties....66
Units 66
Thermal Loads 67
Mesh information 67
6.2. Mesh information - Details....67
Study Results....69
Conclusion 70
6.2.1. Model Information.... 71
Study Properties....72
Units 72

Material Properties....72
Thermal Loads....73
Mesh information....74
6.3. Mesh information - Details....74
Study Results....75
6.3.1. Cooking holder....76
Model Information....76
Study Properties....77
Units....77
Loads and Fixtures....78
Mesh information....79
6.4. Mesh information - Details....79
Resultant Forces....80
6.5. Reaction forces....80
6.6. Reaction Moments....80
6.7. Free body forces....80
6.8. Free body moments....80
Study Results....81
Conclusion....83
6.8.1. Model Information....84
Study Properties....87
Units....87
Loads and Fixtures....88
Contact Information....89
Mesh information....90
6.9. Mesh information - Details....90
6.10. Mesh Control Information:....91
Resultant Forces....91
6.11. Reaction forces....91
6.12. Reaction Moments....91
6.13. Free body forces....91

6.14. Free body moments 91
Study Results 92
Conclusion 95
6.15. MATLAB RESULTS. 96
7. CONCLUSION AND RECOMMENDATIONS 101
Conclusion. 101
7.1. Recommendations. 102
8. REFERENCE LIST. 103
9. APPENDICES. 104

Table of figures.

Figure 1: shows the main two categories of radiation both Beam and diffuse radiation. 4
Figure 2: shows the motion of earth around the sun. 5
Figure 3: shows the apparent path of the sun throughout the year seen from Northern hemisphere. 6
Figure 4: shows the projection of sun's ray in equatorial plane. 7
Figure 5: shows the variation of B constant throughout the year. 8
Figure 6: shows the latitude angle ($\emptyset$). 9
Figure 7: shows the variation of declination (δ) throughout the year. 10
Figure 8: shows the zenith, solar altitude, and solar azimuth angle. 11
Figure 9: shows the angle of incidence (θ) 12
Figure 10: shows the horizontal East-west tracking system. 13
Figure 11: shows the classification of solar cookers. 15
Figure 12: shows the Components of a box solar cooker. 16
Figure 13: shows the Components of a panel solar cooker. 17
Figure 14: shows an example of Collector solar cooker. 17
Figure 15: shows some of concentrating solar cookers. 18
Figure 16: shows the screenshot of Blantyre-Malawi climatic database on RETScreen. 19
Figure 17: shows the screenshot of graph of Blantyre-Malawi climatic database on RETScreen. 20
Figure 18: shows the distribution of solar cooker. 21
Figure 19: shows the geometry of parabola (Stine & Geyer, 2001). 26
Figure 20: shows the parabolas with the same aperture radius and common focus but varied rim angles. 28
Figure 21: shows the 3D map of Ndata area in Thyolo, source: Google map. 32
Figure 22: shows SK-14 parabolic solar cooker. 34
Figure 23: shows PRINCE-15 solar cooker. 36
Figure 24: shows DIY parabolic solar cooker. 37
Figure 25: shows PRINCE-40 (SK-23) parabolic solar cooker design. 39
Figure 26: shows the JDN parabolic solar cooker design. 40
Figure 27: shows heat transfer in cooking section. 47
Figure 28: shows Analogical relationship between electrical and thermal resistance. 51
Figure 29: shows thermal resistance diagram of the cooking section. 51
Figure 30: shows the final assembled drawing. 55
Figure 31: shows the balloon labeling top view. 56
Figure 32: shows the balloon labeling of side view. 57
Figure 33: shows the parabolic dish. 58
Figure 34:shows the supporting Stand. 59
Figure 35: shows the cooking stand 60
Figure 36: shows the cooking section 61
Figure 37: shows the cooking plate 62
Figure 38: shows the solar angle adjusting support. 63
Figure 39: below illustrates solar radiation variation with time. 98
Figure 40: below illustrates solar radiation variation with efficiency. 99

Figure 41: below illustrates solar radiation variation with output energy. 100

Nomenclature.

A	Cross section-area, m
A_a	Aperture area, m^2
d	Diameter, m
$E_{optical}$	Rate of optical radiation
c	Specific heat capacity
hfg	latent heat ($jkg^{-1}k^{-1}$)
I	incident solar flux on the collector plane (Wm^{-2})
m	mass (kg)
Q	heat power (w)
T	temperature
t	time (s)
g	gravitation force
k	thermal conductivity
Ufd,I	internal energy of the food item to be cooked
hfg	specific enthalpy change of evaporation

Subscripts

a	Air, aperture
amb	Ambient
Cav	cavity
Conv	convection
Corr	correct
eff	Effective
ev	Evaporator
i	initial, internal energy

Inner	Inner wall of the receiver
Ins	insulation
l	liquid
lo	loss
par	parabola
rad	radiation
rec	Receiver

Greek Symbols.

γ	Azimuth, un-shading factor
ρ	Density, kg/m^3; reflectivity
η	Efficiency
α	Absorptance
ε	Emissivity, Effectiveness
Ψ	rim angle
φ	Tilt angle, radian
ω	hour angle
σ	Stefan-Boltzmann constant
Δ	Difference

Abbreviations and Acronyms.

BTC	Be the change
JDN	Joseph Daniel Nyirenda
F`UL	Factor of losses thermal

1. INTRODUCTION

1.1. BACKGROUND

Cooking is considered one of humanity's most integral and common activities. Being a process that usually requires a thermal treatment of food, securing the fuel to heat can be as important as providing for the food itself. Many developing countries like Malawi depend on fossil fuels such as charcoal and firewood as fuel for cooking and heating water (NSO, 2018). However, due to their limited resources and greenhouse gas emission, the use of fossil fuels leads to problems such as deforestation, health problems, global warming, climate change, and soil erosion. Using wood for cooking increases the carbon dioxide in the atmosphere due to CO_2 generated by burning lumber and fewer trees consuming it. To salvage the situation, the use of renewable sources is being reconsidered. One of the most common renewable energy sources that have been studied for years is solar energy. A quite different type of program in Malawi was reported at the Kimberly meetings in South Africa in 2000. The country has excellent solar insolation possibilities and severe deforestation in some areas. The Department of Energy Affairs had established a Renewable Energy Program, which promoted a range of renewable devices, including solar cookers (Kimberly, p. 67). The use of solar energy to cook food presents a viable alternative to the use of fuels such as wood, charcoal, and other traditional fuels. Therefore, the applied solar cooking can be used as an effective mitigation tool with regards to global climate change, deforestation, and even economic debasement of the world's poorest people.

1.2. PROBLEM STATEMENT.

Due to over-reliance on charcoal and firewood for preparation of daily meals and heating water for bathing, there is an increase in the rate of cutting down trees which leads to the problem of deforestation which is also directly proportional to soil erosion. Apart from deforestation, the use of charcoal and firewood also produces greenhouse gases such as Carbon dioxide (CO_2) and Methane (CH_4) which are major causes of global warming, climate change, and some health problems such as tuberculosis, lung cancer, asthma, and bronchitis in humans. So, I suggest that the use of solar cookers which are considered renewable energy systems can solve these problems. And also, solar cookers are environmentally friendly with zero emissions. My design which will be called **JOSEPH DANIEL NYIRENDA (JDN) parabolic solar cooker,** have some new physical features which include; having a solar angle adjuster, which will be used to tilt the solar cooker according to the position of the sun to increase the heat conversion efficiency, and another physical feature is that the area of cooking will be glassed to increase thermal storage efficiency of the solar cooker system.

1.3. Literature review.

1.3.1. Introduction to solar cookers.

Solar cookers have a long history back almost the 18th century when Nicholas-de-Saussure built the first-ever fabricated solar box cooker(Otte 2009). Today there are over 60 major designs and more than 100s variations. However, solar cooking has not caught the imagination of the people, except in places where the shortage of conventional fuel like firewood and the like has become very acute(Schäffler and Schäffler n.d.).

1.3.2. Solar energy.

The sun is a sphere with a radius of 6.95×10^{8}m and a distance of 1.5×10^{11}m from the earth. The temperature of the sun is 5777K, and the estimated temperature at the center of the sun is 8×10^{6}K to 40×10^{6}K. The sun is a continual fusion reactor, the main reaction is a process of forming helium (one helium nucleus) by

combining hydrogen. The sun's energy is emitted constantly in all directions, and it is divided into two forms; extraterrestrial and terrestrial.

Earth obtains solar energy from the sun through electromagnetic waves, also known as electromagnetic radiation. Every hour the sun strikes the planet with more energy (4.3×10^{20}J) than the yearly total energy consumption of 4.1×10^{20}J [foster, Ghassemi & Costa 2010, p.4].

Electromagnetic waves can be represented by photons carrying radiant energy or light energy when photons strike matter, the clash triggers a vibration of molecules and these movements will convert the radiant energy of the photons into heat energy (Reusch 2013).

The total amount of solar radiation on a surface is called radiation and can be divided into two main categories: **Beam radiation** and **diffuse radiation.**

Beam radiation- also called direct solar radiation- entails sunrays that have not been scattered by the atmosphere and are received directly from the sun.

Diffuse radiation- concerns both the radiation that has changed its direction due to clouds and particles in the atmosphere (Duffie & Beckman 1991, p.10) and radiation that has hit the ground can be divided into the two subcategories diffuse sky radiation and ground reflected radiation (Ineichen, Guisan & Perez 1990).

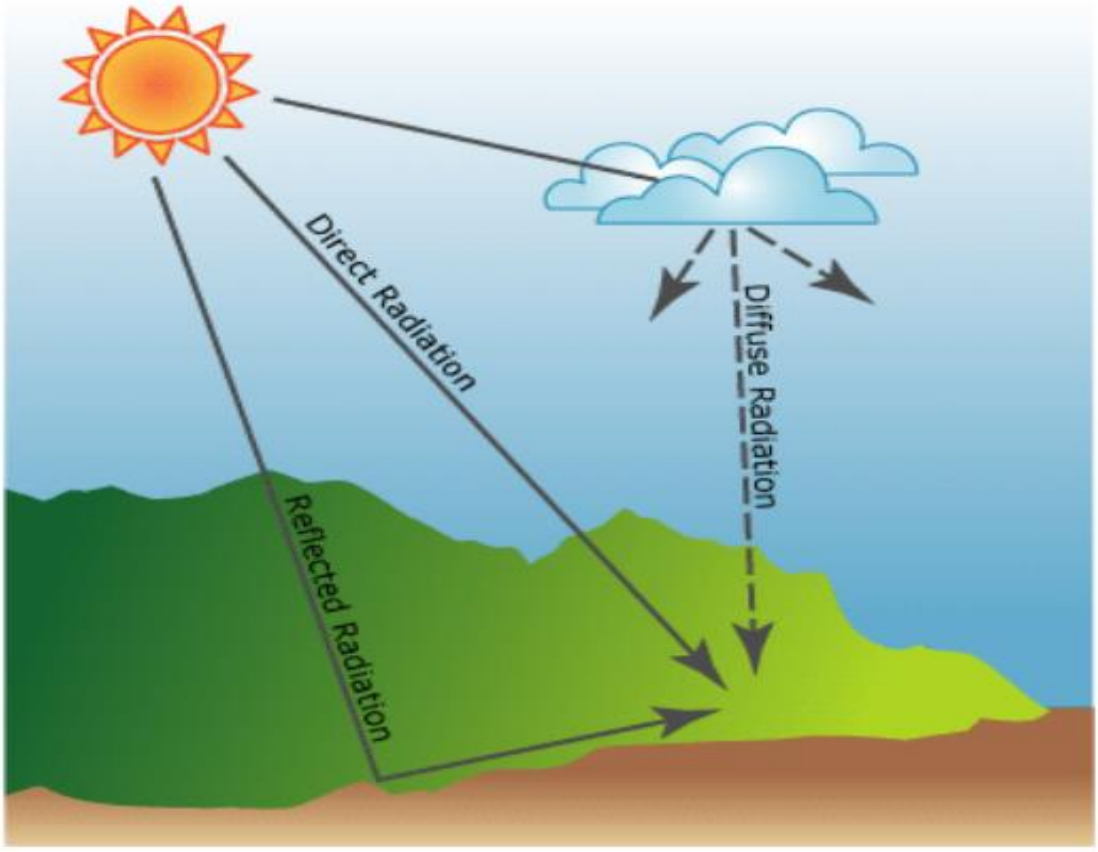


Figure 1: shows the main two categories of radiation both Beam and diffuse radiation.

Irradiance vs. Insolation.

Irradiance is the rate at which radiant energy from the sun strikes a surface, per unit area[w/m^2] while Irradiation is the amount of radiation energy received by a surface, per unit area[j/m^2]. Through integration of the irradiance over a specified time, the Irradiation can be found. It is typical to integrate over an hour and therefore express irradiation in Wh/m^2.

1.3.3. Earth-sun geometric relationship.

The annual amount of solar radiation received by the earth varies due to the changeable distance between the earth and the sun.

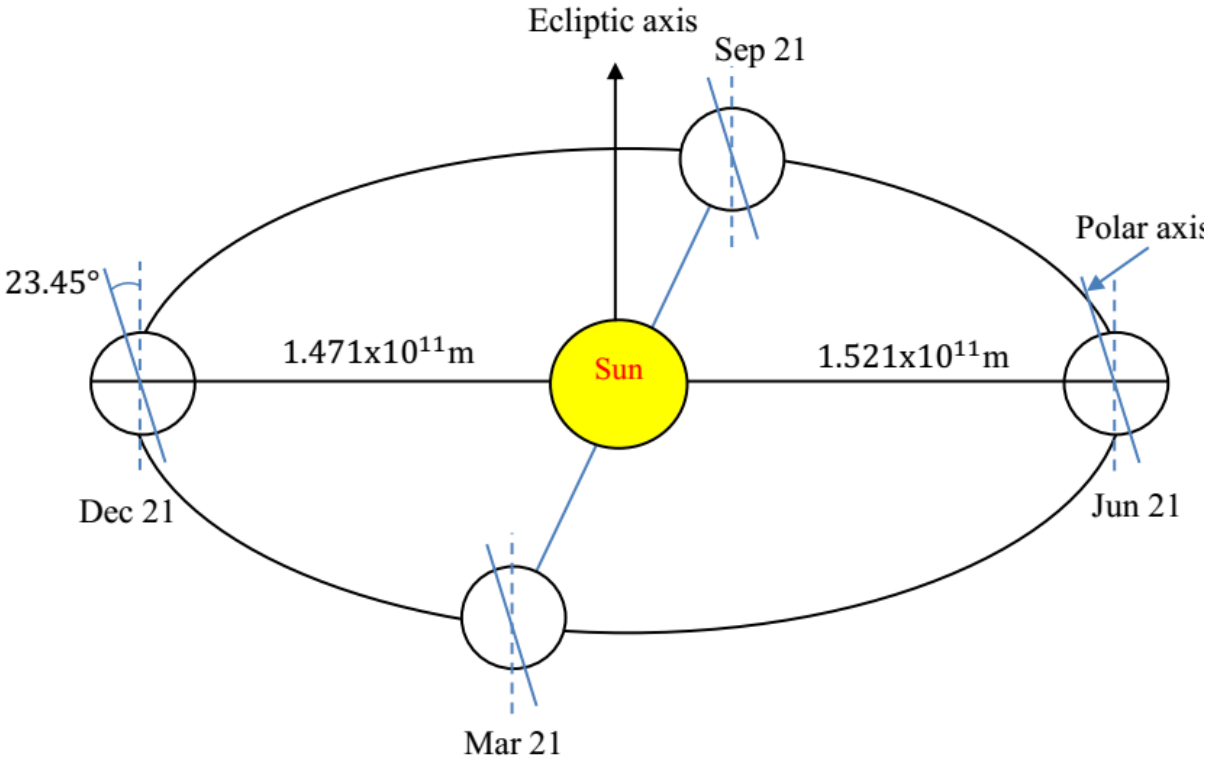


Figure 2: shows the motion of earth around the sun.

The figure 2 shows the motion of earth around the sun.

The Earth-sun distance has a minimum value of 1.47×10^{11}m which is called, perihelion. In the northern hemisphere the shortest day of the year (winter solstice) is on December 21st, which is when the path of the sun in the sky is the lowest. And the maximum value of 1.512×10^{11}m which is called, aphelion, the sun follows a higher and higher path for every day on 21st of March it will reach the **spring equinox,** which is when the sun rises exactly in the east and sets exactly in the west. This day lasts exactly 12 hours and the days will become longer until the summer solstice on 21st of June- the longest day of the year in the Northern hemisphere.

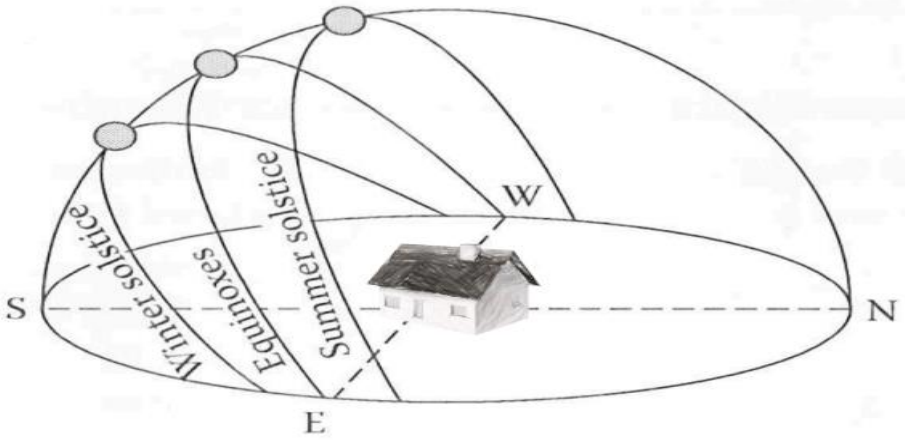


Figure 3: shows the apparent path of the sun throughout the year seen from Northern hemisphere.

From here the sun will start following a lower path again and head towards the same equinox, which (in this direction) is now called the fall equinox. In the southern hemisphere the same cycle follows but in the opposite direction. Therefore, the winter solstice is on 21st of June, fall equinox on, 21st of September and summer solstice on 21st of December (Foster, Ghassemi & Costa 2010, pp.9-10).

Due to the apparent path of the sun permanent solar energy collectors in the Northern hemisphere are recommended to face south while in the southern hemisphere they should face north to receive as much sunshine as possible.

1.3.4. Earth-sun angles.

There are numerous Earth-sun angles need to be explained. They are presented in the following text.

Hour angle (ω): the hour angle can be known as the angle through the earth has to revolve to get the meridian of any point straight under the sun. Hour angle varies throughout the day as seen in the figure below. For any place, at sunrise, the hour angle has maximum negative value of -180^0, then, it slowly increases, 15^0 per hour, while the sun is rising Until it reaches zero at noon. For the period from

afternoon to sunset, hour angle increases from zero to the maximum positive value which is $+180^0$.

The hour angle ω (in degrees) can be calculated from the following equation.

$$\omega = 15(ST - 12)$$

Where ST is the solar local time.

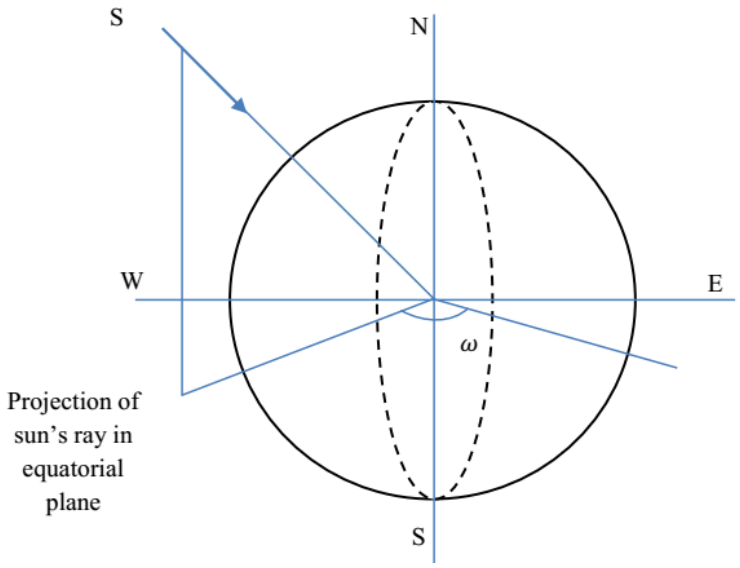


Figure 4: shows the projection of sun's ray in equatorial plane.

Solar local time ST is not same as standard time. Therefore, it is important to convert the local clock time to solar time. The conversion depends on longitude, local standard meridian, and day of the year. It given by the following expression

$$\text{Solar time} = \text{Standard time} + 4(L_{st} - L_{loc}) + E$$

Where L_{st} stands for the standard meridian of local zone time, L_{loc} represent longitude of the location. The term E called the equation of the time (in minutes), and it can be determined applying the following equation

$$E=229.2(0.000075+0.001868CosB-0.032077SinB-0.014615Cos2B-0.04089Sin2B)$$

Where B measured in degrees can be calculated using the next equation

$$B=(n-1)\frac{360}{365}$$

Where n represent the day of the year ($1 \leq n \leq 365$). The equation time is plotted and shown in figure below.

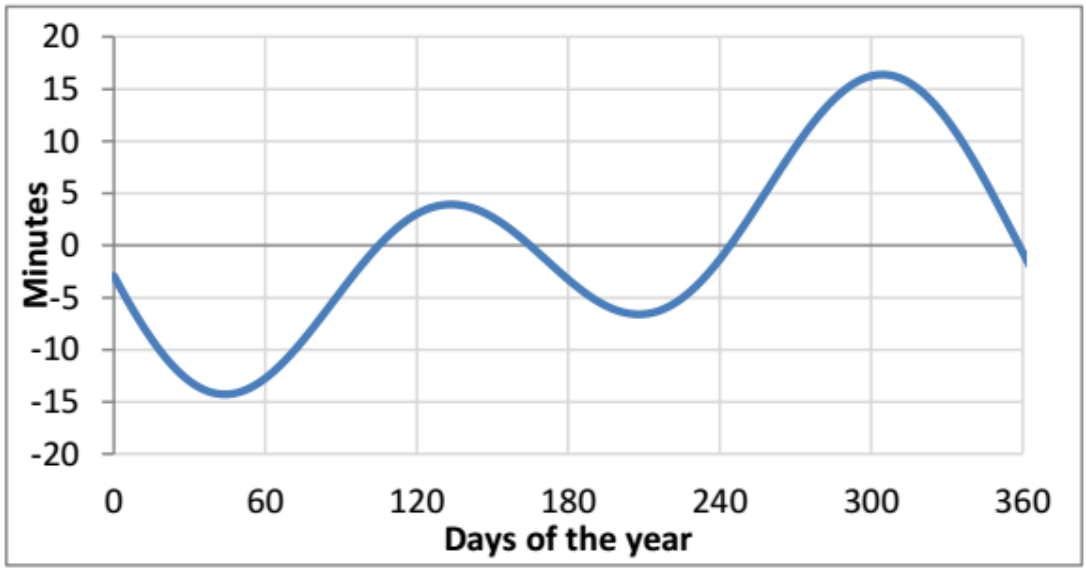


Figure 5: shows the variation of B constant throughout the year.

Latitude angle (Ø) : assume that there is a point P at a location on the earth. By drawing a radical line connecting the earth center with the projection of this radical line on the equatorial plane, an angle is derived and it is known as the latitude angle (Ø) as show in figure below. it varies between +90 and -90 (35.7^0 of thyolo).

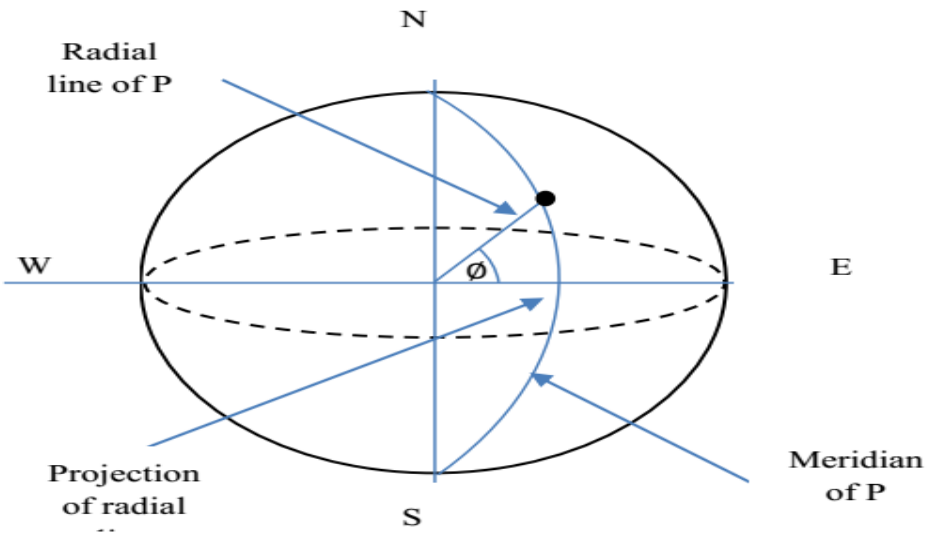


Figure 6: shows the latitude angle ($\emptyset$).

Solar declination (δ) : Solar declination is an angle between a line connecting the earth's and the sun's centers and the projection of the line upon equatorial plane of the earth. The Solar declination varies throughout the year because of the earth's revolving around its axis. It varies between a value of +23.45^0 on June 21 and a value of -23.45^0 on December 21. Solar declination angle can be determined using cooper's equation

$$\delta \text{ (in degrees)} = 23.45 \sin\left[\frac{360}{365}(284+n)\right]$$

Where n represents the day of the year ($1 \leq n \leq 365$). The plotting of the equation is shown in figure below.

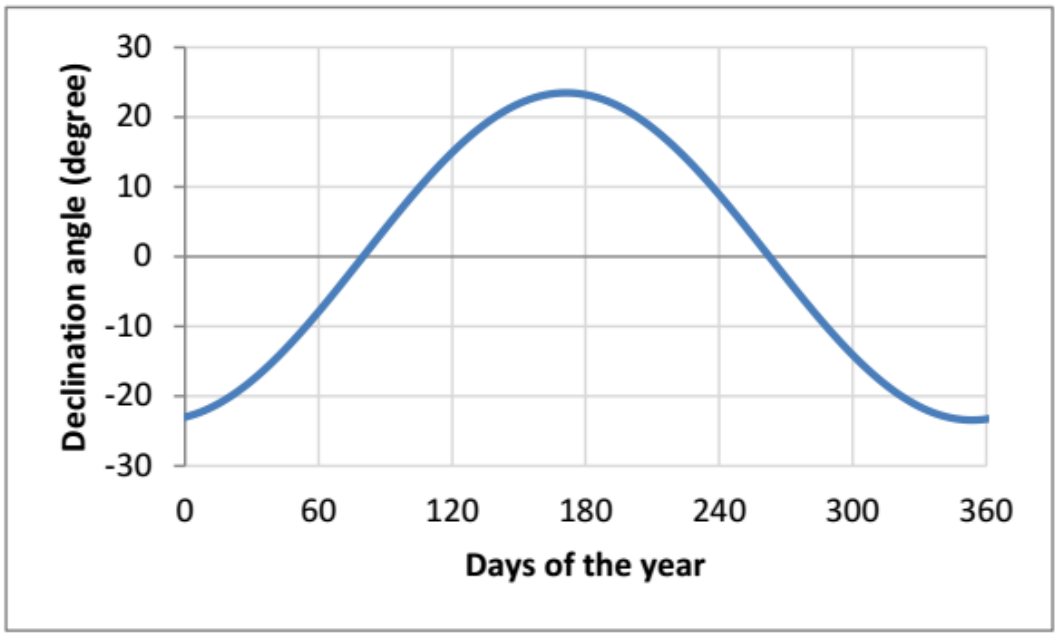


Figure 7: shows the variation of declination (δ) throughout the year.

Zenith angle (θ_z) : Consider a point P on a surface of the earth, the direction PN is called, zenith direction, and the direction SP known as Sun's beam direction. The angle between the zenith angle (θ_z), shown in figure below. At Sunrise or sunset, the zenith angle(θ_z) is about 90^0. However, at noon, the zenith angle become very close to 0^0.

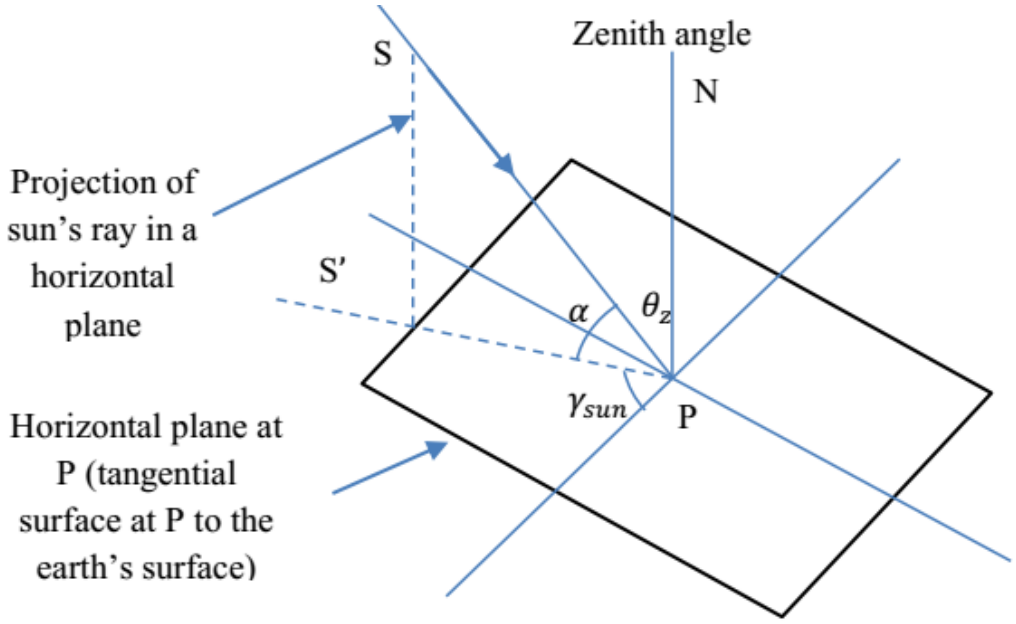


Figure 8: shows the zenith, solar altitude, and solar azimuth angle.

Solar azimuth angle (γsun): The solar azimuth angle is the angle measured between the south direction and the sun's ray as shown in figure above. The expression used to estimate the solar azimuth angle is given by

$$\text{Sin}\ (\gamma sun) = \frac{Cos(\delta)Sin(\omega)}{\cos(\alpha)}$$

Solar altitude (α): the solar altitude angle is the angle between the horizontal direction (S'P) and the sun's beam direction (SP), S'PS is the solar altitude. The summation of zenith angle and solar altitude is equal to 90^0.

$$\theta_z + \alpha = 90$$

The solar altitude angle changes with the sun movement. At sunrise or sunset, the solar altitude angle is near zero while at noon, it becomes near to 90^0. Solar altitude angle can be determined using the following expression

$$\text{Sin}\ (\alpha) = \text{Sin}\ (\emptyset).\text{Sin}\ (\delta) + \text{Cos}\ (\emptyset).\text{Cos}\ (\delta).\text{Cos}\ (\omega)$$

Angle of incidence (θ): According to Duffie, the angle of incidence is defined as the angle between the sun rays hitting a surface and the normal to that surface. The angle of incident varies throughout the day and the year, and it greatly affects the solar energy gained by the receiver. In other words, the radiation is reduced by increase the cosine of this angle. For a plane tilted with an angle of β as shown in the figure below, the angle of incidence correlation is given by

$$\text{Cos}(\theta) = \text{Sin}\delta\text{Sin}\emptyset\text{Cos}\beta - \text{Sin}\delta\text{Cos}\emptyset\text{Sin}\beta\text{Cos}\gamma + \text{Cos}\delta\text{Cos}\emptyset\text{Cos}\beta\text{Cos}\omega + \text{Cos}\delta\text{Sin}\emptyset\text{Sin}\beta\text{Cos}\gamma\text{Cos}\omega + \text{Cos}\delta\text{Sin}\beta\text{Sin}\gamma\text{Sin}\omega$$

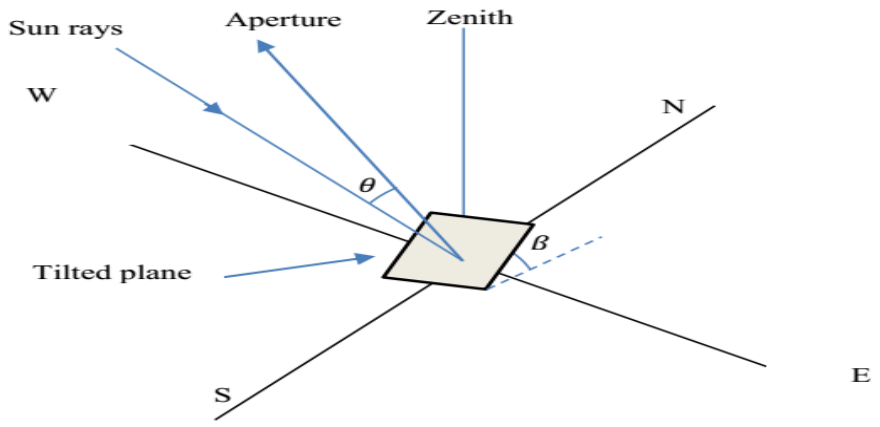


Figure 9: shows the angle of incidence (θ)

In order to maximize the angle of incidence and then maximize the solar radiation, the solar collectors must move in prescribed ways to track the sun. there are two tracking systems of the collectors rotate about two axes which is considered the best way. The second system is that the collectors rotate about axis; horizontal north-south, horizontal east-west, vertical, or parallel to the earth's axis. For the prototype used in this study, the parabolic dish collector rotates about a single axis which is horizontal east-west as seen in the figure below. Thus, the angle of incidence in this case is equal to the zenith angle because the tilting angle β is zero.

$$\text{Cos}\theta = \text{Cos}\,\theta_z$$

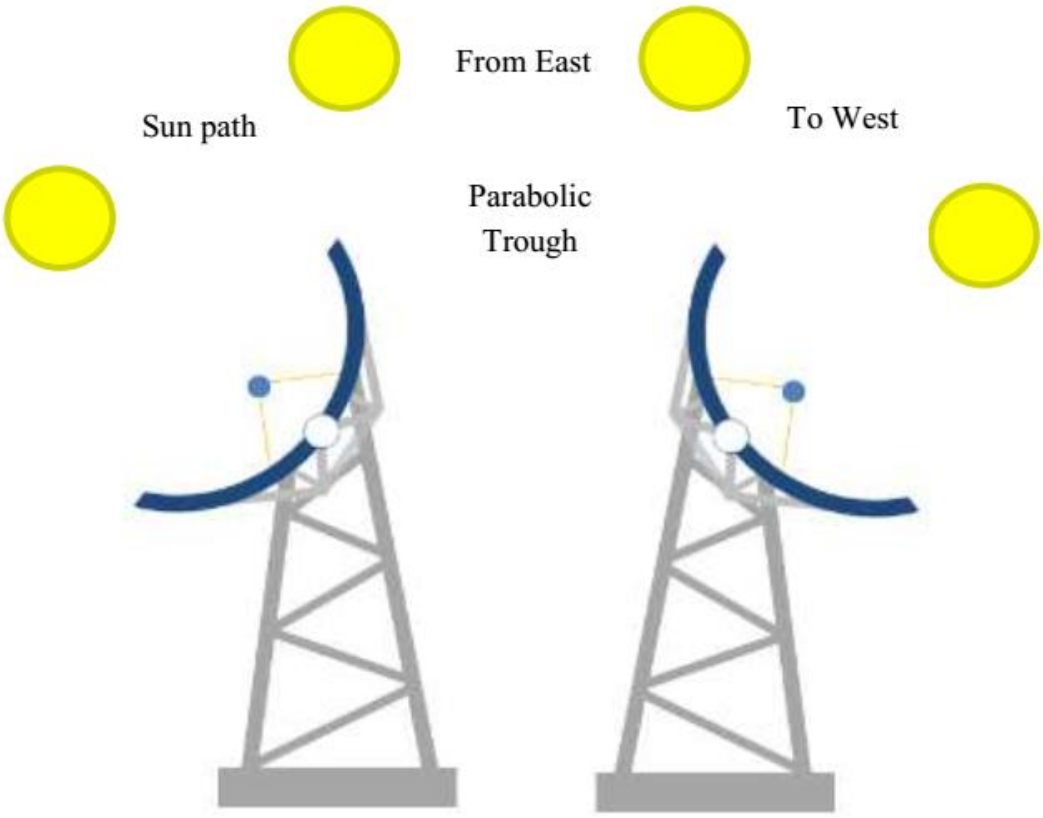


Figure 10: shows the horizontal East-west tracking system.

1.4. History of solar cookers.

Cooking with the energy of the sun is not a new or novel idea. According to Haley and Halacy, his experiment was published in 1767 by a Swiss scientist **Herace-de-Saussure** who also discovered that wooden "hotboxes", produced enough heat to cook the fruit. French scientist Dacurla improved on the hot box design by adding mirrors to reflect more sunlight and insulating the box(Murray et al. 2014).

At the beginning of the years 1900, many Buildings designed to take advantage of solar energy were built using principles of the thermal trap, but they were quickly forgotten and then resumed in the 1930s when several office buildings the double-glazed glass helps with heat retention(Bigalow, Port, and Gasser n.d.). The Second World War took place, but after the war, the need for housing exploded, resulting in new attempts, including solar collectors on the rooftops. The solar cooking

movement began seriously in the middle of the century, with some isolated attempts to arouse an interest in technology. At the end of year 50, Maria Telkes, an MIT scientist who worked on solar cooking her interest led her to build a classic built-in oven, an insulated plywood case with an inclined top of two layers of glass and four large flared reflectors. The design is used, in infinite variation, until today. George Praise former director of the institute of industrial research at the University of Denver, Colorado was also a pioneer of solar technology, including solar cooking(Bigalow et al. n.d.). In the year 1950, he experimented with a model of parabolic solar cooker the name "Umbroiler" because of its structure in the form of an Umbrella. He marketed the design, but it was a commercial failure for the time. After this period, the years of the second half of the 20th century show several individuals and groups experimenting, demonstrating the potential of realizing small and large projects using solar cooking appliances(Anon n.d.). From 1955, a group of individuals in phoenix organized in association for applied solar energy and held its first conference: the America Solar Energy Society and its international counterpart, the international solar energy society. The first seminar on solar cooking was organized in 1981(Murray et al. 2014). The oil shortage of that time was the source of study of the potential of solar energy, with considerable experience in Europe and the United States, as well as in Asia.

1.5. How solar cookers work.

According to the place where you live and how you cook, solar cooking can save you time, effort, and fuel. It is also a fun way to prepare your meals. All foods can be cooked in a type of solar cooker.

Solar cooker: is a device that cooks food using only solar energy in the form of solar radiation. All solar cookers use solar collectors (mostly Aluminum) to trap solar radiation in the form of heat which is concentrated in one place where we can put our pot and start cooking.

1.6. Principle of solar cooking:

Most solar cookers convert sunlight to heat energy that is utilized for cooking. The ability of the solar cooker to collect sunlight is directly related to the projected area of the collector perpendicular to the incident solar beam radiation. The geometric concentration ratio is defined as

$$CR = \frac{A_t}{A_{rc}} \quad (1)$$

Where A_t is the total collector area and A_{rc} is the area of the receiver/absorber surface.

1.7. Types of solar cookers.

A survey of solar cookers worldwide shows that a wide variety of cookers have been designed. However, the available designs of solar cookers fall into four main categories namely, solar box cookers or popularly known as solar ovens, panel cookers, collector cookers, and concentrating or reflector cookers(Patil 2018). The feature common to each design is the sun's rays onto the cooking area and dark inner walls of the cooking area and cooking vessel.

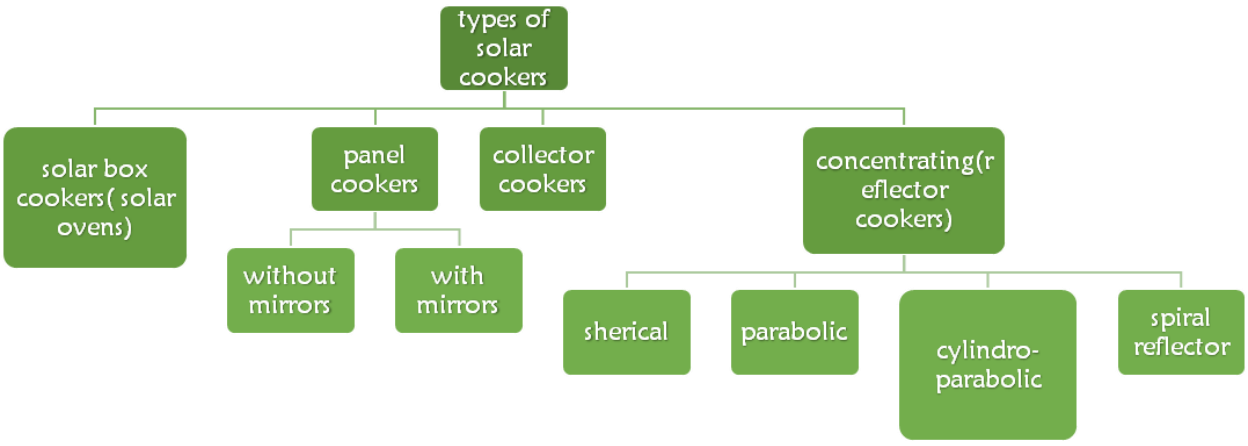


Figure 11: shows the classification of solar cookers.

1. Solar box cooker or solar oven.

It is the most common type of solar cooker made for personal use. It is very simple in construction, consists of a box (square, rectangular, cylindrical) painted black from inside and insulated from all sides except the double-glazed window side is used. Up to four black painted vessels are placed inside the box with the food to be cooked. The cooker takes 1 ½ to 2 hours to cook items such as rice, vegetables.

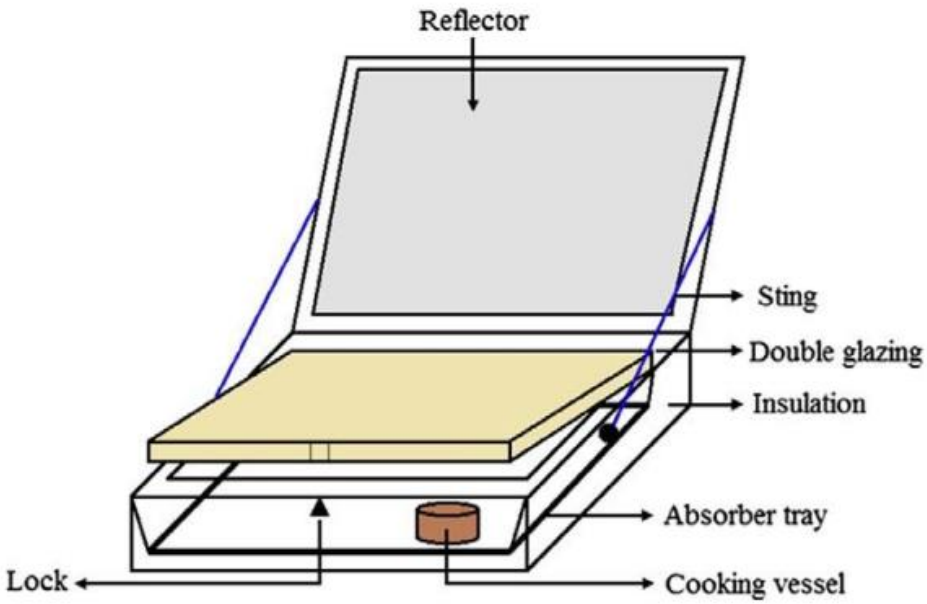


Figure 12: shows the Components of a box solar cooker.

2. Panel Solar Cooker

The panel cooker is quite similar in operation to the solar box cooker. The same principles are employed but instead of an insulated box only, the panel cooker typically relies on large (often multifaceted) reflective panels, which focus the sunlight on a cooking vessel. Panel cookers are the easiest and least costly to make, requiring just four reflective panels and a cooking vessel, but they are unstable in high winds and do not retain as much heat when the sun is hidden behind clouds.

The figure 13

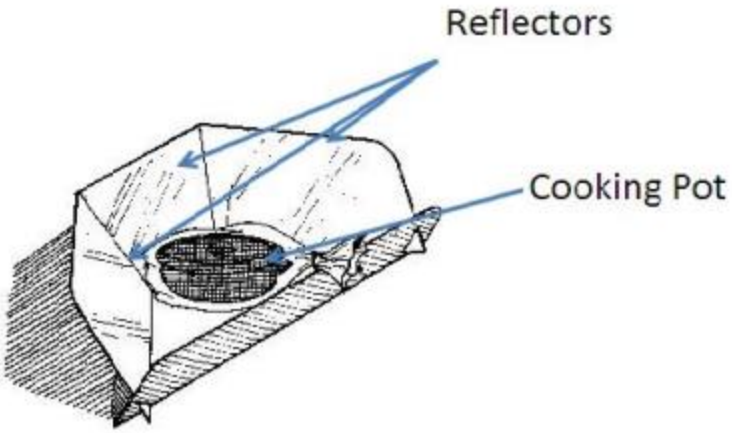


Figure 13: shows the Components of a panel solar cooker.

3. Collector cooker

The collector cooker is made up of two parts that often share a single casing: a collector for the collection of heat and a cooking part for exploiting the yield. A typical collector cooker would consist of a flat plate solar collector, side and head mirrors, and the cooker part. The user is not affected by radiation and heat as the cooking part is separate and protected from radiation. Oil is used as the heat transfer medium to allow higher temperatures to be reached.



Figure 14: shows an example of Collector solar cooker.

4. Concentrating type of solar cooker

It uses the principles of concentrating optics. The concentrating solar cookers primarily consist of a reflector to focus the incident solar radiation on the cooking pot, support with a turning mechanism to keep the reflector facing the sun, and a cooking pot. Hence the cost and size of the reflector are determined by the heating capacity desired. Following are the important types of concentrator type solar cookers (A) Wisconsin solar cooker (Spherical parabolic type, b) Folding Umbrella type solar cooker, c) Paraboloid type solar cooker, d) Lightweight molded aggregate reflector type solar cooker, e) Cylindroid-parabolic solar cooker, f) Multi- mirror or Multi-facet type solar cooker, g) Spiral reflector type solar cooker. Out of these cookers only, the Paraboloid type solar cooker has received commercial attention.

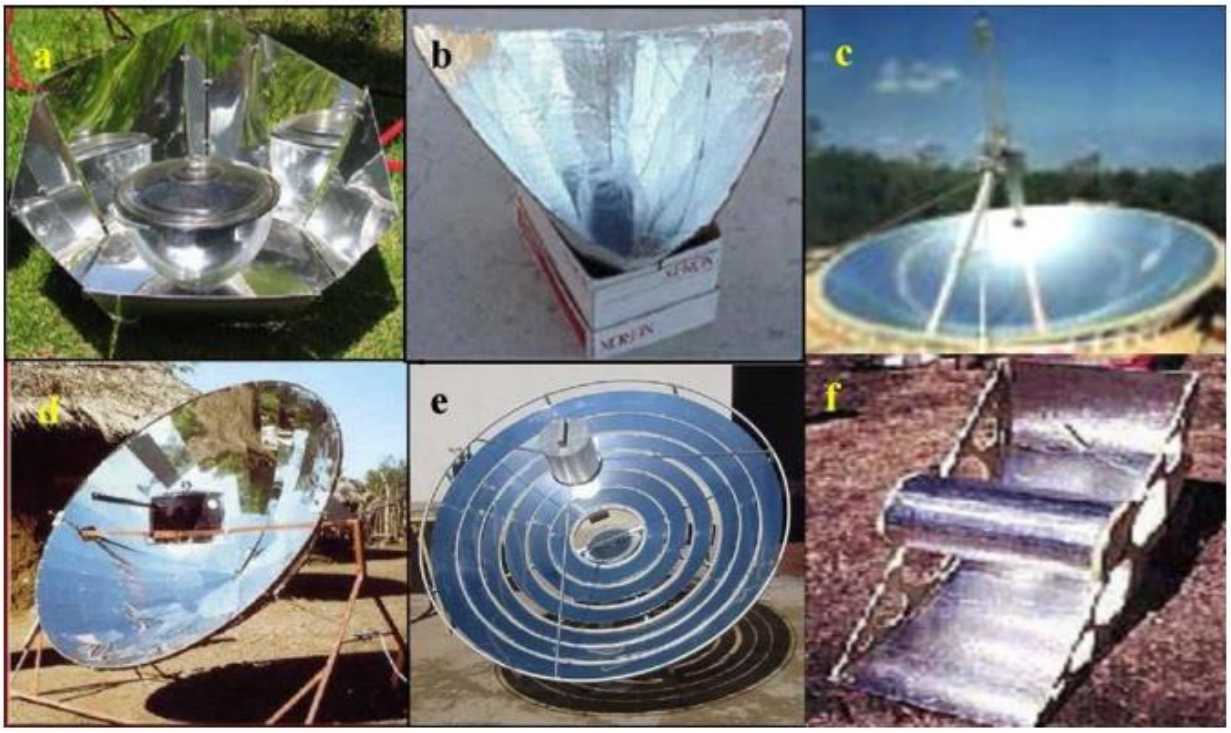


Figure 15: shows some of concentrating solar cookers.

1.8. Sunshine in Malawi.

According to NASA climate database, Malawi has excellent solar radiation with annual avarega of 5.34kWh/m²/day which is possible to be used for cooking directly by using solar cookers. The two figures below shows the annual climatic datebase of Malawi Blantyre produced by NASA using RETScreen software.

RETScreen - Climate database

Map | Search | Data

Country			Malawi	
Province/State				
Climate data location	See map		Blantyre	
Latitude		°N	-15.8	
Longitude		°E	35.0	Source
Climate zone		2A	Hot - Humid	NASA
Elevation		m	611	NASA
Heating design temperature		°C	14.6	NASA
Cooling design temperature		°C	31.9	NASA
Earth temperature amplitude		°C	15.1	NASA

Month	Air temperature	Relative humidity	Precipitation	Daily solar radiation - horizontal	Atmospheric pressure	Wind speed	Earth temperature	Heating degree-days 18 °C	Cooling degree-days 10 °C
	°C	%	mm	kWh/m²/d	kPa	m/s	°C	°C-d	°C-d
January	24.5	78.9%	281.79	5.23	94.1	2.6	25.0	0	450
February	23.9	81.3%	188.44	5.40	94.2	2.7	24.3	0	389
March	23.6	80.2%	149.11	5.41	94.3	2.8	24.0	0	422
April	22.4	74.4%	48.90	5.18	94.6	3.1	22.9	0	372
May	20.7	66.4%	19.53	4.84	94.8	2.9	21.1	0	332
June	18.9	63.5%	15.60	4.38	95.0	3.0	19.3	0	267
July	18.7	59.7%	16.12	4.47	95.1	3.2	19.3	0	270
August	20.9	51.6%	8.37	5.26	95.0	3.6	22.1	0	338
September	24.6	42.5%	9.60	6.11	94.7	4.2	26.5	0	438
October	27.0	43.2%	25.73	6.42	94.5	4.5	29.2	0	527
November	27.4	51.5%	93.00	6.05	94.3	4.0	29.2	0	522
December	25.7	69.0%	199.33	5.31	94.2	3.0	26.6	0	487
Annual	**23.2**	**63.4%**	**1,055.52**	**5.34**	**94.6**	**3.3**	**24.1**	**0**	**4,812**
Source	NASA	NASA	NASA	NASA	NASA	NASA	NASA	NASA	NASA
Measured at					m	10	0		

Figure 16: shows the screenshot of Blantyre-Malawi climatic database on RETScreen.

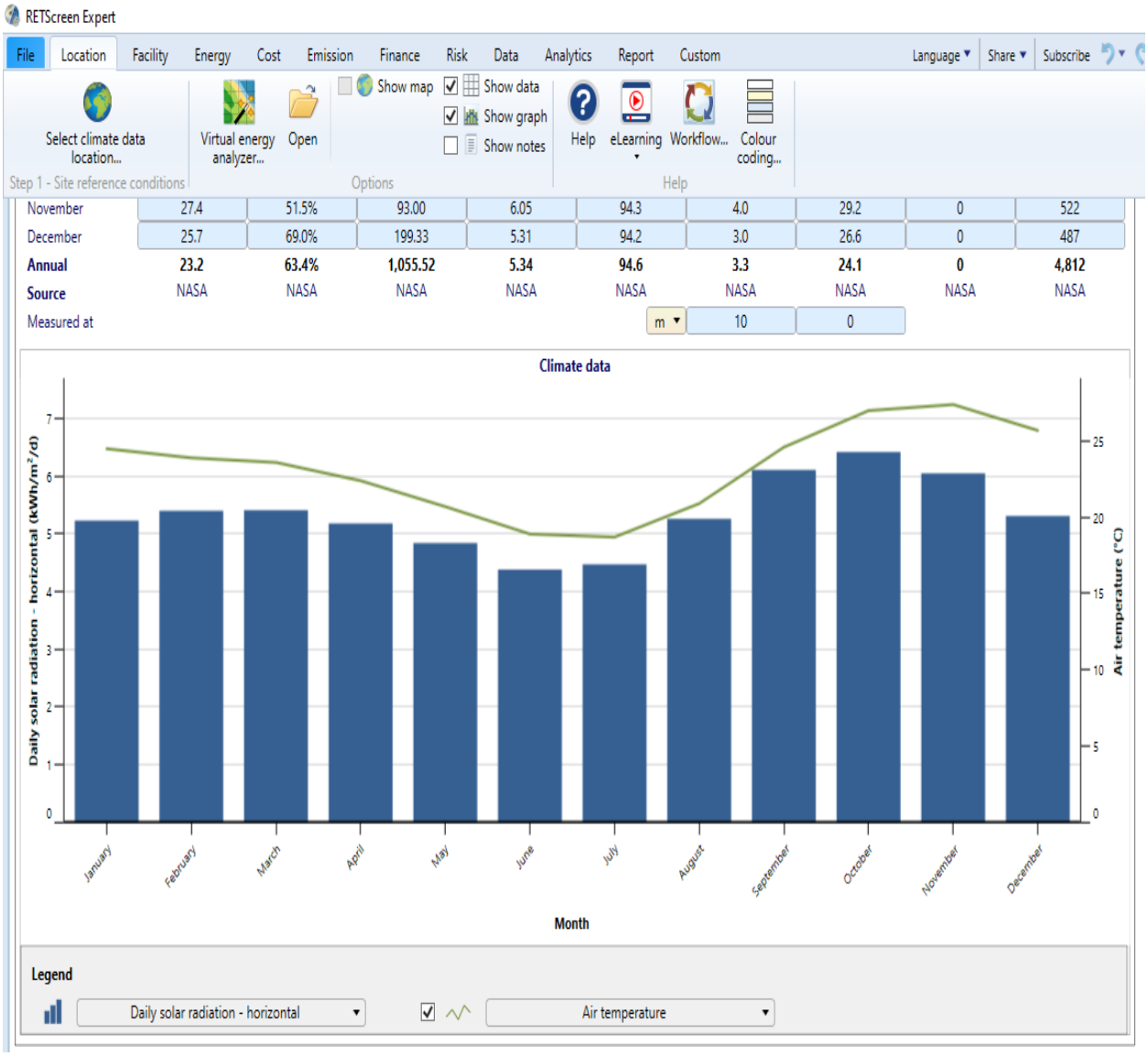


Figure 17: shows the screenshot of graph of Blantyre-Malawi climatic database on RETScreen.

As we can see from the figure (16) on the column of Daily solar radiation horizontal we can observe that Malawi reach the maximum of solar radiation up to 6.42kWh/m²/d during October and only reaches the minimum of 4.38kWh/m²/d in June which is steal enough solar radiation to cook food of more than 10 people.

1.8.1. Available solar cookers in Malawi

Department of Energy Affairs a quite different type program in Malawi was reported on that the [Kimberly meetings] in South Africa in 2000. The country has excellent solar insolation possibilities, and severe deforestation in some areas. The department of Energy Affairs has established a renewable energy program, which promoted a range of renewable devices, including solar cookers. Using box cookers sold through a micro-financing scheme, the project intended to establish distribution centers across the country



Figure 18: shows the distribution of solar cooker.

A private business, the Zako solar cookers industry was the principal manufacturer of ovens, and nongovernmental organizations were assisting in the distribution.

As unusual sponsor of solar cooking in Malawi has been then non-profit organization, peace child international. One of its programs called **Be the change (BTC)** challenged young people to make a difference in their communities. In Malawi a portion of youth action work focused on solar cooking. One young man proposed to his colleagues that they make and sell solar cookers as a BTC project. By 2001, the group had been able to

provide 50 village families with solar cookers in 9 different villages. The group reached out for support from organization in Germany and Austria, and was also aided in locating reflective materials by a Malawi business, universal industries. (Source: solar cooker review, November 2001).

The table below shows the types of available solar cookers in Malawi.

Types of cooker	Advantages	Disadvantages
Solar box cooker T= 150^{0}C	• Uses both direct and diffuse radiation • Requires little intervention by the user • Very easy and safe to use • High acceptance angle • High tolerance for tracking error	• Slow even cooking i.e. 1.5 – 2 hours • Not use for frying/chapatti making
Panel cooker T=200-250^{0}C	• Better performance than box cooker	• Poor performance on cloudy conditions • Relies more on reflected radiation
Collector cooker	• Use both direct and diffuse radiation • Simple, safe and convenient to use	• Complicated to build. • Expensive

Concentrating (reflector) cooker $\eta = 50\%$	• Quite efficient • Can achieve extremely high temperatures 300 – 350^{0}C • Cooking is quicker (1/2 to 1 hour)	• Difficult to make and use (complex design) • Requires the user's attention.

1.8.2. Solar cookers are needed due to

1. High cost or Unavailability of commercial fuels – Kerosene, Coal, cooking gas, and Electricity.
2. *Deforestation is* caused by increasing firewood consumption.
3. Use of dung and agricultural waste as fuels instead of for *soil enrichment*.
4. Diversion of human resources for fuel collection.

1.8.3. Advantages of solar cookers.

1. No attention is needed during cooking as in other devices.
2. No smoke evolution, thus clean.
3. No pollution, thus environment friendly.
4. Vitamins of food are not destroyed; therefore, solar-cooked food is with natural taste, aroma, and healthier.
5. Available every day, thus *renewable*.
6. Solar Energy does not contribute to global warming, acid rain, or smog.
7. Solar Energy systems are maintenance-free and long-lasting.

1.8.4. Disadvantages of solar cookers.

1. Many solar-powered cookers are large and bulky to carry.
2. More time is required for the cooking process.
3. The initial cost of an efficient solar cooking system is high.
4. Solar energy concentration is influenced by the presence of clouds or pollution in the air.
5. Food cannot be cooked at night.

1.9. Outline of thesis.

The thesis is divided into nine chapters. This chapter is the introduction, which gives a general highlight of the existing problem of using fossil fuels such as charcoal and firewood as fuel for cooking and heating water for different purposes. The same chapter also include a review of existing literature on research that has been conducted on solar cookers here in Malawi. Chapter 2, shows the main objective and specific objectives. Chapter 3, shows the theoretical part of parabolic solar cookers. Chapter 4, shows the methodology, which includes design specification and concept evaluation using Pugn matrix. Chapter 5 shows the design calculation, detailed drawing of the solar cooker and material selection. Chapter 6, shows the simulation and results of the designed solar cooker. Chapter 7, explains the conclusions and the recommendations of the study. Chapter 8, shows the reference list. Chapter 9, which is appendix shows the mathematical code for my design which helps to find efficiency, power output, power losses, and concentration ration of the design.

2. STUDY OBJECTIVES.

The main objective is to design a parabolic solar cooker.

2.1. specific objectives:

- To identify available solar cookers in Malawi
- To identify a suitable model of the solar cooker in Malawi.
- To integrate thermal energy storage into the design to store energy and for longer and better heat distribution in the solar cooker.
- To develop a high-performance but low-cost domestic solar cooker.

3. THE THEORETICAL PART OF SOLAR COOKERS.

3.1. Dish theory: parabolic dish Geometry.

The parabolic dish was selected as a concentrator in this study because it has the potential to meet both the medium and high temperature needs of human and has been identified to be most efficient in terms of heat generation. A parabolic dish concentrates the incoming solar radiation to a point. When the sun shines on this concentrator, it reflects the rays of the sun to a receiver that is placed at its focus point. The parabola occurs when the locus of a point has the ability to realign itself such that its distance from a stationary point and a fixed line is always the same. As shown if the figure below

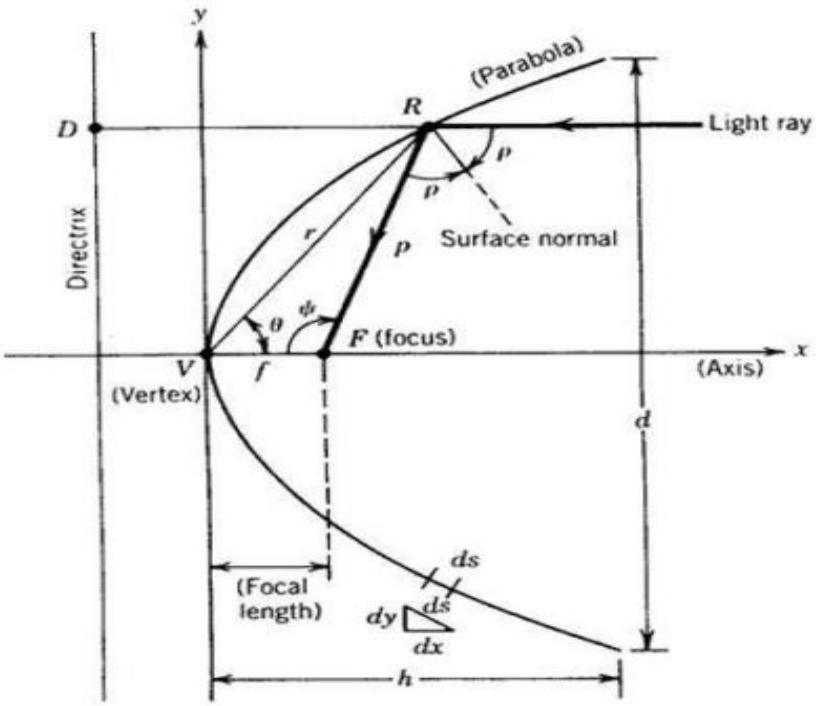


Figure 19: shows the geometry of parabola (Stine & Geyer, 2001).

This is shown explicitly in figure, where the Directix represent the fixed line, the stationary point is the focus represented by F, and the axis of parabola is the imaginary line drawn passing the point F and at a right angle to the Directix. The

vertex (V) of the parabola is the point at which the axis of the parabola, and it is also a point that is located at the midpoint between the focus (F) and Directix of a parabola.

Taking the origin as vertex V in figure above, and the x-axis along the parabola, the equation of parabola can be expressed as

$$Y^2 = 4fx \tag{2}$$

Where f is the focal length (distance VF, which is form the vertex to the focus). When the point of origin is shifted to the focal left-hand side of the origin the equation would become

$$Y^2 = 4f(f + x) \tag{3}$$

The parabolic radius(P) is the distance from the focus to the curve, and Ψ is the angle measured from line VF. With the origin still at F, these parameters can be related by an equation.

$$P = \frac{2f}{1 + cos\Psi} \tag{4}$$

All the ray from the sun reach the earth in parallel form; therefore, all incident rays on the parabolic dish axis are reflected back to the focal point **f** as shown in the figure below by the thick line in the figure; the reflected angle is same as the incident angle in accordance with Snell's law, which states that the angle of incidence and reflected angle are equal. From figure(n) above, it can be observed that an expression can be developed as

$$\Psi = 2P \tag{5}$$

All parabolic equations derived thus far are imaginary, as they work for parabolas with infinitely continuous curve length, but they are useful because they form the basis on which the size of different parabola can be determined, depending on where the curve is truncated, as shown in the figure (n), where all parabolas in it have the same point focus and aperture diameter, but different rim angles (Ψ). The point or extent of truncation of parabola is often defined in terms of rim angle Ψ, or of the ratio to aperture diameter (f/d)

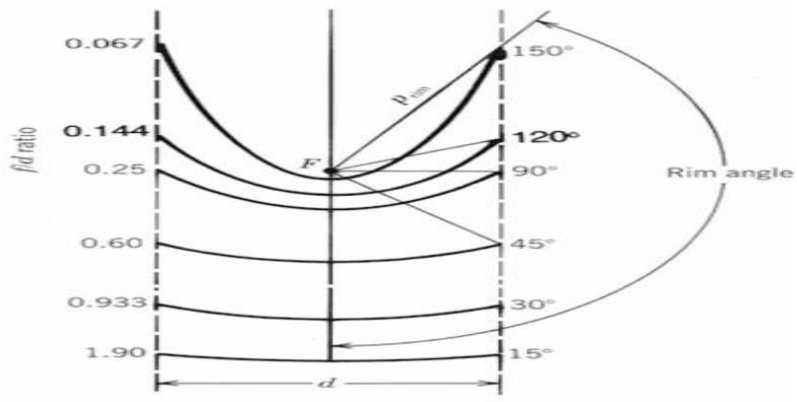


Figure 20: shows the parabolas with the same aperture radius and common focus but varied rim angles.

From the figure it can be seen that the smaller the rim angle, the further the focal point moves away from the parabolic curves. Also, the parabolas with the higher rim angles are less flat, deeper and their focal point closer to their parabolic curves. From the two figures above, another; parameter, h_{par} (which is the height of the curve), can be defined as the maximum or farthest distance from (V) that the vertex is to a straight line drawn across the circular aperture part of a parabola, as shown explicitly in figure (n). The relationship between the height of the curve, h_{par}, and the diameter of the aperture (d) and the focal length (f) can be then stated as

$$F = \frac{d^2}{16h} \tag{6}$$

In a like manner, the rim angle may be found in terms of the parabola dimensions

$$\tan\Psi = \frac{1}{\frac{d}{8h} + \frac{2h}{d}} \tag{7}$$

Where f is the focal length, d is the distance across the aperture (or opening) of the parabola and h is the distance from the vertex to the aperture. The cross-sectional area of the space enclosed between a parabola and normal to the axis is given by this area should not be confused with the reflecting surface area of a parabolic dish or their aperture areas.

$$\tan\Psi = \frac{{}^{f}/_{d}}{2(\frac{f}{d})^2 + \frac{1}{8}} \tag{8}$$

$$\frac{f}{d} = \frac{1}{4\tan({}^{\Psi}/_{2})} \tag{9}$$

The focal point of the dish is of the inmost importance, as it is the place through which all the reflected rays pass and it is also the point where the most thermally effective reflected shape of the sun is formed.

3.2. Solar Energy collection.

Harnessing enough solar energy for a desired system and reducing the likely losses in the

selected system are the two major issues that drive the modelling of any solar heat

process and application (Duffie & Beckman, 2013). In order to address these issues, this subsection discusses the type of solar collector used, how the collector reflects the rays of the sun, the type of receiver adopted, how the reflected energy will be collected in terms of heat energy in the receiver, as well as the heat transfer analysis involved. First was necessary to understand how solar energy collection is achieved and what type of collector must be used to achieve the aim of having a heat output of around 200 to 220 °C in the cooking section.

According to Al-Soud et al. (2010), a solar collector is a device that is used to convert direct radiation from the sun to electricity and/or heat. CSP has been identified as the best way to generate heat energy from the sun (Kalogirou, 2009). The parabolic dish type was selected for this study. The principle of operation of this type of system is that the parabolic dish faces the sun and then reflects the rays of the sun to a solar receiver.

Before discussing the details of the parts responsible for solar energy collection, the background overall equations are presented for guidance in the energy balance. In a separate heat transfer analysis for concentrating systems, Shuai et al. (2008) and Reddy and Sendhil Kumar (2009) showed that, in order to carry out a credible energy balance in thermal solar energy-collecting systems, it is often better to single out the collector and receiver and then balance the energy in and out of them. The overall energy balance in this subsection therefore can be written in terms of the rate of useful energy (Q̇ u), the rate of optical radiation that is incident on the receiver from the dish (Eoptical), and the rate at which there are thermal energy losses in the receiver (Q̇ loss), expressed by Stine and Geyer (2001) as

$$\dot{Q}_u = E_{optical} - \dot{Q}_{loss} \tag{10}$$

The setup under consideration in this report is an indirect system that involves a heat transfer fluid; therefore, the useful heat energy ($\dot{Q}_u$) can be expressed in terms of the heat that is added to the oil while it travels through the receiver, as

$$\dot{Q}_u = mc_p(T_{out} - T_{in}) \tag{11}$$

Now that the governing equations are known, the various parts of the solar energy
collection subsystem will be presented in the following sections.

3.3. Geometric concentration Ratio (CR_g).

Geometric concentration ratio is the area of the collector aperture A_a divided by the surface area of the receiver A_r

$$\mathrm{CR_g} = \frac{A_a}{A_y} \tag{12}$$

4. METHODOLOGY.

4.1. Introduction

This chapter gives an outline of research methods that were followed in the study to come up with my new design. It provides information on the study site, product specification used to evaluate different available design concept, and finally it shows the pugh matrix selection which helped me to come up with my new design.

4.2. Setting/study site.

The study was conducted at Malawi University of science and technology (MUST). Which is located in Goliat, Thyolo District, TA Ngolongoliwa which is made of a population of 33,839 is according to the national demographics' statistics (2018) which most of the people rely on charcoal and firewood as a source of energy for cooking and heating water for bathing. Malawi University of Science and Technology (MUST) is found at coordinates of *15.9020S, 35.2168E, and* is 36.6 kilometers from the center of Blantyre city.



Figure 21: shows the 3D map of Ndata area in Thyolo, source: Google map.

4.3. Product specification.

The design was specified based on the following product design specification:

a. Performance

- The performance was based on how fast, slow, rate of working, and tolerance of speed.

b. Environment

- How the surrounding environment affected the efficiency of the Solar cooker by looking at the surroundings, temperature, humidity, and pressure range.

c. Maintenance

- Based on whether the solar cooker will requires regular maintenance and the availability of spare parts.

d. Cost

- How expensive or cheap is the product as a result of materials used and cost of manufacturing.

e. Size and Weight

- Portability of the parabolic solar cooker.

f. Choice of material

- Mainly focuses on the durability of materials used, cost, and the availability of the materials.

g. Safety

- The safety was based on the legislation and standards covering the aspects such as EEC legislation on product liability and particular specifications relevant to particular areas such as BS 5724. Safety Requirements on Hospital Medical Electrical Equipment.

h. Competition

- A thorough analysis of competitors was carried out, including a comprehensive literature search, patents and product literature search relating not only to the proposed product area, but also to the product area.

i. Ergonomics

- It is necessary to clarify the possible nature of the interaction of the product with man. What height, reach, forces and operating torques are acceptable to the user. Postures and lighting should be considered.

k. Shipping

- How product will be delivered. By land, sea or air – home or overseas, what type and size of truck, pallet container, or type of aircraft used for the type of product under consideration.

4.4. Conceptional Evaluation.

Three conceptual designs which are now commercialized on the solar cooker markets were obtained including the fourth one SK-14 which is now commonly used by many people in different countries and it have standard parameters which produces the efficiency of around 55% where used as my reference point on my conceptual generation and evaluation.

SK-14 parabolic concentrator concept



Figure 22: shows SK-14 parabolic solar cooker.

Principle

SK-14, is a solar concentrator developed by Dr.Ing. Dieter Siefert. It is a concentrating type parabolic dish solar cooker useful for households and small establishments. A typical dish solar cooker has an aperture diameter of 1.4 meter and focal length 0.28 meter. The reflecting material used for fabrication of this cooker is anodized aluminum sheet which has a reflectivity of over 80%. The tracking of the cooker is manual and thus has to be adjusted in 15 to 20 minutes during cooking time. It has a delivering power of about 0.4 kW which can boil 2 to 3 liters of water in half an hour. The temperature achieved at the bottom of the vessel could be around 300 ^{0}C to 400 ^{0}C which is sufficient for roasting, frying and boiling. The cooker having a thermal efficiency of around 55% can meet the needs of around 4-8 peoples and can be used from one hour after sunrise to one hour before sunset on clear days. The cost of the cooker may vary from Rs. 3,500 to Rs. 6,000 depending on the type of reflectors used and the salient features provided by the manufacturers.

Operation

Different solar cooker has different working principle but most of them have same basic principle. Food cooks faster when it is in smaller pieces. Usually, small pieces of food placed in solar cooker. potatoes are normally cut into in small piece and cook. They should not whole. For simple cooking like melting butter it is not necessary. If we have to cook different foods, then put them in different pots. After that pot is placed on cooking area of the solar cooker. Food that cook quickly that should place latter. Rice for lunch might be started early in the morning. Depending on size and capacity of solar cooker, quantity of cooked food, family can use one or more cooker. Solar cooker turned towards the sun and left until and unless food is cooked. Solar cookers may be checked every one to turn the dish towards the sun. Make ensure about shadow of nearly building or tree. Cooking being used, quantity of food, air temperature, wind and latitude

also effect on performance. By using large solar collectors, it might be possible to cook rice for four people in four hours, melting butter in 15 minutes.

PRINCE-15 (Fabricated) parabolic concentrator concept.



Figure 23: shows PRINCE-15 solar cooker.

Principle

It is a concentrating type parabolic dish solar cooker with square geometry and useful for households and autoclaving. A typical dish solar cooker has dimension of 1250 mm × 1250 mm and focal length 0.460 meter. The reflecting material used for fabrication of this cooker is anodized aluminum sheet which has a reflectivity of over 80%. The tracking of the cooker is manual and thus has to be adjusted in 15 to 20 minutes during cooking time. It has a delivering power of about 0.6 kW which can boil 2 to 3 liters of water within 20 m minutes. The temperature achieved at the bottom of the vessel could be around 350 ^{0}C to 400 ^{0}C which is sufficient for roasting, frying and boiling. The

cooker having a thermal efficiency of around 62% can meet the needs of around 8 peoples. PRINCE- 15 is a concentrator with square or rectangular dish shape. This shape permits use of same sized strips of steel to make bowl. This makes the bowl sturdy. As the members of the dish have same geometric shape this reflector is easy to assemble even by novice people with the help of construction manual.

ADVANTAGES OF PRINCE-15 DESIGN.

- Cooking is quicker (1/2 to 1 hour).
- Quite efficient.
- Can achieve extremely high temperature 300 ^{0}C to 350 ^{0}C.

DISADVANTAGES OF PRINCE-15 DESIGN.

- Difficult to make and use (complex design)
- Requires the user's attention.
- Relatively high cost
- Safety problems (burns or eye damage)
- Strong reliance on direct beam.

DIY parabolic solar cooker concept



Figure 24: shows DIY parabolic solar cooker.

Principle

A DIY-parabolic solar cooker has high reflectivity which uses heavy duty aluminum foil to concentrate light coming from sun on a small cooking area, but it is depend on geometry of cooking surface. Solar cookers are typically designed to achieve temperature 300 ^{0}C to 400 ^{0}C on a sunny day. Solar cookers concentrate sunlight on cooking pan. Interaction between receiver material and sunlight converts sunlight into heat energy. Pots and pan used for cooking must be in black color only. It is most important to insulate the cooker simply by using glass lid on pot. It minimizes convection loss of heat energy in the solar cooker.

ADVANTAGES OF DIY DESIGN.

- Cooking is quicker (1/2 to 1 hour).
- highly efficient.
- Can achieve extremely high temperature 300 ^{0}C to 350 ^{0}C.
- Use locally available materials
- It is cheap compared to other parabolic solar cookers

DISADVANTAGES OF DIY DESIGN.

- Difficult to make and use (complex design)
- Requires the user's attention.
- Safety problems (burns or eye damage)
- Strong reliance on direct beam.

SK-23, PRINCE-40 Design Concept.



Figure 25: shows PRINCE-40 (SK-23) parabolic solar cooker design.

Principle

PRINCE-40 are the community solar cookers. It is a concentrating type parabolic dish solar cooker, with cooking capacity: 40-50 people. It has a dish diameter of 2.3m, aperture area 4m^2, heat rate at the pot is at 2.5 kw, and it cost: Rs. 20,000, and the material used for forming dish is best quality German reflectors with more than 85% reflectivity. The PRINCE-40 unit is designed, manufactured, tested, and commercialized by PRINCE.

ADVANTAGES OF PRINCE-40 DESIGN.

- Cooking is quicker (1/2 to 1 hour).
- Quite efficient.
- Can achieve extremely high temperature 300 ^{0}C to 400 ^{0}C.

DISADVANTAGES OF PRINCE-40 DESIGN.

- Difficult to make and use (complex design)
- Requires the user's attention.

- Relatively high cost
- Safety problems (burns or eye damage)
- Strong reliance on direct beam.

Joseph Daniel Nyirenda (JDN) concept.

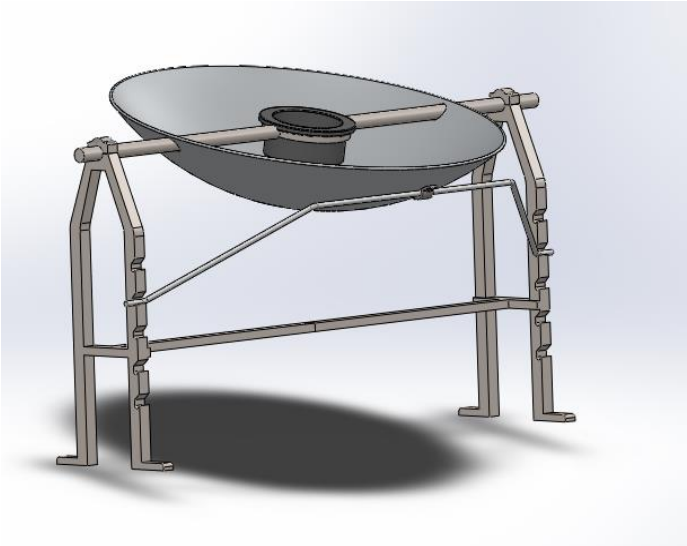


Figure 26: shows the JDN parabolic solar cooker design.

Principle

JDN parabolic solar cooker was designed to use locally available materials such as plywood to create a parabolic dish which will be covered by heavy duty aluminum foil to concentrate light coming from sun on a small cooking area. A double glass with hemispheric shape will be placed at the bottom of cooking area which will be made of ceramic to act as both thermal insulation and thermal storage, in order to achieve an accurate theoretical analysis of this type of solar cooking section. The parabolic dish has a diameter of 1.4m and a focal length of 0.28m. The sun tracking of the cooker is manual and thus has to be adjusted with solar angle adjuster every 1 hour with respond to calibrated solar angle adjusting slot. It has a delivering power of about 0.6kW and produces the temperature range of 350^{0}C to 400^{0}C. and it has the overall thermal efficiency of 0.796

Advantages.

- Highly efficient
- Use locally available materials
- Can achieve extremely high temperature 350^{0}C to 450^{0}C
- It is cheap compared to another existing parabolic solar cookers.
- Easy to use

Disadvantages.

- Difficult to make
- Requires the user's attention
- Safety problem (eye damage)

The table shows pugh matrix selection.

Design specification	PRINCE-40 (SK-23) Design	DIY-Design	Prince-15 Design	JDN Design	Ref (SK-14)
Performance	+	0	+	+	0
Environment	+	+	+	+	0
Cost	-	+	-	+	0
Size and weight	-	+	-	+	0
Choice of material	+	+	+	+	0
Safty	+	+	+	+	0
Competition	+	-	+	+	0
Ergonomics	-	+	+	+	0

Shipping	-	+	-	0	0
Sum of +	**5**	**7**	**6**	**8**	
Sum of -	**4**	**1**	**3**	**0**	
Total	**1**	**6**	**3**	**8**	
Rank	**4**	**2**	**3**	**1**	

now by using pugh matrix and taking SK-14 as reference point, JDN-design has a top score of 8 according to the specification selected. So, my design was proved to be better than already existing designs.

5. EMBORDIMENT AND DETAILED DRAWINGS.

5.1. Introduction

This chapter firstly, outline the important formulas used in design calculation, then the detailed drawing of my design with is specific materials and dimensions, and it describes why those materials and dimensions.

5.2. Design calculations

To accomplish the design and simulation, different equations were used. For better accumulating heat without letting pass the fresh air, is good to choose the depth of the parabola. The designed parabolic solar cooker is composed of a parabola whose diameter is 1.42m and its depth 0.25m, with aluminum foil of 1mm thickness.

The equation giving focal distance (F) is given by Kalbande [200]

$$\mathrm{F} = \frac{d^2}{16h} \tag{13}$$

The parabola surface is:

$$A = \frac{8 \times \pi \times f^2}{3}\left[\left(\frac{d}{4 \times f}\right)^2 + 1\right)^{\frac{3}{2}} - 1] \tag{14}$$

The half aperture surface is:

$$\tan\Psi = \frac{1}{\frac{d}{8h} + \frac{2h}{d}} \tag{15}$$

The heat balance of the solar concentrator with permanents rate is given by Zereli [2004]

$$P_a = P_u + P_e \quad (16)$$

Where

P_a – is absorptive radiation power, W

P_u – useful power, W

P_e – is thermal losses power, W

The radiation absorptive power can be calculated by:

$$P_a = EC_i A\rho\gamma\tau\alpha \quad (17)$$

Where

E – is illumination on the level of the concentrator, W/m^2

C_i – is idea concentration

A – area of the parabolic concentrator, m^2

ρ – the parabola coefficient of reflexion

γ – the absorber coefficient of interception

τ – is cooking pot transmittivity

α – is the cooking pot absorptivity

The coefficient of interception is given by the following equation

$$\gamma = 1 - \exp\left[-820\left(0.7\frac{r}{f}\right)^2(1 + \cos(\emptyset_0))\right] \quad (18)$$

Where

r – is Exergy

f – focal distance

The power of heating is given as follow

$$Q_{heat} = \frac{M_w C_w \Delta T_{\infty-95}}{\Delta t} \quad (19)$$

To compare the various cookers in various countries and under various climate, Funk [2000] has shown that the power of radiation is standardize to 700 w/m^2

The standard power is expressed then by:

$$P_s = \frac{(M_w C_w)(T_{wf} - T_{wi})}{600} \times \frac{700}{I_b} \quad (20)$$

"600" represents the time interval of measured in seconds.

The thermal losses factor is given by the center of energy studies [2006]

$$F'UL = \frac{(MC)'w}{A_{pot}\tau_0} \quad (21)$$

$$(MC)'w = M_{pot}.C_{pot} + M_w.C_w \quad (22)$$

Where

F·UL – factor of losses thermal

M_{pot} – mass of empty pot with lid, kg

M_w – mass of water, kg

C_w – specific heat of water, J/kg.K

C_{pot} – Specific heat of matter of the pot of cooking, J/kg.K

τ_0 – cooking time constant.

The optical effectiveness factor is given by the centre of energy studies [2006] and kumar [1995]

$$F'\eta_0 = \frac{\frac{(F'UL)A_{pot}}{A_{parabole}}\left[\left(\frac{T_{wf}-T_a}{Ib}\right)-\left(\frac{T_{wi}-T_a}{Ib}\right)e^{\frac{-\tau}{\tau_0}}\right]}{1-e^{\frac{-\tau}{\tau_0}}} \quad (23)$$

η_0: the optical efficiency of the collector.

Thus, the quantity of thermal energy produced by solar collector is described by the output of the collector which is given by Schwarzer [2007] and Kundarpur [2006]

$$\eta = \frac{(M_w \times C_w + M_{pot} \times C_{pot})(T_{wf}-T_{wi})}{A_{parabole} \times \int_0^t Ib.dt} \quad (24)$$

Overall thermal efficiency is calculated by the following equation (El-sebaii and Ibrahim 2005).

$$\eta_u = \frac{M_f C_f \Delta T_f}{I_{av} A_c \Delta t} \quad (25)$$

Where:

η_u - over thermal efficiency (%)

M_f – Mass of cooking fluid (kg)

C_f – Specific heat of cooking fluid (j/kg.K)

ΔT_F – difference between the maximum and ambient air temperature.

I_{av} – average solar intensity (W/m^2) during the time interval.

A_c – is the aperture area (m^2) of the cooker.

Δt – time required to achieve maximum temperature of the cooking fluid(s).

5.3. Heat transfer in cooking section

The model for analysis of the solar cooking pot presented by EL-Kassaby (1991) and modified by Amer (2003) and Kimarmbo 2007, who worked backed from the energy supplied to the food to analyses their systems.

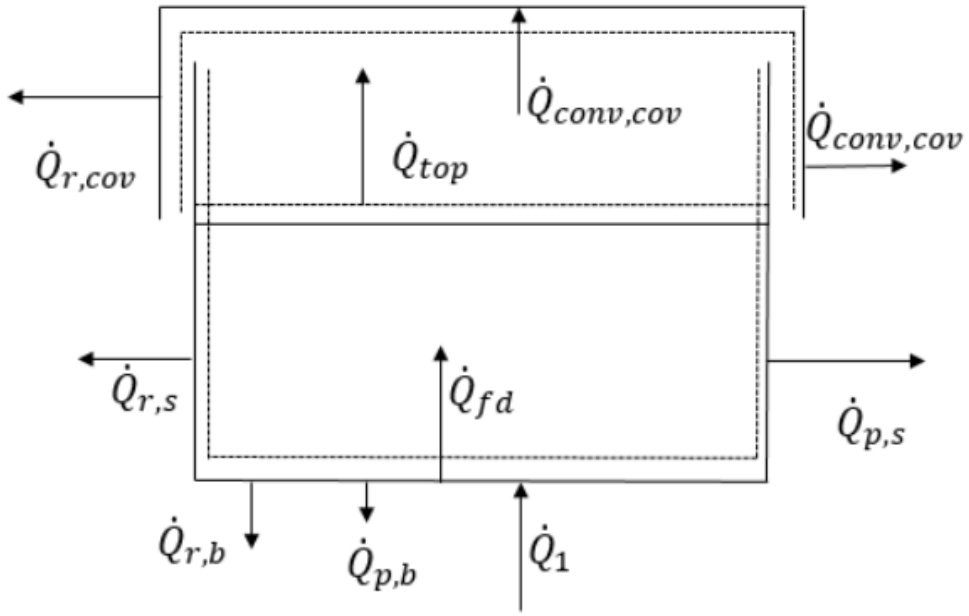


Figure 27: shows heat transfer in cooking section.

In this system, however, $\dot{Q}_{fd}$ represents the energy supplied to whatever is being heated up in the pot (food, pancake, water, etc.). The work that this energy performs can be divided into two. First it has to raise the internal energy of the food, $U_{fd,i}$, and second, it has to overcome the convective losses through the air top of the pot, as $\dot{Q}_{top}$.

$$\dot{Q}_{fd} = \dot{Q}_{top} + \dot{Q}_{fd,i} \tag{26}$$

Writing equation (26) explicitly in terms of the instantaneous temperature of the food $\frac{dT_{fd}}{dt}$, the mass of food that is cooked, M_{fd}, the specific heat capacity of the

food and the heat transfer coefficient between the inside of the cooking pot and the food being cooked are shown in equation

$$\dot{Q}_{fd} = \dot{Q}_{top} + m_{fd}c_{fd}\frac{dT_{fd}}{dt} = h_{fd}A_{fd}(T_{pot} - T_{fd}) \quad (27)$$

The heat energy from the tank is transferred to the cooking pot through the aluminum plate which is painted black, represented as $\dot{Q}_1$, and this energy is transferred to the food as $\dot{Q_{fd}}$, which is expressed in equation (26) and (27) to perform the two functions, thermal insulation and thermal storage. The energy lost through convection from the side walls of the cooking pot is represented as $\dot{Q_{p,s}}$ and that lost from the bottom of the pot to the surroundings is $\dot{Q_{p,b}}$. The radiation from the bottom of the pot to the and from the sides to the cover is presented by $\dot{Q_{r,b}}$ and $\dot{Q_{r,s}}$ respectively. These energies can all be combined in an energy balance equation, represented as

$$\dot{Q} = m_{pot}c_{pot}\frac{dT_{pot}}{dt} + \dot{Q}_{fd} + \dot{Q}_{p,s} + \dot{Q}_{p,b} + \dot{Q}_{r,s} + \dot{Q}_{r,b} \quad (28)$$

Where:

$$\dot{Q}_{p,s} = h_g A_{side}(T_{pot} - T_a) \quad (29)$$

$$\dot{Q}_{p,b} = h_a A_{top}(T_{pot} - T_a) \quad (30)$$

$$\dot{Q}_{p,b} = \sigma\varepsilon_{pot}A_{pot}({T_{top}}^4 - {T_a}^4) \quad (31)$$

$$\dot{Q}_{p,b} = \sigma A_{side}({T_{top}}^4 - {T_a}^4) \quad (32)$$

The air trapped between the tank cover and the inside part of the pot section was also modelled, because it was expected to transfer the heat to and/ or get the heat from both the pot and the pot cover. This can be expressed as

$$\dot{Q}_{p,s} + \dot{Q}_{top} + \dot{Q}_{p,s2} = m_a c_a \frac{dT_g}{dt} \tag{33}$$

Where the newly introduced convection term, $\dot{Q}_{p,s2}$, for the air trapped in the cooking section is defined as follows:

$$\dot{Q}_{p,s2}, = h_g A_{cov}(T_{cov} - T_g) \tag{34}$$

Two types of cooking can be performed with the experimental setup: the first is cooking under direct sunshine, where the top of the cooking section is left exposed to direct sunshine, and the second is when the top part of the cooking section is covered with insulators. When cooking was done in sunshine and top of the cooking section in the storage tank was not covered with insulation to allow additional direct heating from sunshine, it was necessary to model the exposed cover into the set of defined equations, because the cover of the pot was also expected to receive direct irradiation from the sun and to gain heat from the inner part of the pot through convection $\dot{Q}_{p,s2}$. It was also expected to store some heat as latent internal energy, and to lose heat to the atmosphere through radiation ($\dot{Q}_r$) and convection ($\dot{Q}_{conv}$). The energy balance for this expression is given below, where $\dot{Q}_2$ is the secondary direct irradiation falling on the cooking section.

$$\dot{Q}_2 + \dot{Q}_{rs} = \dot{Q}_{p,s2} + \dot{Q}_{p,s2} + \dot{Q}_{cov}, cov \frac{dT_{cov}}{dt} \tag{35}$$

Where

$$\dot{Q}_2 = A_{cov}\alpha_{cov} I \tag{36}$$

$$\dot{Q}_r = \sigma \varepsilon_{cov} A_{cov} (T_{cov}{}^4 - T_a{}^4) \quad (37)$$

$$\dot{Q}_{cov,} conv = h_a A_{cov} (T_{cov}{}^4 - T_a{}^4) \quad (38)$$

Rearranging the above equations to form a forst-order differential equation that can be solved numerically gives the following sets of equations:

$$\frac{dT_{fd}}{dt} = F_{fd}(T_{fd}, T_{pot}, t) \quad (39)$$

$$\frac{dT_{pot}}{dt} = F_{pot}(T_{fd}, T_{pot}, T_g, T_{cov}, t) \quad (40)$$

$$\frac{dT_g}{dt} = F_g(T_{fd}, T_{pot}, T_g, T_{cov}, t) \quad (41)$$

$$\frac{dT_{cov}}{dt} = F_{cov}(T_{fd}, T_{pot},, T_{cov}, t) \quad (42)$$

The above equations can be solved using the fourth-order range-Kutta method for numerical solutions of first-order differential equations. The Chapra and Canale (2003) model was used to generate the results.

An alternative way solves the heat transfer in the cooking section is by using the thermal resistance method. Figure (28) shows an alternative method to analyses the heat flow in the cooking section by using the concept of thermal resistance. This resolves heat transfer as basic electricity equation, V=IR, with V the electrical potential current I, analogical to the rate of heat transfer, and the resistance R relating to thermal resistance, as shown in the figure below

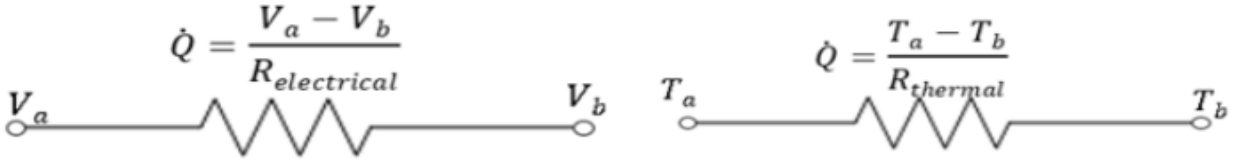


Figure 28: shows Analogical relationship between electrical and thermal resistance.

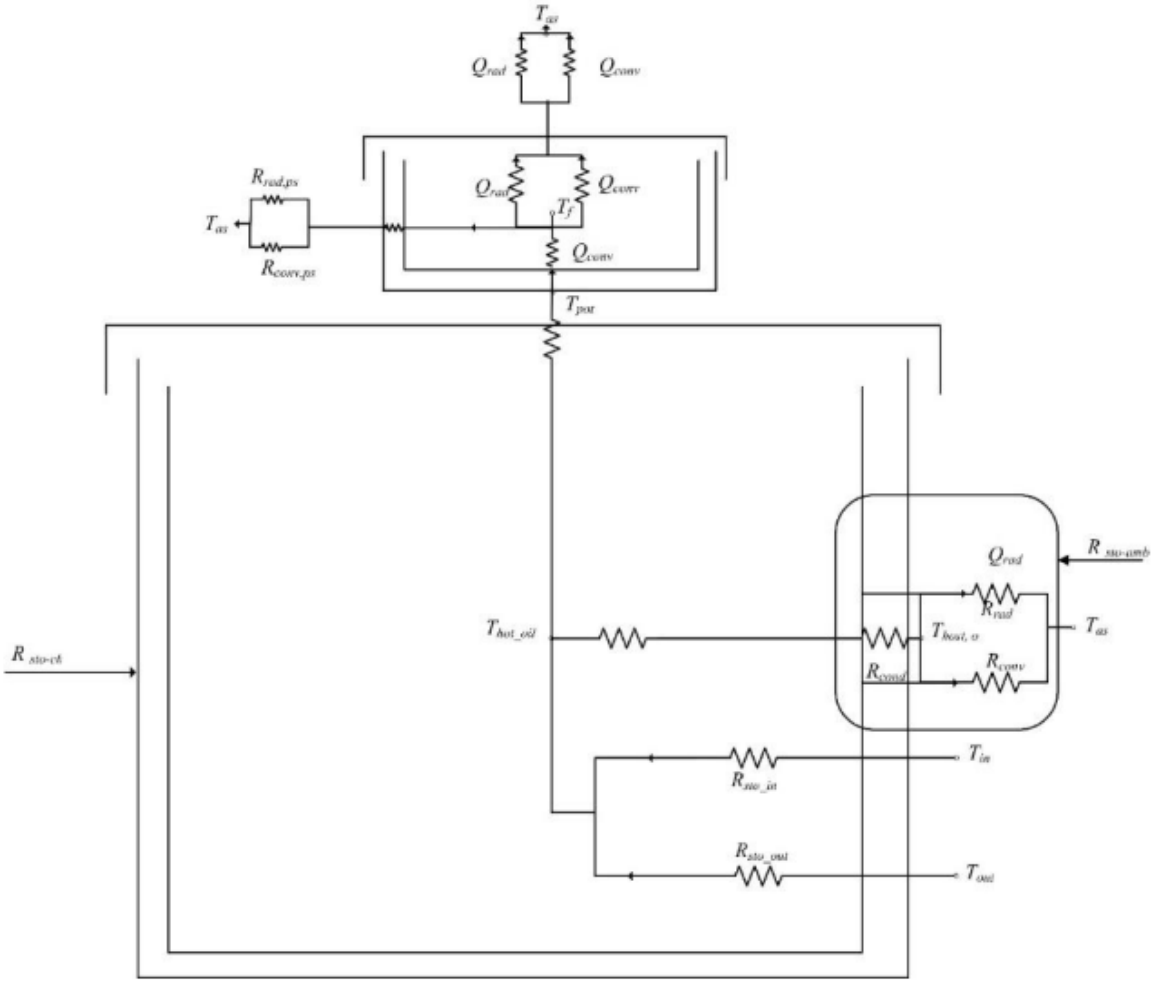


Figure 29: shows thermal resistance diagram of the cooking section.

The analogy in figure (29) can be used to solve the energy equation using the resistances shown in figure (28). the various heat transfer modes with resistance analysis are shown in the set of equations below:

$$R_{conv} = \frac{1}{hA} \tag{43}$$

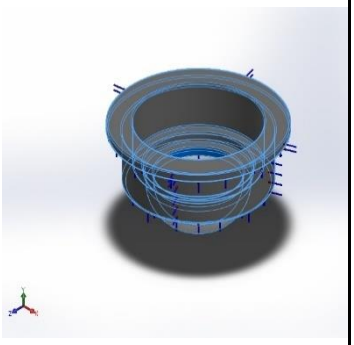
$$R_{cond} = \frac{\Delta x}{kA} \tag{44}$$

$$R_{rad} = \frac{1}{\varepsilon \sigma A (T_a{}^2 + T_b{}^2} \tag{45}$$

MATERIAL SELECTION.

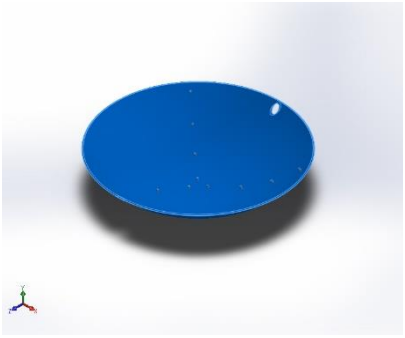
The choice of materials was firstly based on availability of materials (locally available material) and then the properties of that material was also the second criteria used in selecting the materials.

Cooking section.

Model Reference	Properties	Components
	Name: Ceramic Porcelain Model type: Linear Elastic Isotropic Default failure criterion: Mohr-Coulomb Stress Thermal conductivity: 1.4949 W/(m.K) Specific heat: 877.96 J/(kg.K) Mass density: 1,864.29 kg/m^3	SolidBody 1(Revolve3) (parabolic cooking area)
Curve Data:N/A		

I choose this material because is made from sand and it has good thermal insulation us we can see on the table on thermal conductivity which is very small compared to other thermal insulation materials.

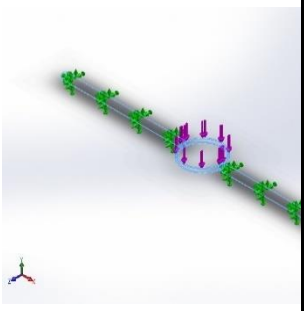
Parabolic Dish.

Model Reference	Properties	Components
	Name: Aluminium foil Model type: Linear Elastic Isotropic Default failure criterion: Unknown Thermal conductivity: 30 W/(m.K) Specific heat: 850 J/(kg.K) Mass density: 267.569 kg/m^3	SolidBody 1(Cut-Extrude1) (parabolic dish)
Curve Data:N/A		

The parabolic dish will be formed with plywood which will be cover by the heavy-duty aluminum heavy duty. These are locally available materials and easily be replace during maintenance because they are cheap.

Cooking stand.

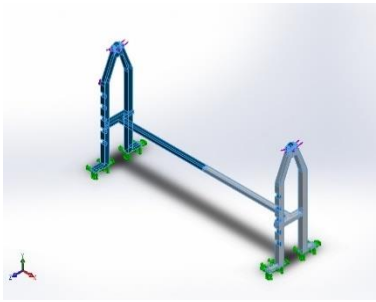
Material Properties

Model Reference	Properties	Components
	Name: Stainless Steel (ferritic) Model type: Linear Elastic Isotropic Default failure criterion: Max von Mises Stress Yield strength: 1.72339e+08 N/m^2 Tensile strength: 5.13613e+08 N/m^2 Elastic modulus: 2e+11 N/m^2 Poisson's ratio: 0.28 Mass density: 1,873.74 kg/m^3 Shear modulus: 7.7e+10 N/m^2 Thermal expansion coefficient: 1.1e-05 /Kelvin	SolidBody 1(Cut-Extrude2)(cooking holder)
Curve Data:N/A		

I choose the stainless steel because it has more strength to with stand high forces and pressure during cooking. And the steel is plenty available in different areas.

Supporting Stand.

Material properties.

Model Reference	Properties	Components
	Name: Pine (HARDWOOD) Model type: **Linear Elastic Isotropic** Default failure criterion: **Unknown** Yield strength: **2e+07 N/m^2** Elastic modulus: **3e+09 N/m^2** Poisson's ratio: **0.29** Mass density: **159.99 kg/m^3** Shear modulus: **3e+08 N/m^2**	**SolidBody 1(Cut-Extrude2[2])(stand),** **SolidBody 2(Cut-Extrude7[1])(stand),** **SolidBody 3(Cut-Extrude7[2])(stand),** **SolidBody 4(Mirror6[2])(stand)**
Curve Data:N/A		

I choose pine because it is locally in many areas of the country and it is also cheap. It also has a strength to withstand high pressures ca the table indicates.

5.4. Detailed Drawings

5.4.1. Final design

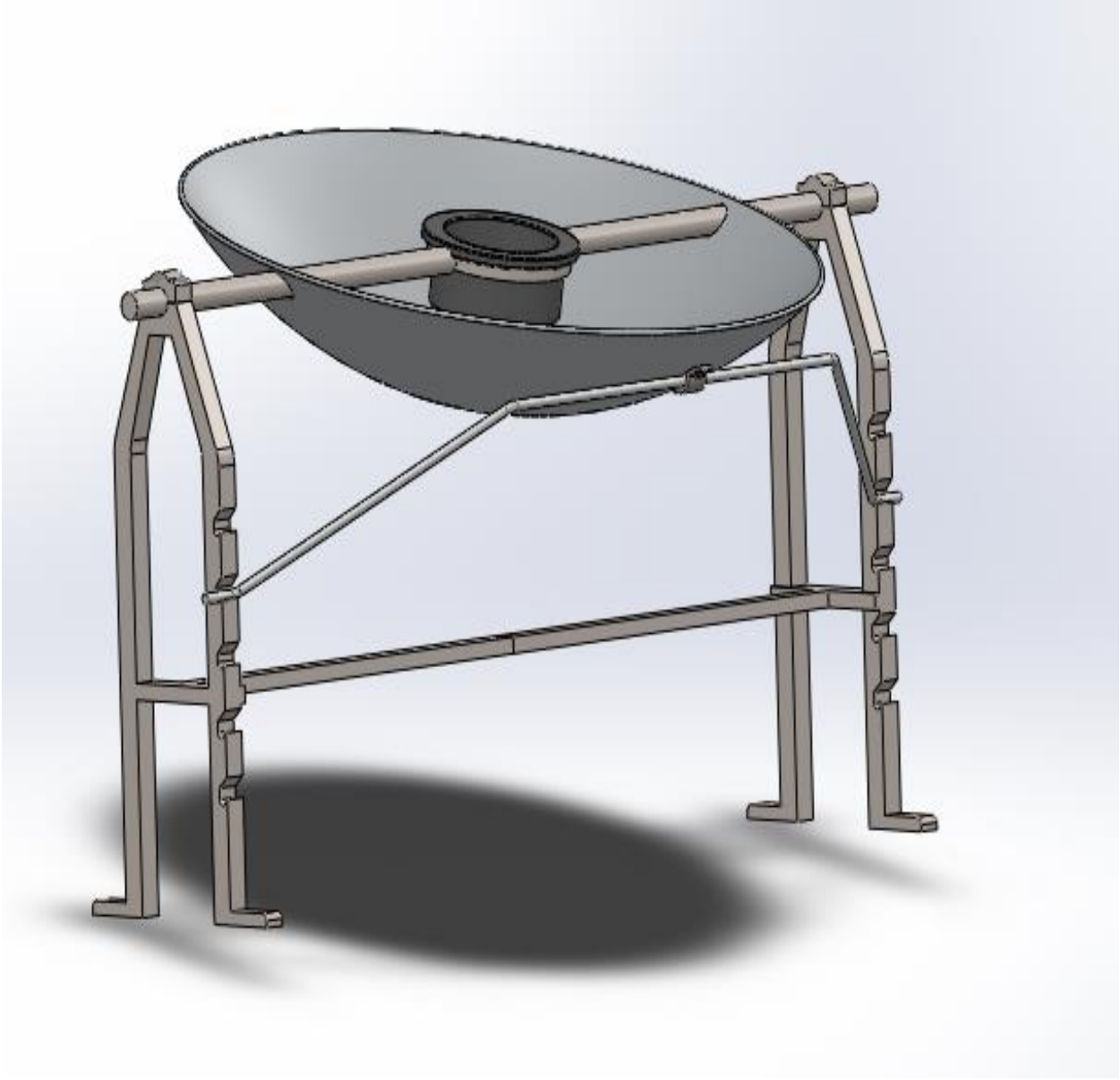


Figure 30: shows the final assembled drawing.

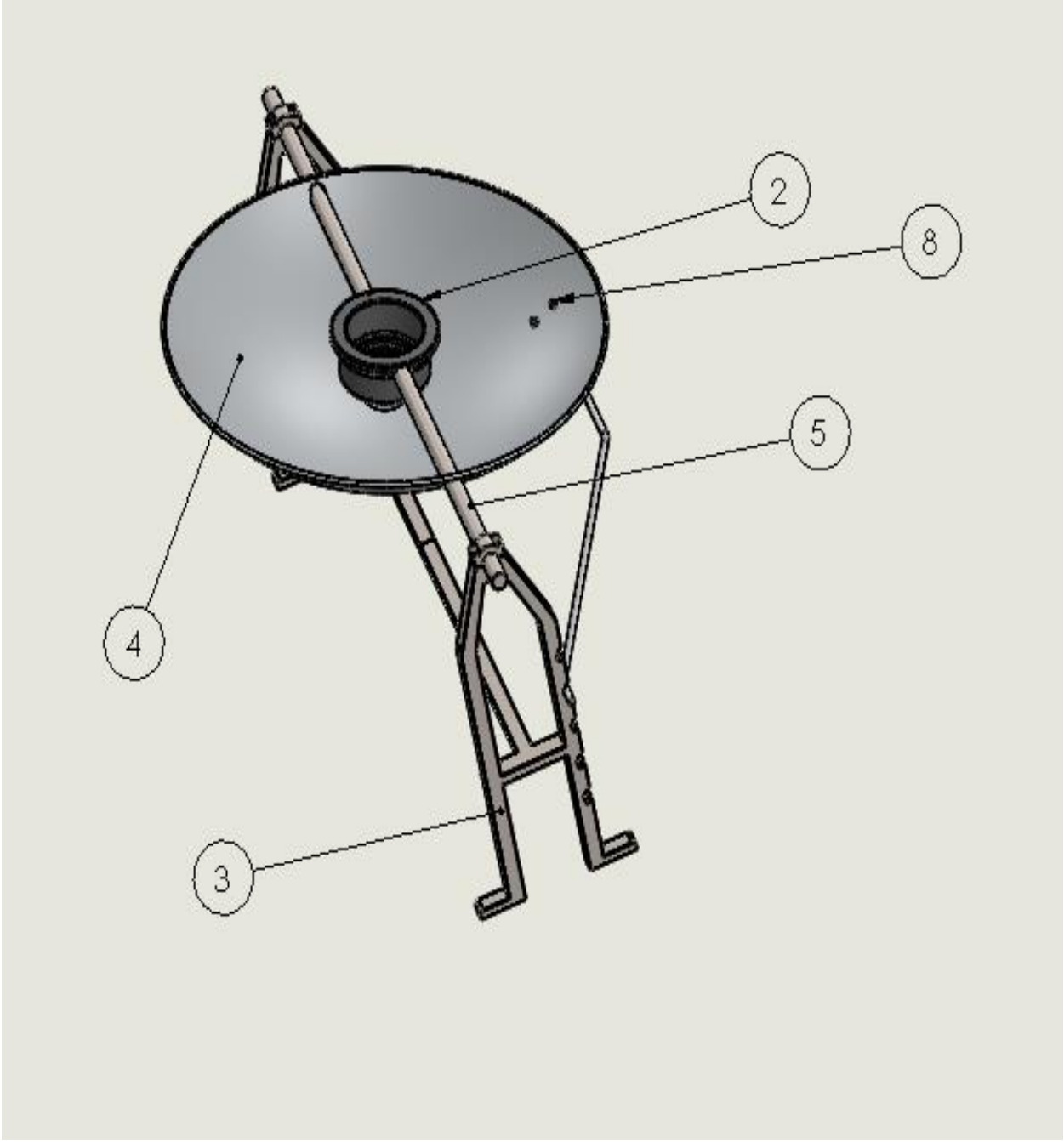


Figure 31: shows the balloon labeling top view.

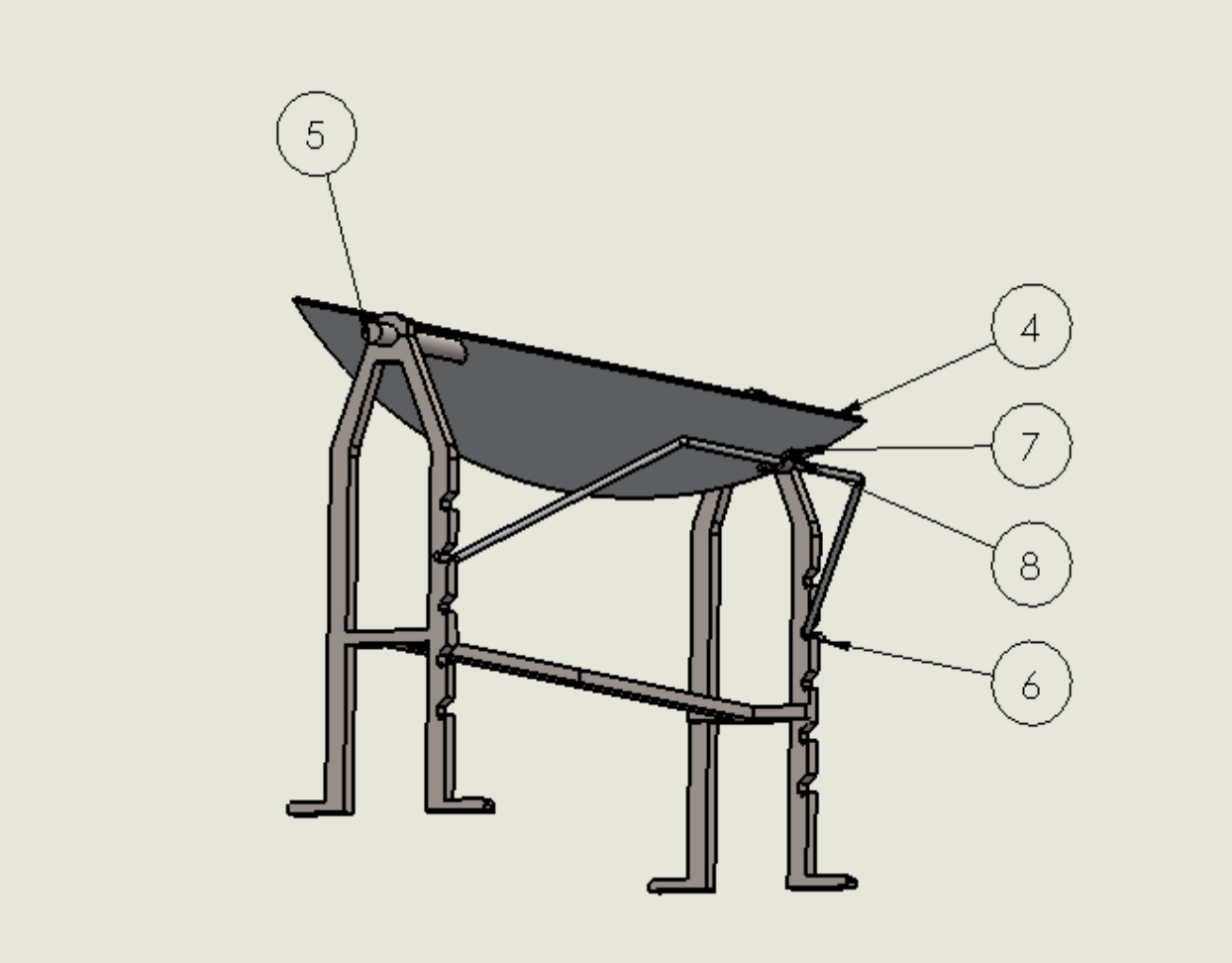


Figure 32: shows the balloon labeling of side view.

KEY

1= Assembled drawing (Full body)

2= cooking chamber

3= Supporting stand

4= Parabolic dish

5= Cooking stand

6= Dish adjusting stand

7= Dish adjusting stand holder

8= hinge

5.4.2. Parabolic dish.

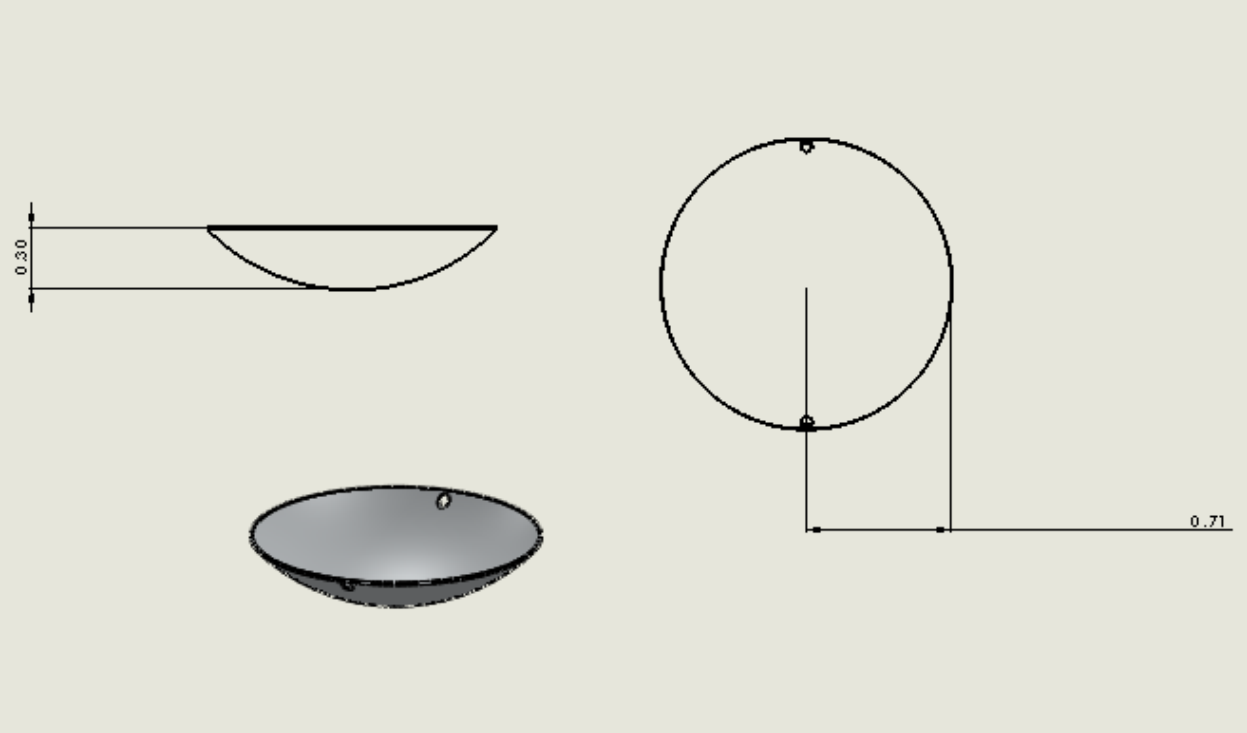


Figure 33: shows the parabolic dish.

The parabolic dish was designed to have a diameter of 1.42m because that size is the one with high concentration ratio of about 7001.089 according to the theoretical part of parabola and is also the size which many commonly used solar cookers with high efficiency used. The dish will have a height of 0.3m in order to provide the theoretical focal distance of 0.25m.

The dish will be made by simple locally available materials manly ½-inch plywood (for panel form), heavy-duty aluminum foil, sheet of paper and large corrugated cardboard box(es). This material is easily accessible and cheap for easily maintenance in different areas.

5.4.3. Supporting stand.

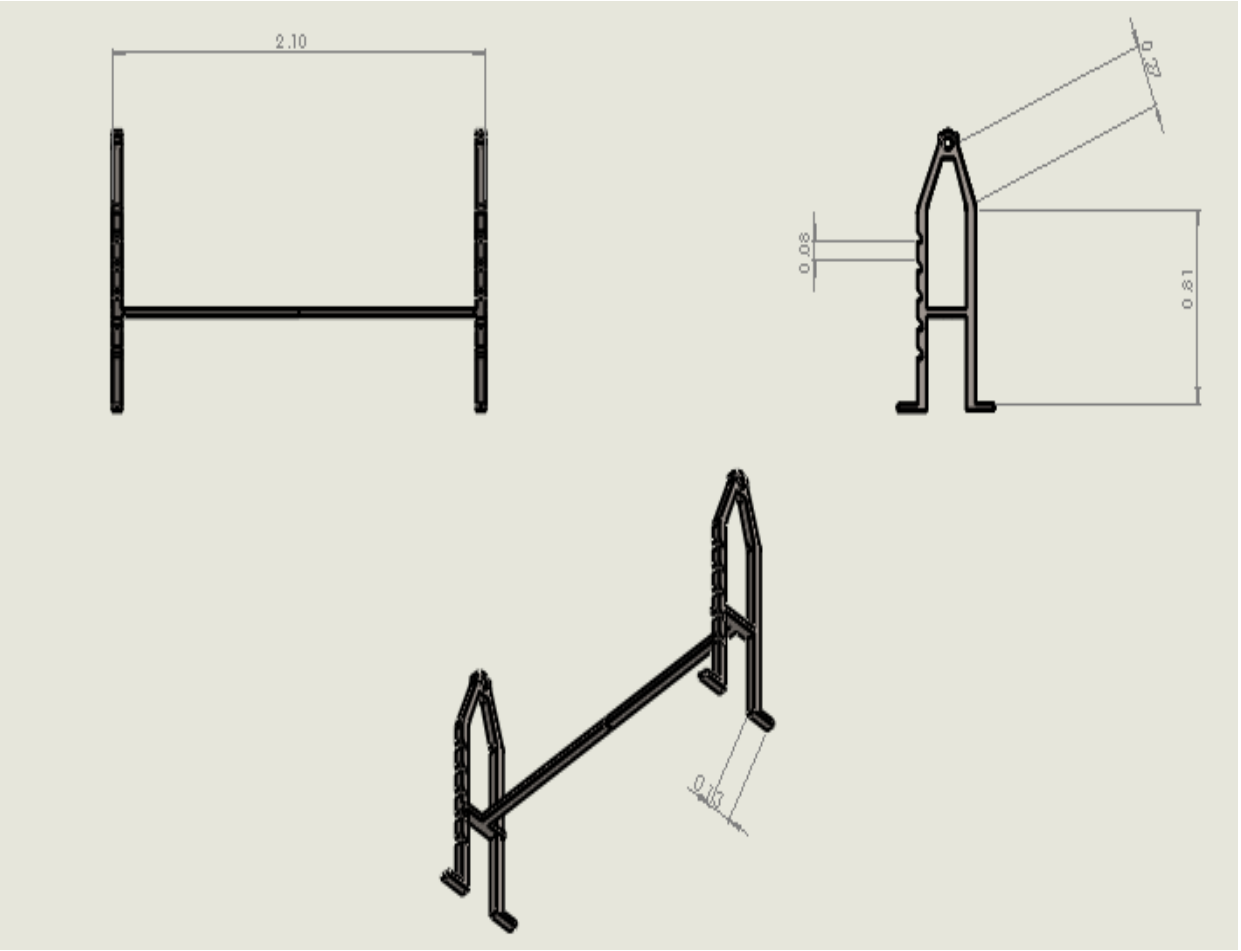


Figure 34:shows the supporting Stand.

The supporting stand will be made with hard wood (pine) for easily accessible and cheap for everyone to afford it. The stand is 2.1m wide and 1.2m high, and it also have dish adjusting slots with the distance of 0.08cm between each adjusting slot. This was done in order to manually track the sun position to increase the systems efficiency of converting sunlight into heat energy. The spacing was done after the calculation of sun position after every one hour during the day.

5.4.4. Cooking stand.

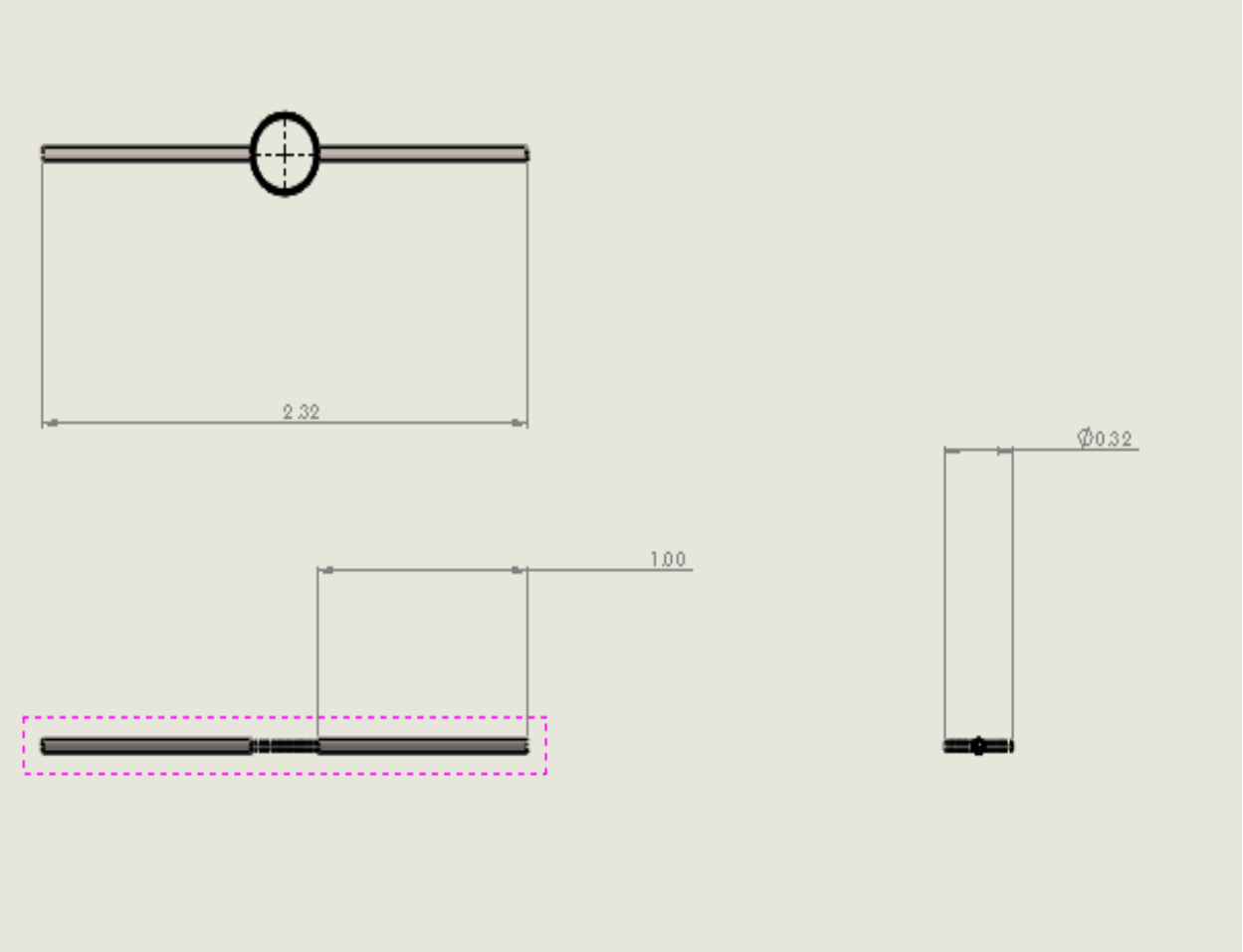


Figure 35: shows the cooking stand

The cooking stand will be made with gavanized/ stanless steel inorder to withstand the forces and pressure during cooking and have enough strength to hold the pot and cooking chamber together at the same time. The cooking stand is 2.32m long with the circle of 0.32m at the center which holds the cooking chamber.

5.4.5. Cooking area with thermal storage part.

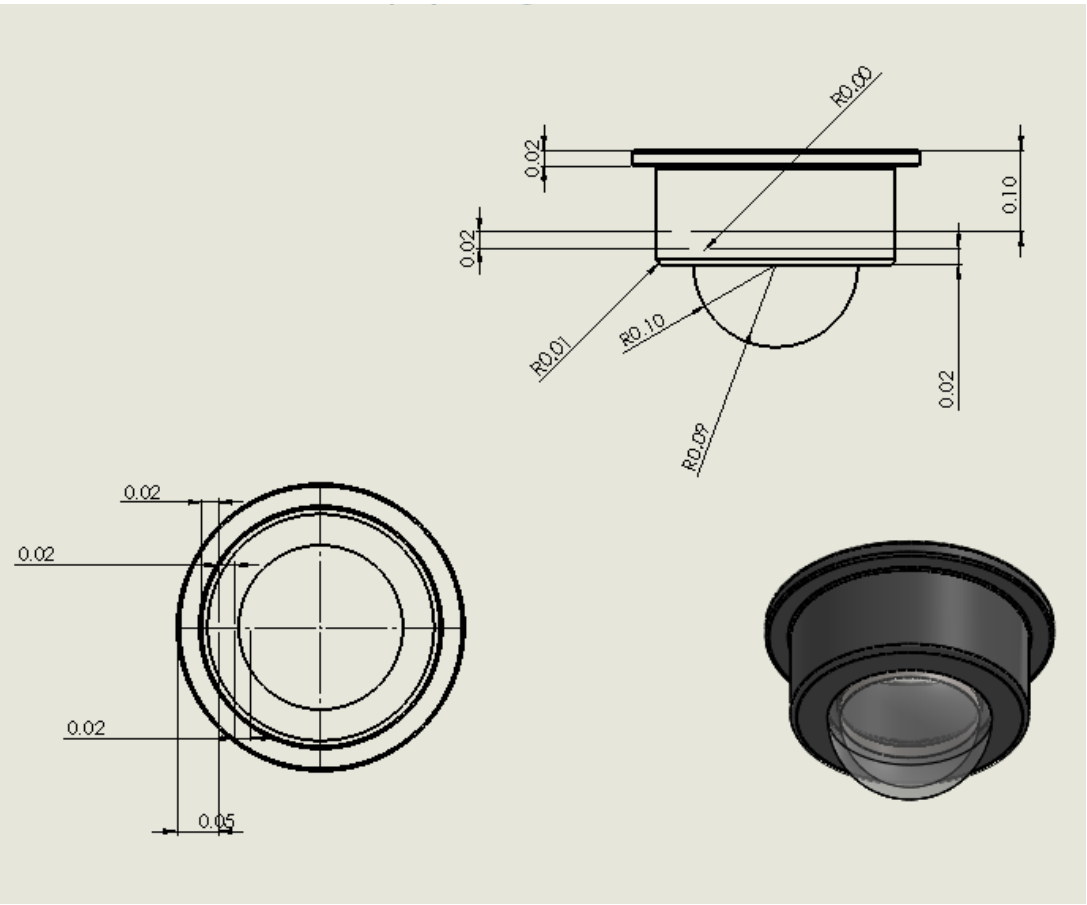


Figure 36: shows the cooking section

Cooking section

A double glass with hemispheric shape will be placed at the bottom of cooking area which will be made of ceramic to act as both thermal insulation and thermal storage, in order to achieve an accurate theoretical analysis of this type of solar cooking section. Inside the cooking chamber there is a space where the black plate will be placed to close the open part of the double glassed hemisphere to create a heat storage tank. The first assumption made was that a constant heat is supplied to the pot. If the cooking is done in a shaded place (clouds) or in a place where there is no direct exposure of the cooking pot to the sun, the energy stored from the hemi-spherical double glass is modelled as the only energy supplied to the cooking plate. However, if the cooking is done outside, an

additional direct irradiation from the sun should be added to the energy input as the secondary irradiation falling on the pot

5.4.6. Cooking plate

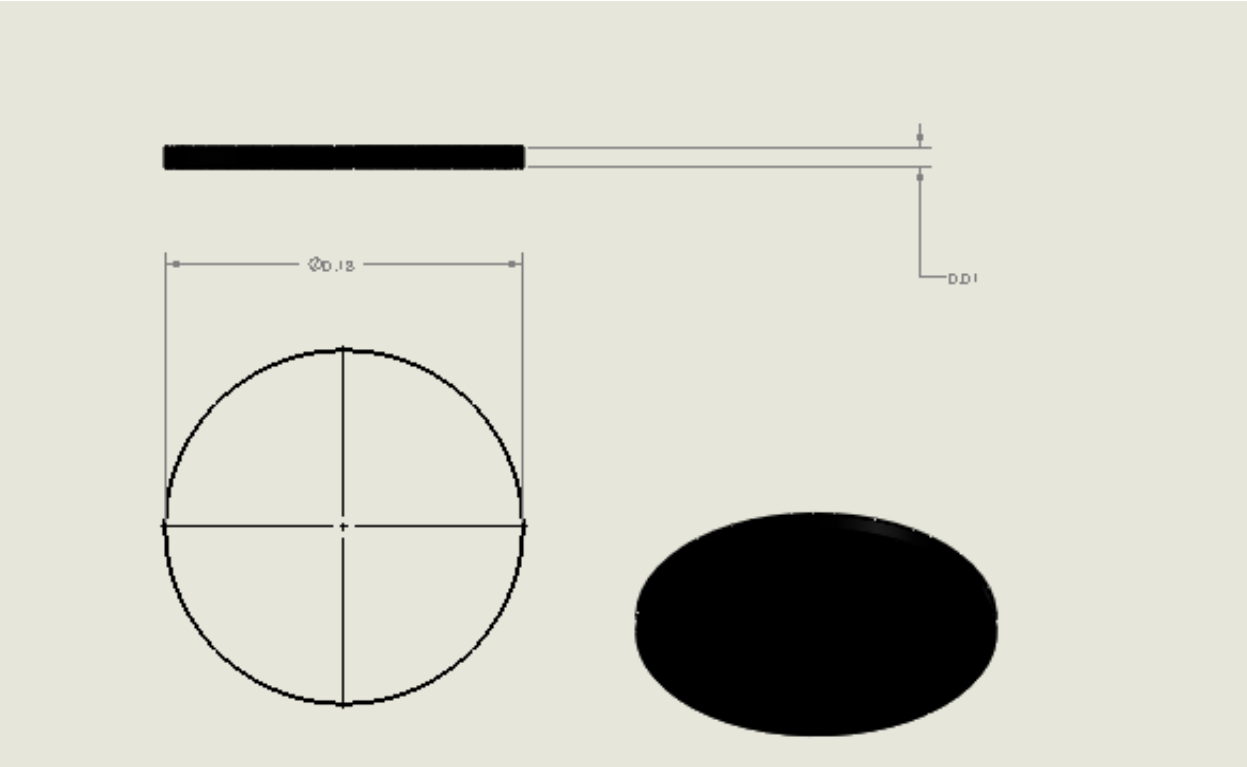


Figure 37: shows the cooking plate

The cooking plate will be made with aluminum metal which will be painted black for easily heat transfer from the thermal storage tank to the cooking pot. It will have a diameter of 0.18m which fits the base of the cooking chamber as designed.

5.4.7. Dish adjusting support.

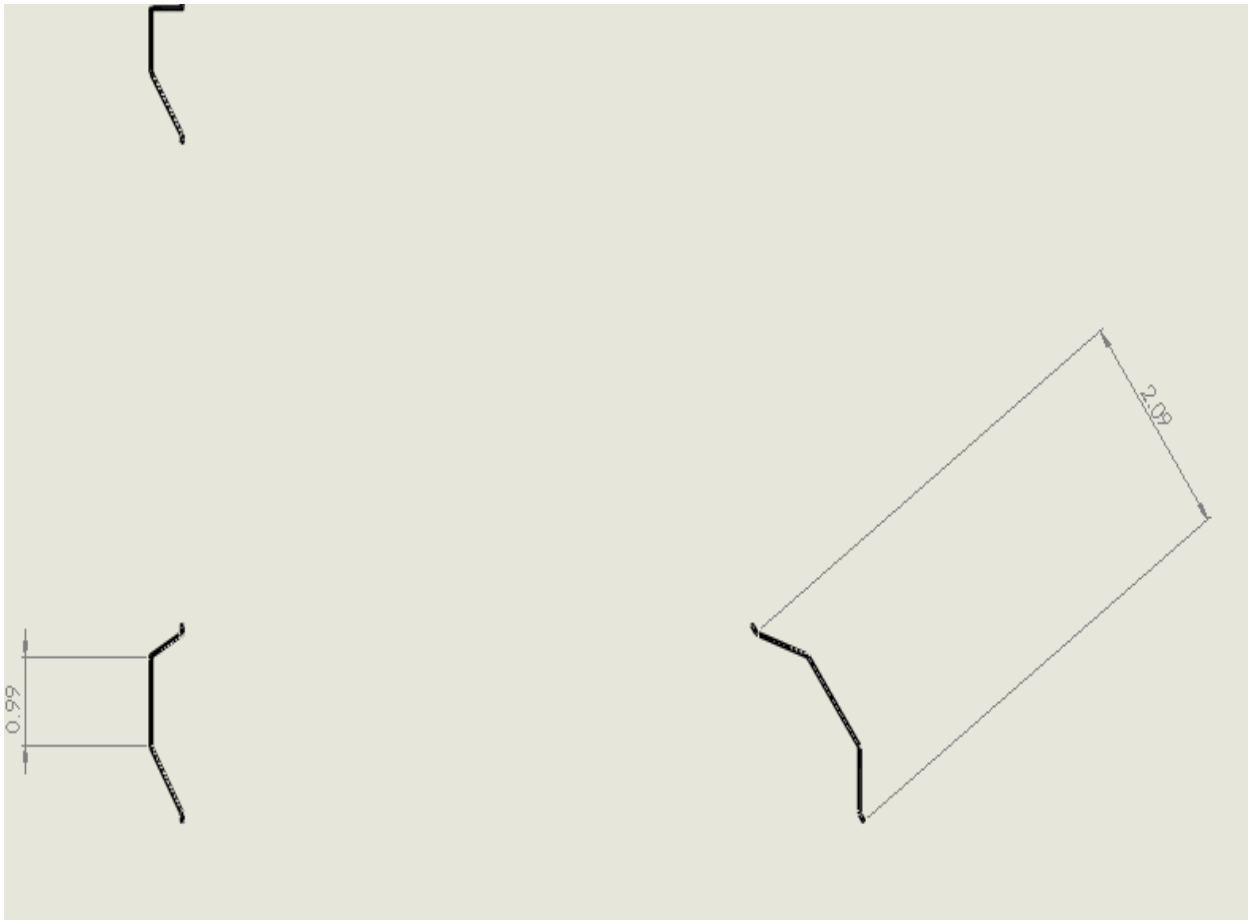


Figure 38: shows the solar angle adjusting support.

The dish adjusting angle support will be made with the metallic rode which will be 2.09m long and 0.01m diameter. The dimensions where selected according to the size of support stand to reach the adjusting slot. The adjusting angle support will be helping the dish to be adjusted in different positions according to the sun's position in the sky.

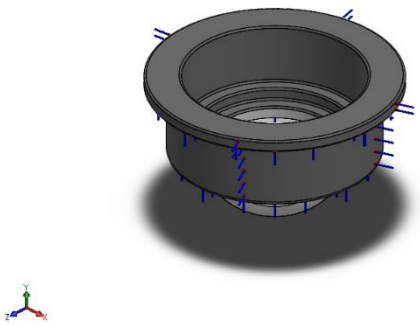
6. SIMULATION AND RESULTS.

I used SOLIDWORKS and MATLAB to do simulation of my design by finding out how it will perform on the actual ground and finding out design's efficiency. I used solid works to find how heat will be transferred with the selected materials, and also finding out the force and pressure the machine can withstand during cooking while MATLAB program helps to calculate the geometrical concentration parameters, the parameter of heat transfer, and calculating the efficiencies of different diameters of parabolic concentrator.

6.1. SOLIDWORKS RESULTS.

Thermal analysis simulation

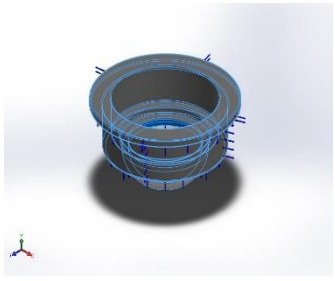
6.1.1. Model Information



Model name: parabolic cooking area

Current Configuration: Default

Solid Bodies

Document Name and Reference	Treated As	Volumetric Properties	Document Path/Date Modified
Revolve3 	Solid Body	Mass:8.5575 kg Volume:0.00459021 m^3 Density:1,864.29 kg/m^3 Weight:83.8635 N	C:\Users\JDNide\Documents\parabolic solar cooker\parabolic cooking area.SLDPRT May 3 06:20:30 2021

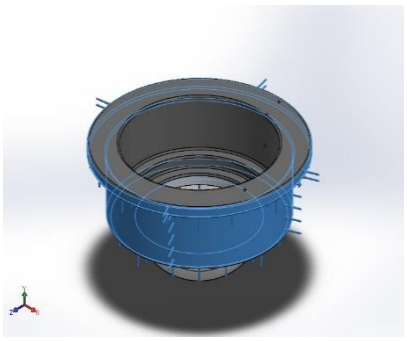
Study Properties

Study name	Thermal Analysis 1
Analysis type	Thermal (Steady state)
Mesh type	Solid Mesh
Solver type	FFEPlus
Solution type	Steady state
Contact resistance defined?	No
Result folder	SOLIDWORKS document (C:\Users\JDNide\Documents\parabolic solar cooker)

Units

Unit system:	SI (MKS)
Length/Displacement	Mm
Temperature	Kelvin
Angular velocity	Rad/sec
Pressure/Stress	N/m ^ 2

Thermal Loads

Load name	Load Image	Load Details
Temperature-1		**Entities:** 4 face(s) **Temperature:** 663 Kelvin

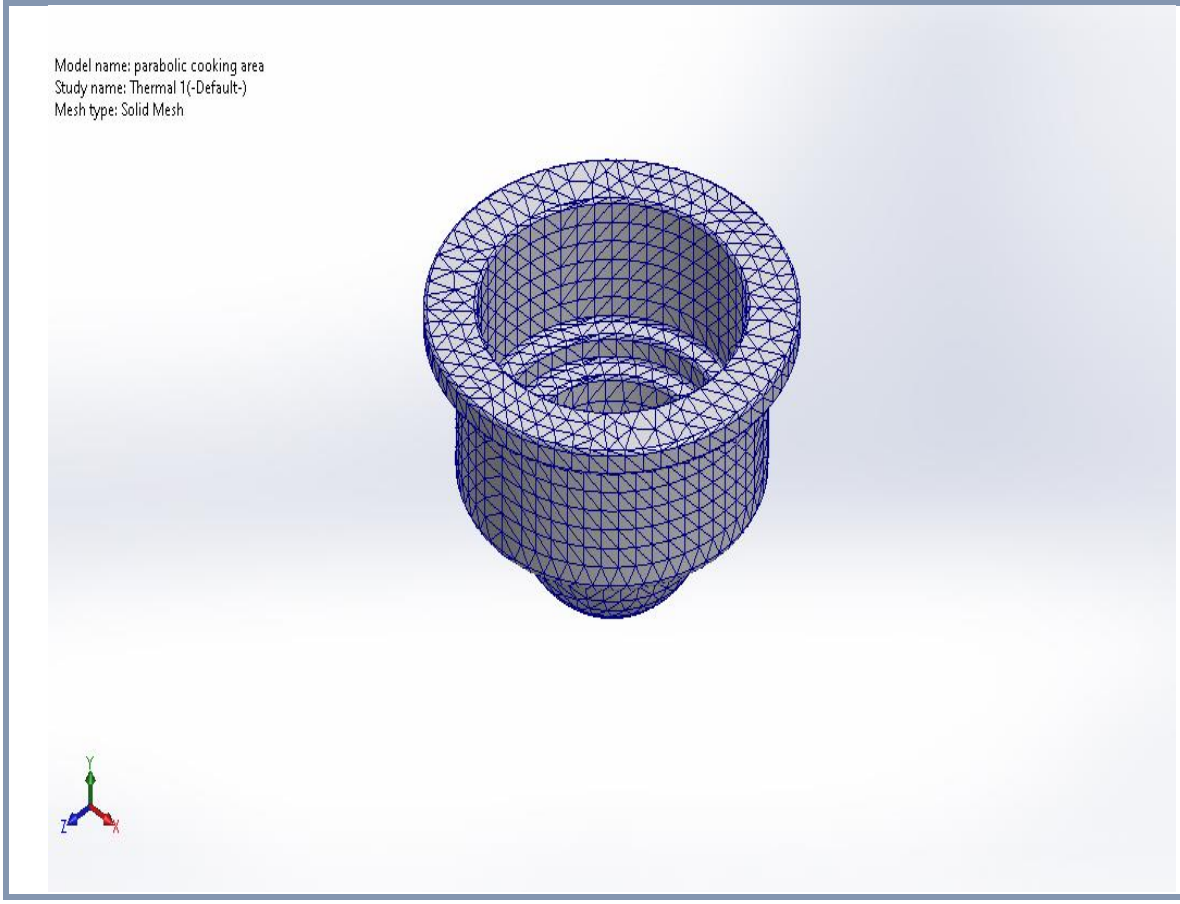
Mesh information

Mesh type	Solid Mesh
Mesher Used:	Standard mesh
Automatic Transition:	Off
Include Mesh Auto Loops:	Off
Jacobian points for High quality mesh	16 Points
Element Size	0.0166222 m
Tolerance	0.00083111 m
Mesh Quality	High

6.2. Mesh information - Details

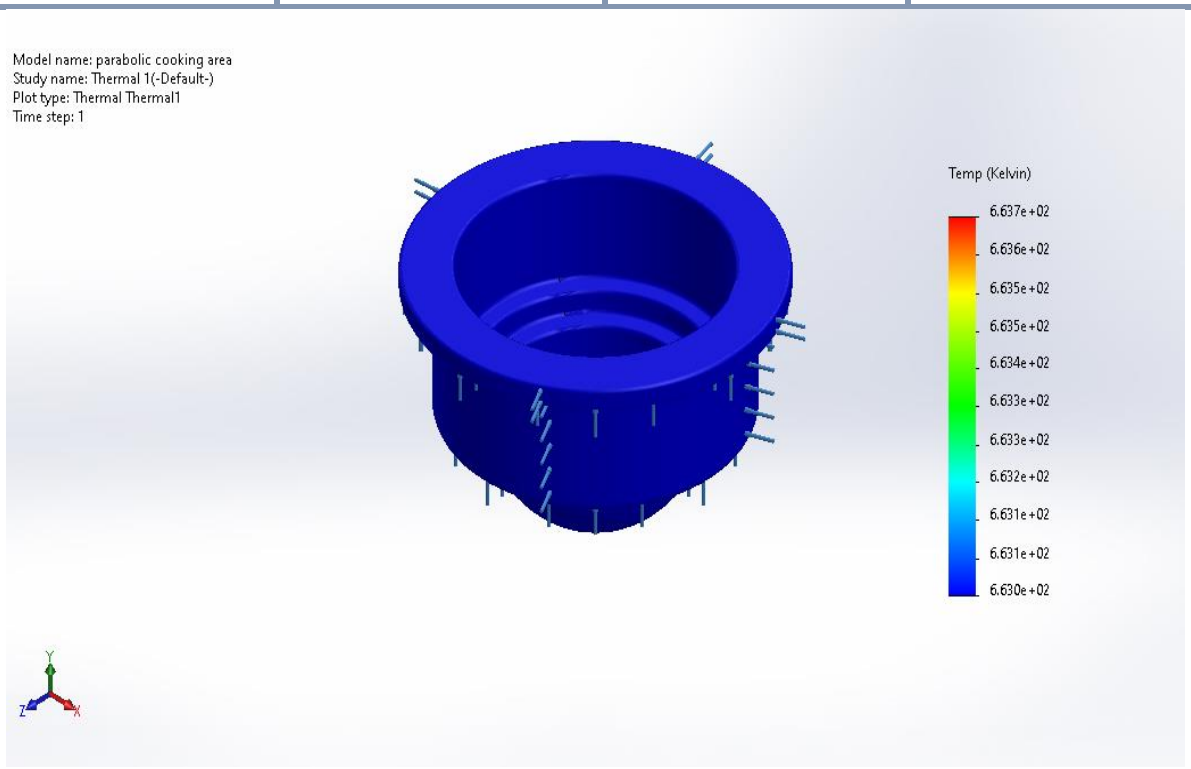
Total Nodes	18223
Total Elements	10460
Maximum Aspect Ratio	15.849
% of elements with Aspect Ratio < 3	86.8

% of elements with Aspect Ratio > 10	0.00956
% of distorted elements(Jacobian)	0
Time to complete mesh(hh;mm;ss):	00:00:05
Computer name:	



Study Results

Name	Type	Min	Max
Thermal1	TEMP: Temperature	6.630e+02Kelvin Node: 1	6.630e+02Kelvin Node: 1



parabolic cooking area-Thermal 1-Thermal-Thermal1

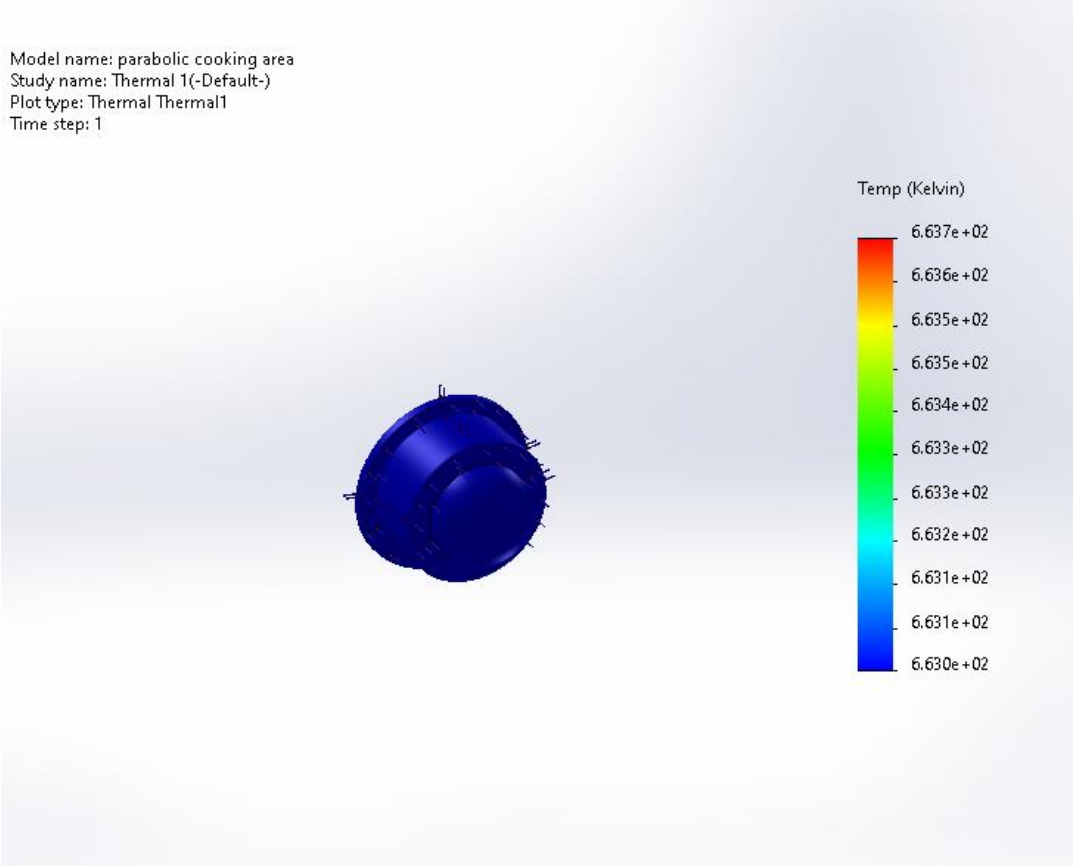
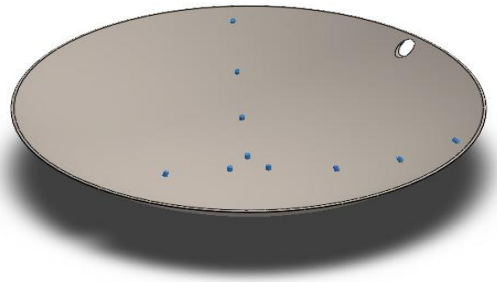


Image-1

Conclusion

As shown in the diagram above, there is the temperature scale on the right side of the diagram which shows temperature ranges starting from 663 K up to 667 K. The diagram shows blue color which means that the heat outside the ceramic will remain less than the maximum temperature of 663 K produced by the solar cooker. This shows that the ceramic material will be good enough to keep the inside heart without losing more heat due to heart transfer, mostly conduction and radiation.

6.2.1. Model Information

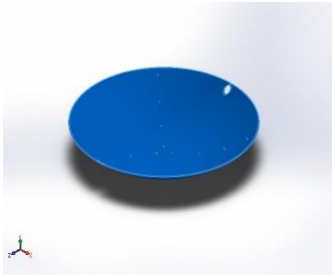




Model name: parabolic dish

Current Configuration: Default

Solid Bodies

Document Name and Reference	Treated As	Volumetric Properties	Document Path/Date Modified
Cut-Extrude1 	Solid Body	Mass:5.0725 kg Volume:0.0189577 m^3 Density:267.569 kg/m^3 Weight:49.711 N	C:\Users\JDNide\Documents\parabolic solar cooker\parabolic dish.SLDPRT May 14 02:41:22 2021

Study Properties

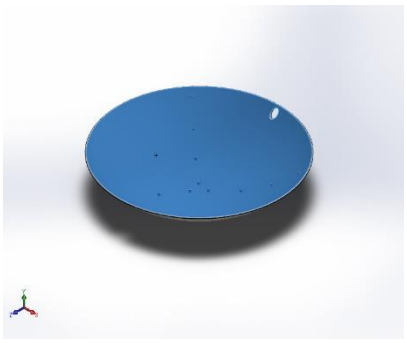
Study name	Thermal (solar radiation) analysis
Analysis type	Thermal(Steady state)
Mesh type	Solid Mesh
Solver type	FFEPlus
Solution type	Steady state
Contact resistance defined?	No
Result folder	SOLIDWORKS document (C:\Users\JDNide\Documents\parabolic solar cooker)

Units

Unit system:	SI (MKS)
Length/Displacement	Mm
Temperature	Kelvin
Angular velocity	Rad/sec
Pressure/Stress	N/m ^ 2

Material Properties

Thermal Loads

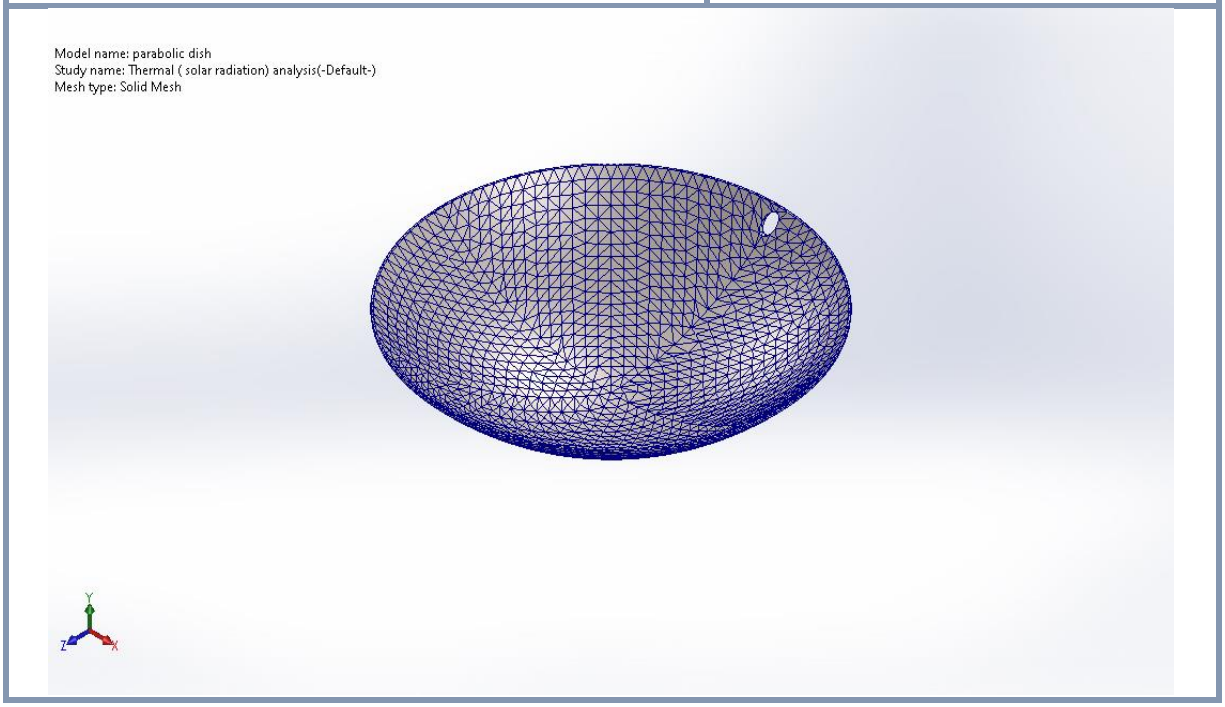
Load name	Load Image	Load Details
Heat Power-1		**Entities:** 1 face(s) **Heat Power Value:** 600 W

Mesh information

Mesh type	Solid Mesh
Mesher Used:	Standard mesh
Automatic Transition:	Off
Include Mesh Auto Loops:	Off
Jacobian points for High quality mesh	16 Points
Element Size	0.0391517 m
Tolerance	0.00195758 m
Mesh Quality	High

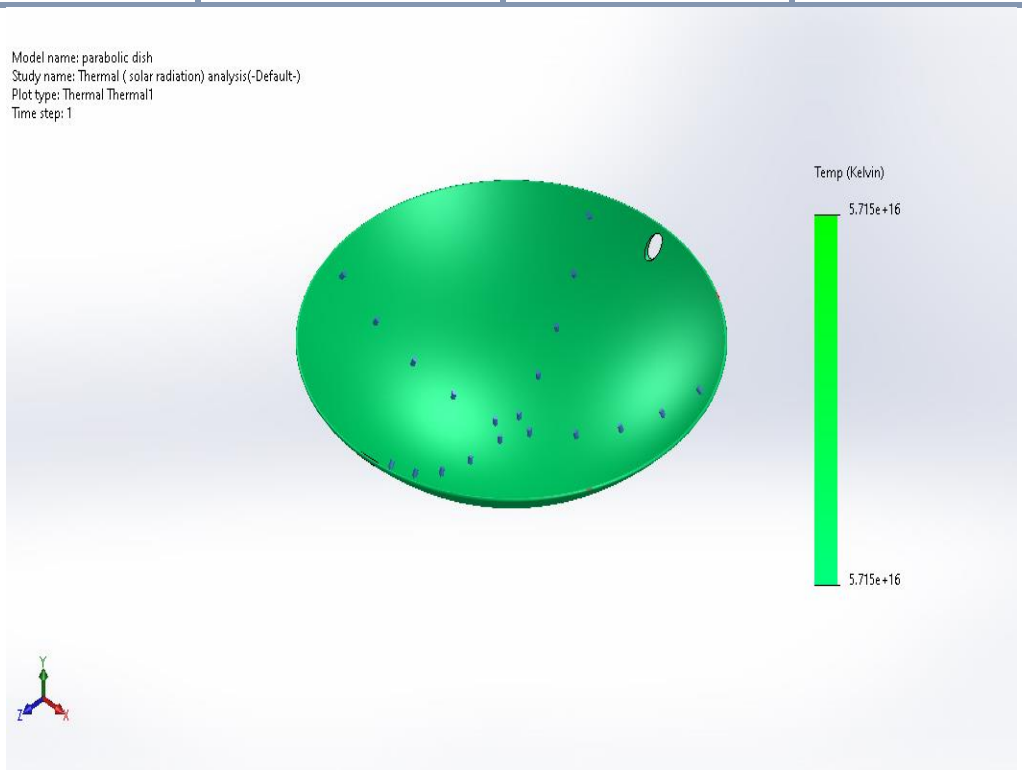
6.3. Mesh information - Details

Total Nodes	16353
Total Elements	8084
Maximum Aspect Ratio	46.025
% of elements with Aspect Ratio < 3	8.86
% of elements with Aspect Ratio > 10	1.29
% of distorted elements(Jacobian)	0
Time to complete mesh(hh;mm;ss):	00:00:06
Computer name:	



Study Results

Name	Type	Min	Max
Thermal1	TEMP: Temperature	5.715e+16Kelvin Node: 1	5.715e+16Kelvin Node: 2



parabolic dish-Thermal (solar radiation) analysis-Thermal-Thermal1

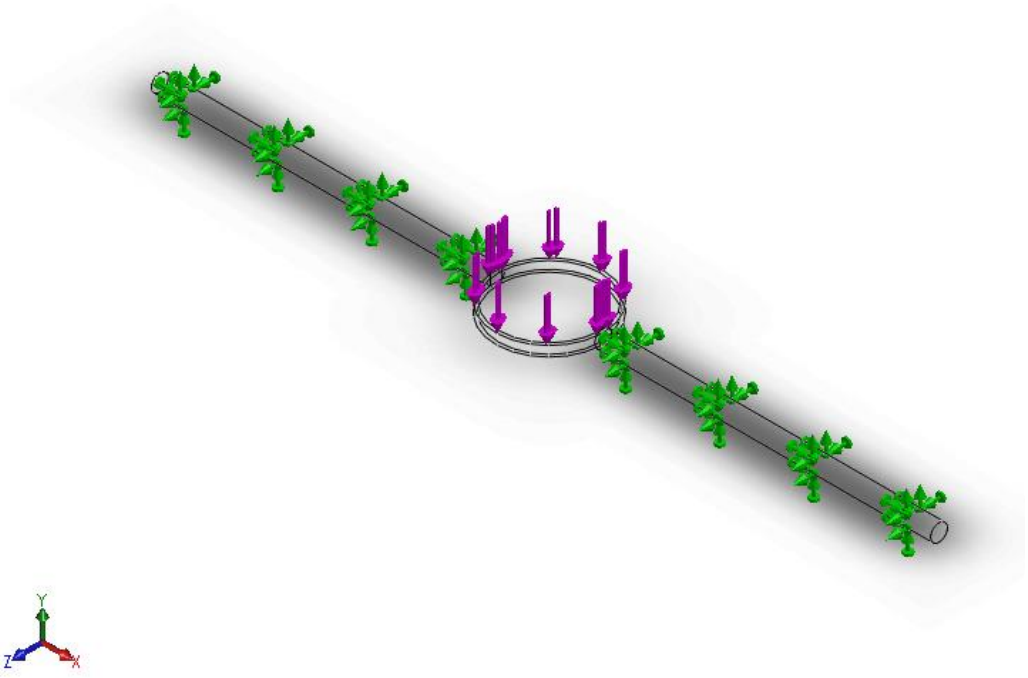
Conclusion

As we can see of the diagram above there is a scale on the right side of the diagram which shows the scientific notation of temperature range from 572K and above that. The parabolic dish shows the color of approximately 572K which is enough to produce the temperature which can cook food of more people in less than an hour.

Force and pressure simulations

6.3.1. Cooking holder

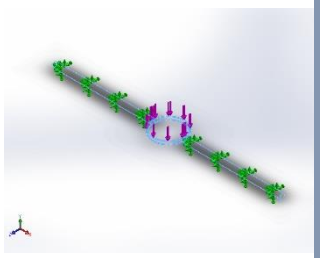
Model Information



Model name: cooking holder

Current Configuration: Default

Solid Bodies

Document Name and Reference	Treated As	Volumetric Properties	Document Path/Date Modified
Cut-Extrude2 	Solid Body	Mass:7.9044 kg Volume:0.00421851 m^3 Density:1,873.74 kg/m^3 Weight:77.463 N	C:\Users\HP\Desktop\parabolic solar cooker\cooking holder.SLDPRT May 3 22:55:10 2021

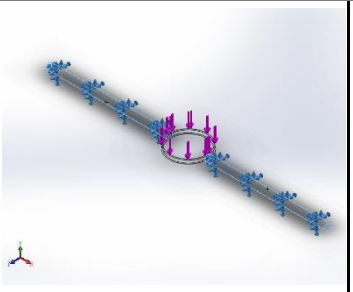
Study Properties

Study name	Static 2
Analysis type	Static
Mesh type	Solid Mesh
Thermal Effect:	On
Thermal option	Include temperature loads
Zero strain temperature	298 Kelvin
Include fluid pressure effects from SOLIDWORKS Flow Simulation	Off
Solver type	FFEPlus
Inplane Effect:	Off
Soft Spring:	Off
Inertial Relief:	Off
Incompatible bonding options	Automatic
Large displacement	Off
Compute free body forces	On
Friction	Off
Use Adaptive Method:	Off
Result folder	SOLIDWORKS document (C:\Users\HP\Desktop\parabolic solar cooker)

Units

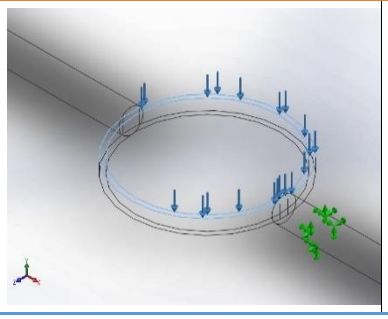
Unit system:	SI (MKS)
Length/Displacement	mm
Temperature	Kelvin
Angular velocity	Rad/sec
Pressure/Stress	N/m^2

Loads and Fixtures

Fixture name	Fixture Image	Fixture Details
Fixed-1		Entities: 2 face(s) Type: Fixed Geometry

Resultant Forces

Components	X	Y	Z	Resultant
Reaction force(N)	0.00166414	99.9841	-0.0195355	99.9841
Reaction Moment(N.m)	0	0	0	0

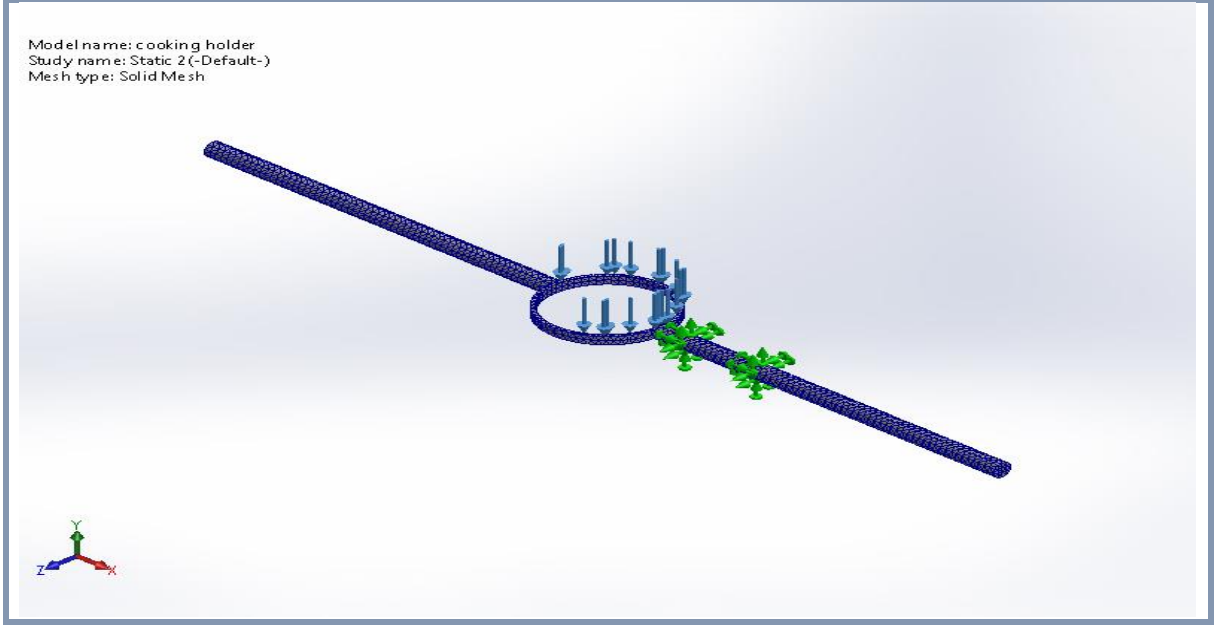
Load name	Load Image	Load Details
Force-1		Entities: 1 face(s) Type: Apply normal force Value: 100 N

Mesh information

Mesh type	Solid Mesh
Mesher Used:	Standard mesh
Automatic Transition:	Off
Include Mesh Auto Loops:	Off
Jacobian points for High quality mesh	16 Points
Element Size	0.0161609 m
Tolerance	0.000808045 m
Mesh Quality	High

6.4. Mesh information - Details

Total Nodes	11803
Total Elements	6296
Maximum Aspect Ratio	7.3019
% of elements with Aspect Ratio < 3	99.1
% of elements with Aspect Ratio > 10	0
% of distorted elements(Jacobian)	0
Time to complete mesh(hh;mm;ss):	00:00:03
Computer name:	JDNide



Resultant Forces

6.5. Reaction forces

Selection set	Units	Sum X	Sum Y	Sum Z	Resultant
Entire Model	N	0.00166414	99.9841	-0.0195355	99.9841

6.6. Reaction Moments

Selection set	Units	Sum X	Sum Y	Sum Z	Resultant
Entire Model	N.m	0	0	0	0

6.7. Free body forces

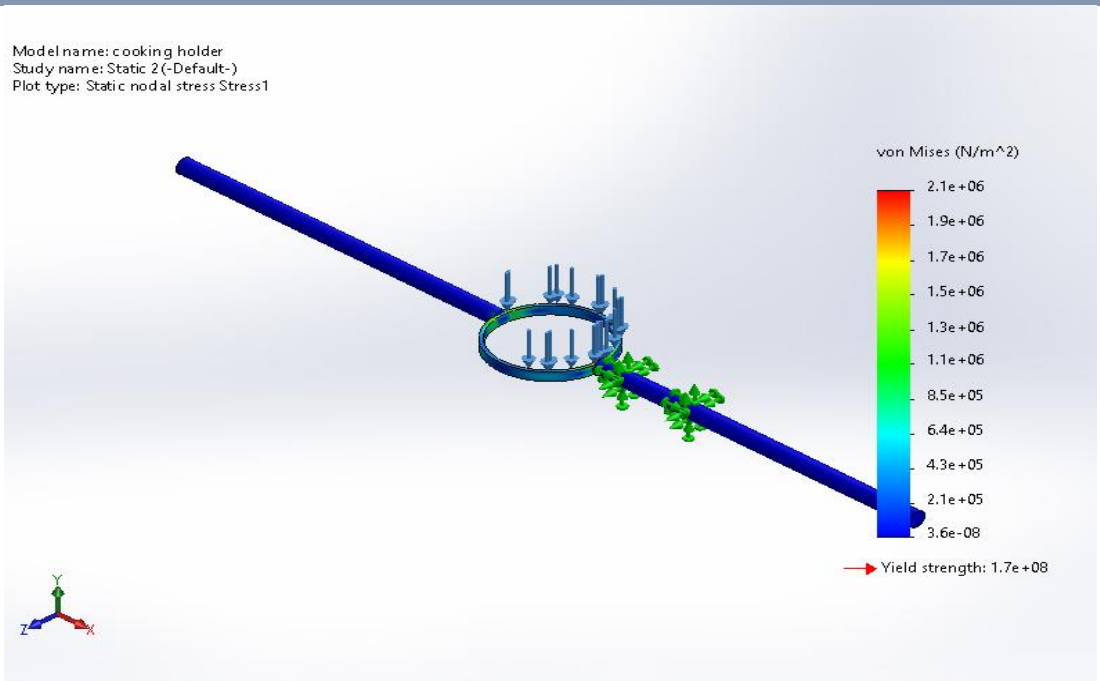
Selection set	Units	Sum X	Sum Y	Sum Z	Resultant
Entire Model	N	0.0357944	0.0149854	-0.0367592	0.0534512

6.8. Free body moments

Selection set	Units	Sum X	Sum Y	Sum Z	Resultant
Entire Model	N.m	0	0	0	1e-33

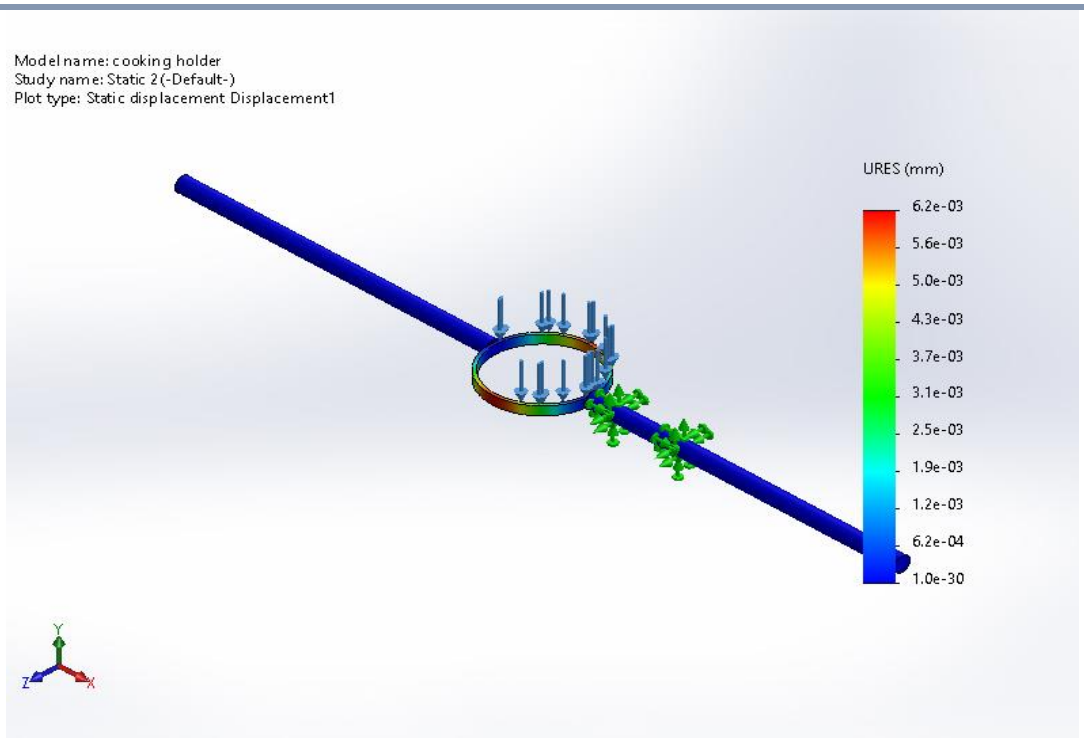
Study Results

Name	Type	Min	Max
Stress1	VON: von Mises Stress	3.6e-08N/m^2 Node: 6788	2.1e+06N/m^2 Node: 5296



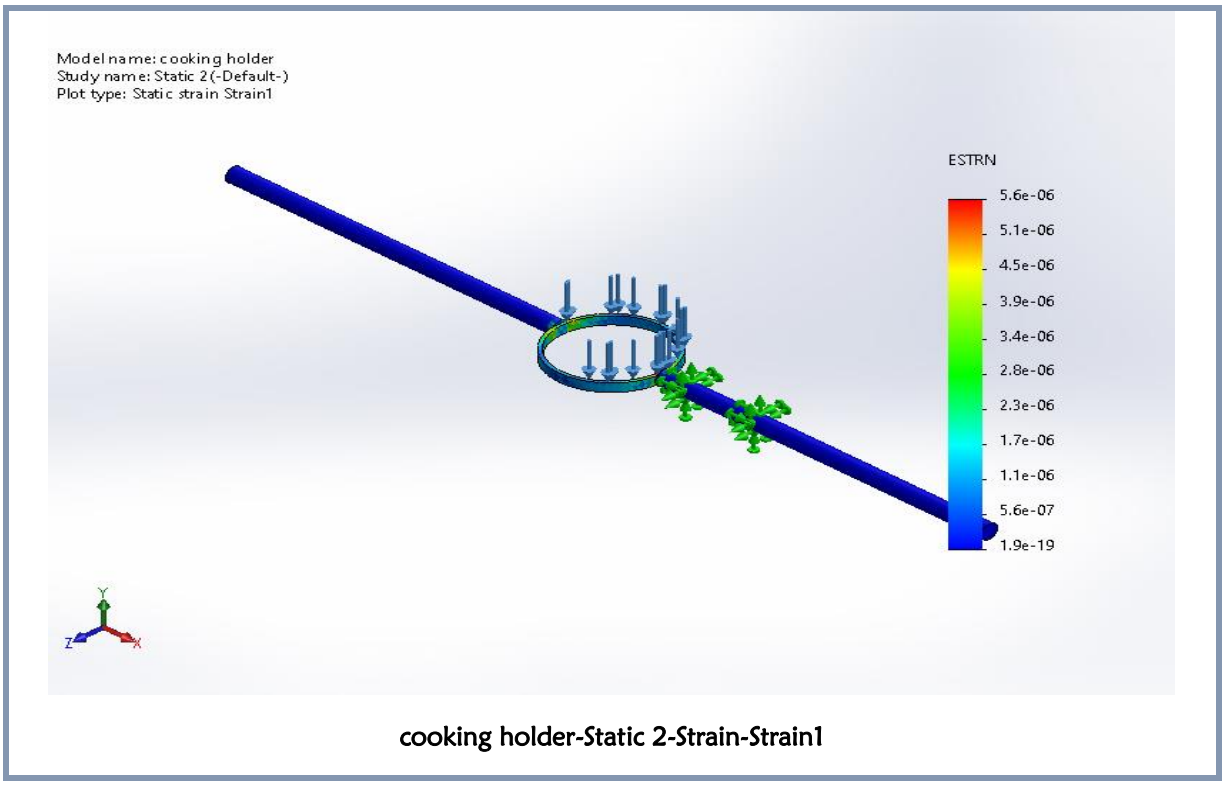
cooking holder-Static 2-Stress-Stress1

Name	Type	Min	Max
Displacement1	URES: Resultant Displacement	0.0e+00mm Node: 124	6.2e-03mm Node: 1033



cooking holder-Static 2-Displacement-Displacement1

Name	Type	Min	Max
Strain1	ESTRN: Equivalent Strain	1.9e-19 Element: 3027	5.6e-06 Element: 3802

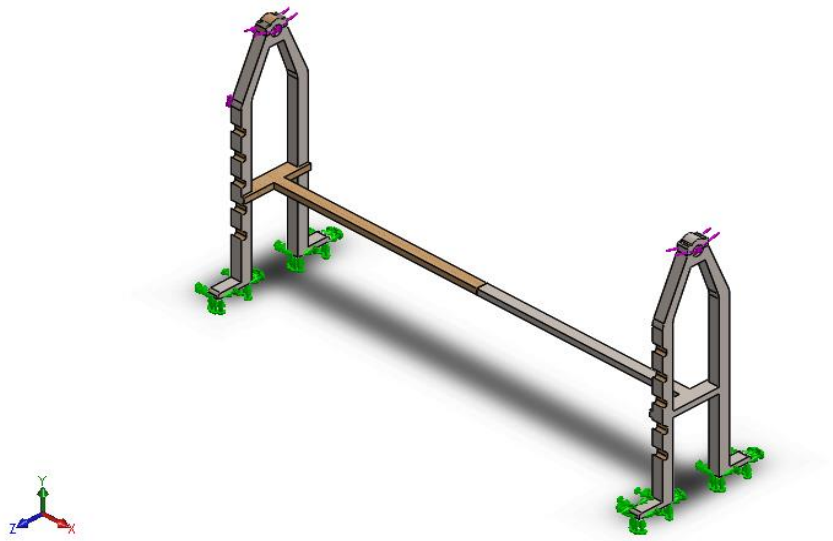


cooking holder-Static 2-Strain-Strain1

Conclusion

As we can see from the diagram of force and strain above. It shows that the cooking stand can withstand the force of greater than 100N without damaging or deforming the structure of cooking stand

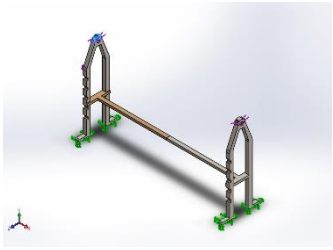
6.8.1. Model Information

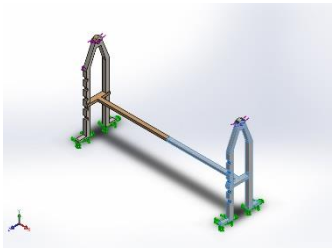
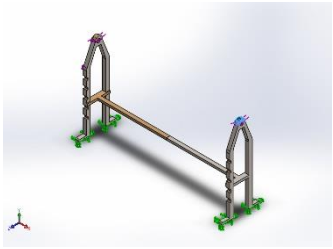


Model name: stand

Current Configuration: Default

Solid Bodies

Document Name and Reference	Treated As	Volumetric Properties	Document Path/Date Modified
Cut-Extrude2[2] 	Solid Body	Mass:0.0260565 kg Volume:0.000162863 m^3 Density:159.99 kg/m^3 Weight:0.255354 N	C:\Users\HP\Desktop\parabolic solar cooker\stand.SLDPRT May 9 19:42:34 2021
Cut-Extrude7[1] 	Solid Body	Mass:1.20615 kg Volume:0.00753893 m^3 Density:159.99 kg/m^3 Weight:11.8203 N	C:\Users\HP\Desktop\parabolic solar cooker\stand.SLDPRT May 9 19:42:34 2021

Cut-Extrude7[2] 	Solid Body	Mass:1.20615 kg Volume:0.00753893 m^3 Density:159.99 kg/m^3 Weight:11.8203 N	C:\Users\HP\Desktop\parabolic solar cooker\stand.SLDPRT May 9 19:42:34 2021
Mirror6[2] 	Solid Body	Mass:0.0260565 kg Volume:0.000162863 m^3 Density:159.99 kg/m^3 Weight:0.255353 N	C:\Users\HP\Desktop\parabolic solar cooker\stand.SLDPRT May 9 19:42:34 2021

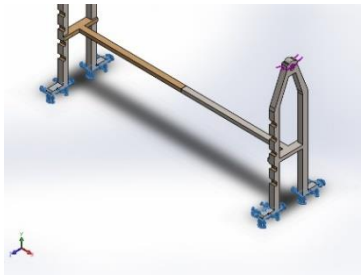
Study Properties

Study name	force n pressure simultion of stnd
Analysis type	Static
Mesh type	Solid Mesh
Thermal Effect:	On
Thermal option	Include temperature loads
Zero strain temperature	298 Kelvin
Include fluid pressure effects from SOLIDWORKS Flow Simulation	Off
Solver type	FFEPlus
Inplane Effect:	Off
Soft Spring:	Off
Inertial Relief:	Off
Incompatible bonding options	Automatic
Large displacement	Off
Compute free body forces	On
Friction	Off
Use Adaptive Method:	Off
Result folder	SOLIDWORKS document (C:\Users\HP\Desktop\parabolic solar cooker)

Units

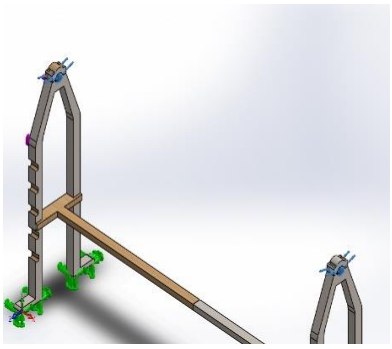
Unit system:	SI (MKS)
Length/Displacement	mm
Temperature	Kelvin
Angular velocity	Rad/sec
Pressure/Stress	N/m^2

Loads and Fixtures

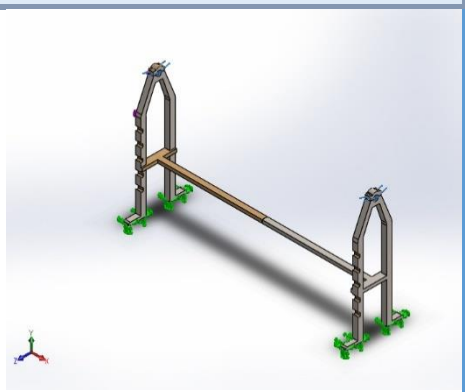
Fixture name	Fixture Image	Fixture Details
Fixed-1		Entities: 1 edge(s), 4 Type: Fixed Geon

Resultant Forces

Components	X	Y	Z
Reaction force(N)	-0.476104	195.559	0.0190201
Reaction Moment(N.m)	0	0	0

Load name	Load Image	Load Details
Force-1		Entities: 2 face(s) Type: Apply normal force Value: 150 N

Contact Information

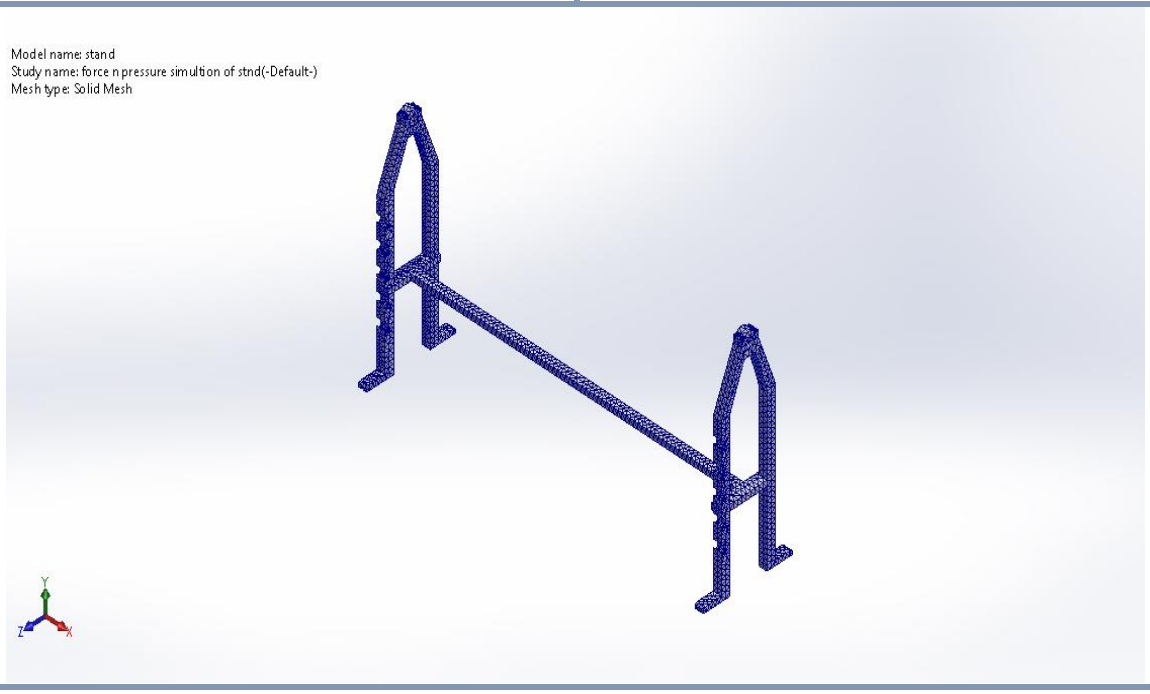
Contact	Contact Image	Contact Properties
Global Contact		Type: Bonded Components: 1 component(s) Options: Incompatible mesh

Mesh information

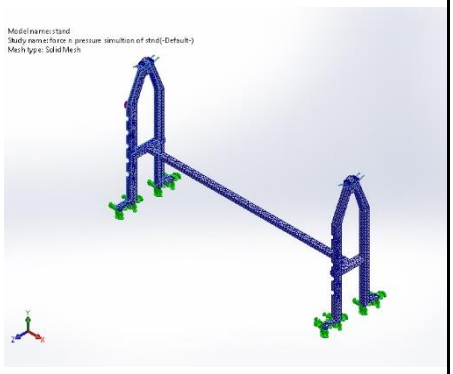
Mesh type	Solid Mesh
Mesher Used:	Standard mesh
Automatic Transition:	Off
Include Mesh Auto Loops:	Off
Jacobian points for High quality mesh	16 Points
Element Size	0.0248848 m
Tolerance	0.00124424 m
Mesh Quality	High

6.9. Mesh information - Details

Total Nodes	25511
Total Elements	13467
Maximum Aspect Ratio	22.305
% of elements with Aspect Ratio < 3	91.3
% of elements with Aspect Ratio > 10	0.163
% of distorted elements(Jacobian)	0
Time to complete mesh(hh;mm;ss):	00:00:08
Computer name:	JDNide



6.10. Mesh Control Information:

Mesh Control Name	Mesh Control Image	Mesh Control Details
Control-1		Entities: 1 face(s) Units: m Size: 0.0161751 Ratio: 0.0161751

Resultant Forces

6.11. Reaction forces

Selection set	Units	Sum X	Sum Y	Sum Z	Resultant
Entire Model	N	-0.476104	195.559	0.0190201	195.56

6.12. Reaction Moments

Selection set	Units	Sum X	Sum Y	Sum Z	Resultant
Entire Model	N.m	0	0	0	0

6.13. Free body forces

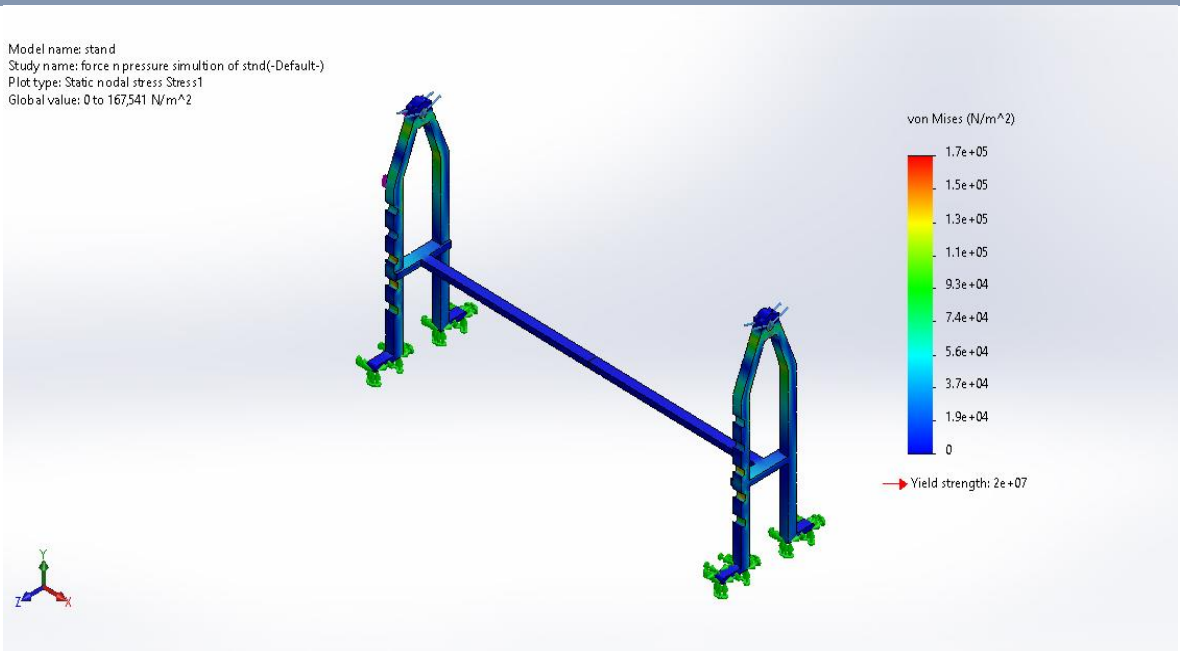
Selection set	Units	Sum X	Sum Y	Sum Z	Resultant
Entire Model	N	-0.0204279	0.175659	0.214255	0.277811

6.14. Free body moments

Selection set	Units	Sum X	Sum Y	Sum Z	Resultant
Entire Model	N.m	0	0	0	1e-33

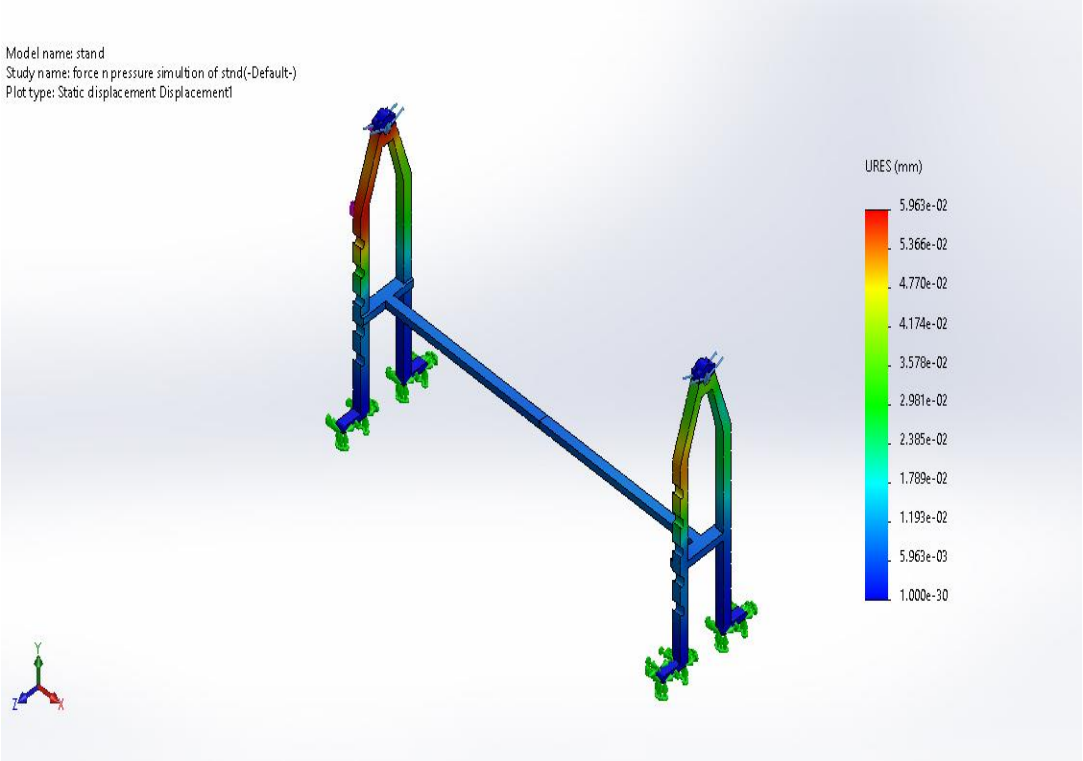
Study Results

Name	Type	Min	Max
Stress1	VON: von Mises Stress	0N/m^2 Node: 1	1.7e+05N/m^2 Node: 10635



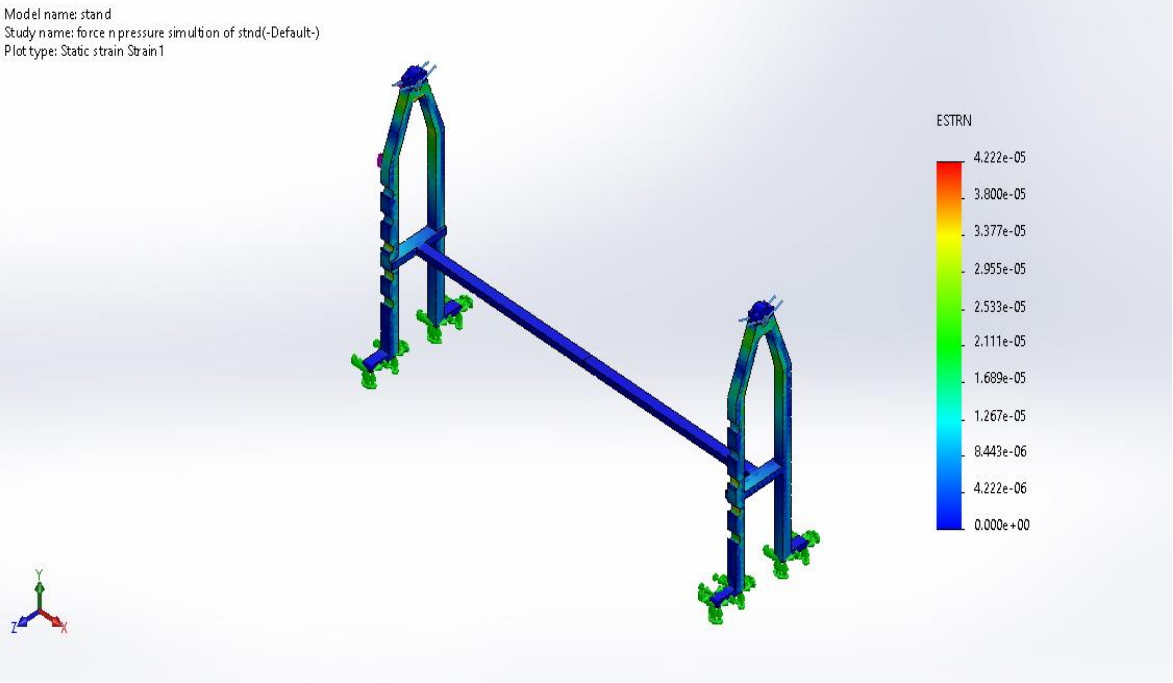
stand-force n pressure simultion of stnd-Stress-Stress1

Name	Type	Min	Max
Displacement1	URES: Resultant Displacement	0.000e+00mm Node: 1	5.963e-02mm Node: 1166



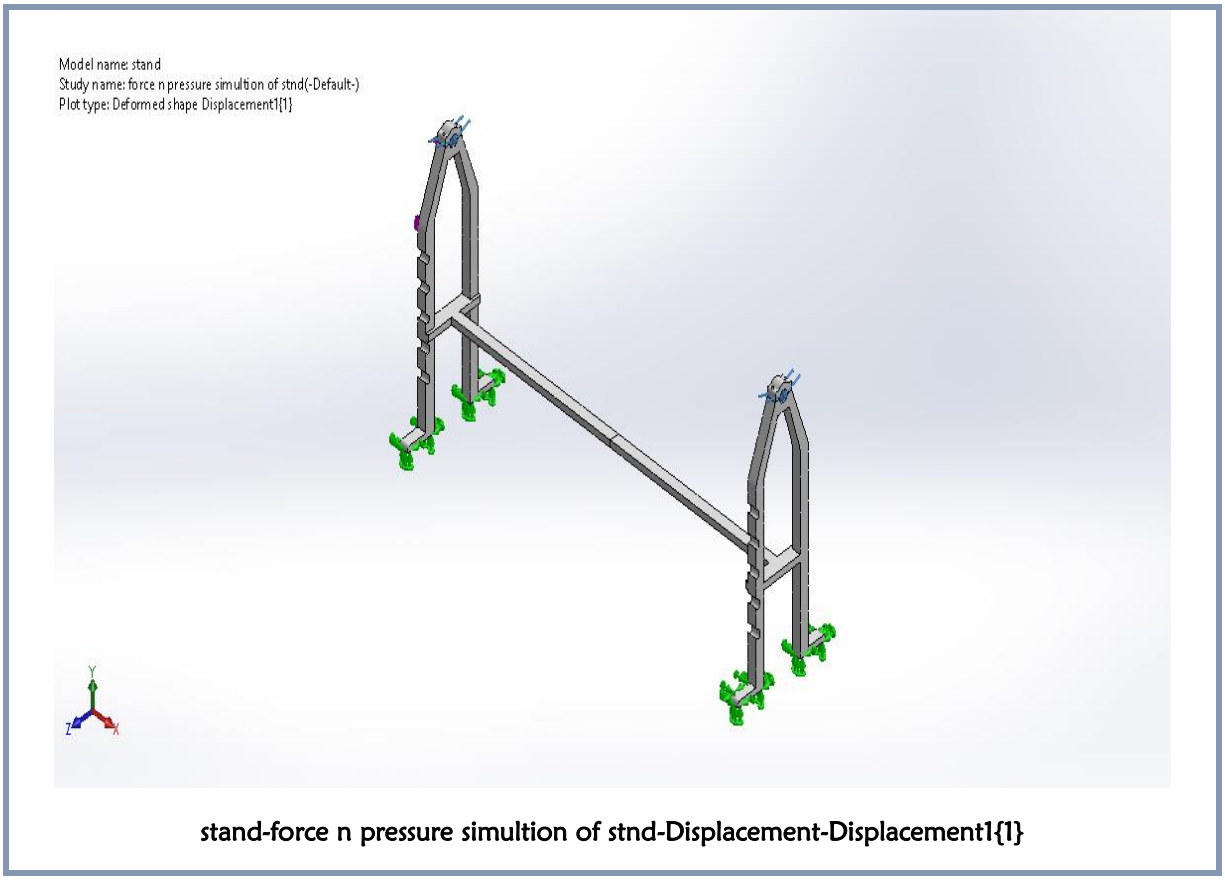
stand-force n pressure simultion of stnd-Displacement-Displacement1

Name	Type	Min	Max
Strain1	ESTRN: Equivalent Strain	0.000e+00 Element: 1	4.222e-05 Element: 6406



simultion of stnd-Strain-Strain1

Name	Type
Displacement1{1}	Deformed shape



stand-force n pressure simultion of stnd-Displacement-Displacement1{1}

Conclusion

The solidworks results show that the supporting stand will be able to withstand the force of more than 150N during cooking.

6.15. MATLAB RESULTS.

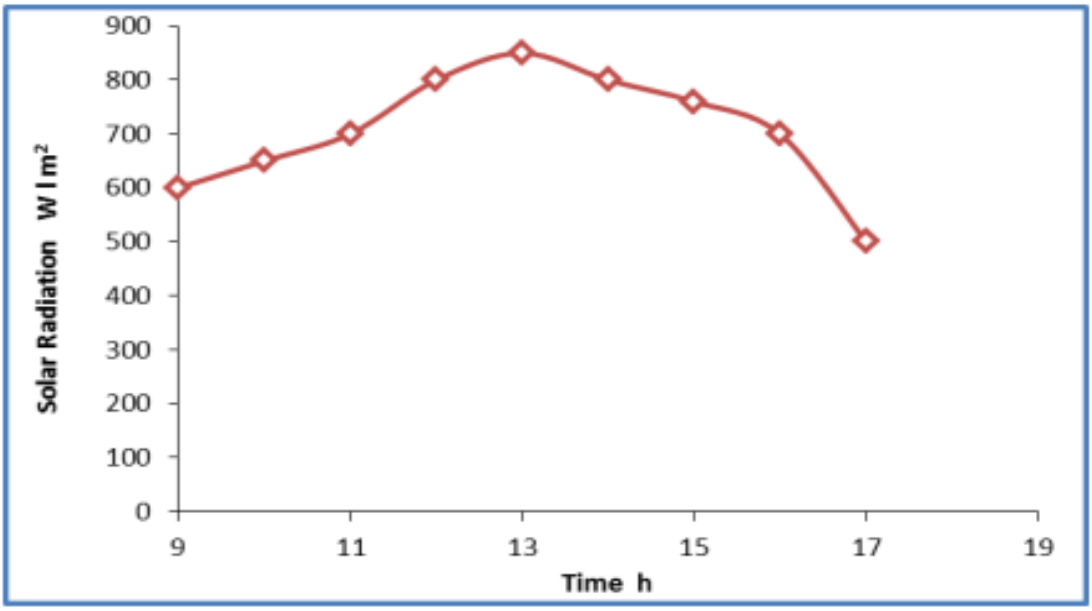
By using the program coded using MATLAB, we can design any concentration and calculate the parameters of heat transfer and their efficiencies. The table below shows geometrical concentration parameter by using the program for many concentrations.

d(m)	h(m)	f(m)	f/d	Ψ	Sa	H	S	C
1.42	0.25	0.5041	0.355	70.308	0.00022	0.02	0.000226	7001.389
2.5	0.3	1.3020	0.520833	51.282	0.01836	0.26	0.018369	267.094
3	0.35	1.6071	0.535714	50.033	0.03391	0.27	0.033912	208.3333
3.5	0.4	1.9140	0.546875	49.134	0.05495	0.28	0.05495	175
4	0.45	2.2222	0.555556	48.455	0.08195	0.29	0.081954	153.2567
4.5	0.5	2.5312	0.5625	47.924	0.11539	0.3	0.115395	137.7551
5	0.55	2.8409	0.568182	47.498	0.15574	0.31	0.155744	126.0081

And from study solar radiation with time and wind speed, we can calculate inlet and outlet temperature for receiver with time by using the program we can calculate heat transfer and calculate the heat lose energy and useful energy for any solar system. The table below shows heat transfer by measuring temperature and solar radiation, and by using the information in table above.

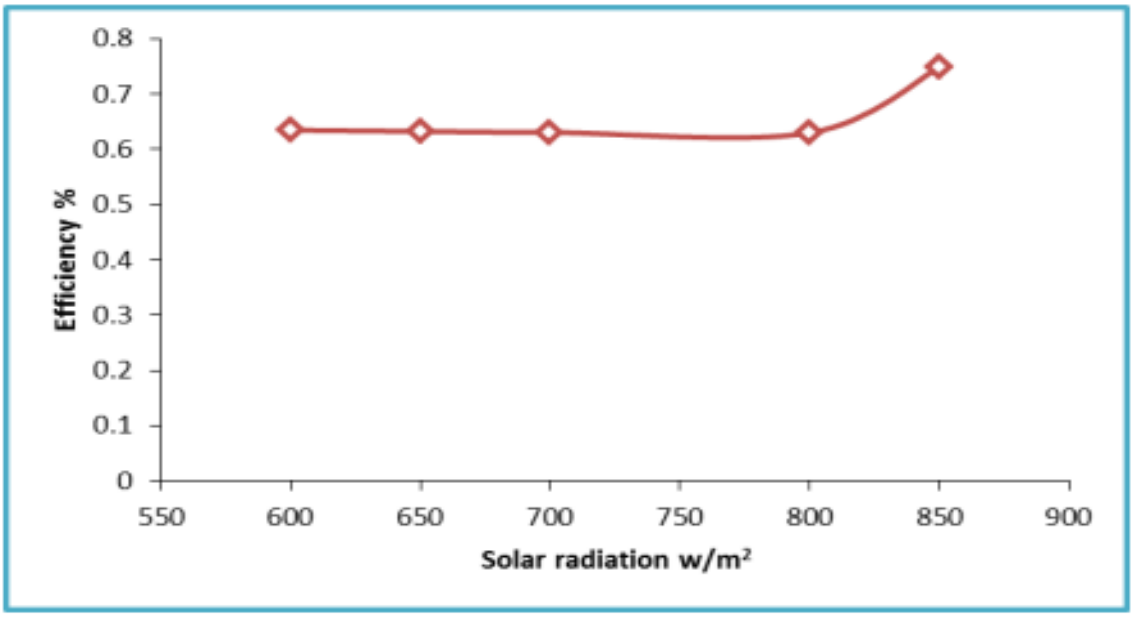
Qloss W	Ps-m	τ_g	αr	S	Aa	Ia W/m²	Qopt W	Qopt KW	Qout	$\eta collector$
5.301893	1	1	0.8	1	3.14	550	1381.6	1.3816	1376.298	0.79693
10.60379	0.8	1	0.8	1	3.14	600	1205.76	1.20576	1195.156	0.634372
15.90568	0.8	1	0.8	1	3.14	650	1306.24	1.30624	1290.334	0.632207
21.20757	0.8	1	0.8	1	3.14	700	1406.72	1.40672	1385.512	0.630351
26.50946	0.8	1	0.8	1	3.14	800	1607.68	1.60768	1581.171	0.629447
31.81136	0.8	1	0.95	1	3.14	850	2028.44	2.02844	1996.629	0.748081
37.11325	0.8	1	0.95	1	3.14	800	1909.12	1.90912	1872.007	0.745226

Figure 39: below illustrates solar radiation variation with time.



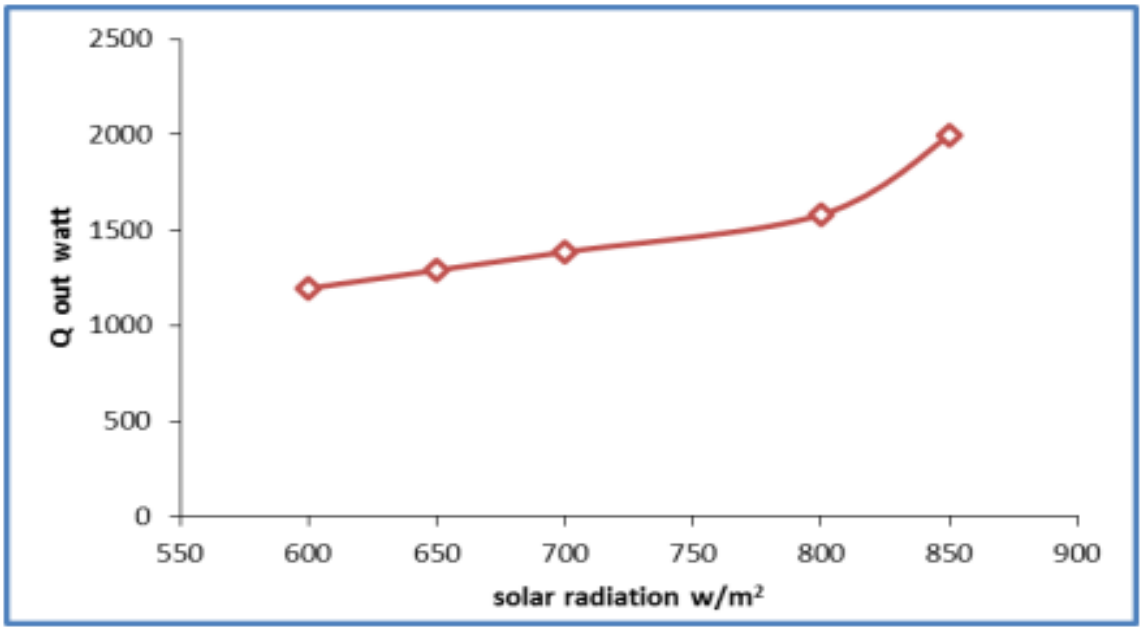
According to the graph, we can see that on the average daily basis according to the year, the solar radiation increases from 600W/m² when the time is at 9:00 hours and continue increases until reaching the peak of 850W/m² when time is around 13:00 hours. After reaching the peak at round 13:00 hours, the solar radiation start decreasing as the time goes during the day until it reaches the minimum cooking solar radiation of 400W/m² when time reaches 15:00 hours.

Figure 40: below illustrates solar radiation variation with efficiency.



According to the graph, we can see that the minimum efficiency the solar cooker can reach is greater than 0.6 even when the solar radiation is at 600W/m² and remains at the same level of efficiency until the solar radiation increases greater than 800W/m² is when the efficiency also increases up to the maximum efficiency of 0.79 ≈ 0.8 when the solar radiation is at 850W/m².

Figure 41: below illustrates solar radiation variation with output energy.



According to the graph, as the solar radiation increases the output energy of the solar cooker also increases with the possibility of the maximum of 2000W when the solar radiation reaches 850W/m².

7. CONCLUSION AND RECOMMENDATIONS.

Conclusion.

Solar cookers are gradually gaining ground and a lot of research is being undertaken to ensure that they compete favorably with other conventional cookers. In this report, the concept of cooking with the sun was proven to be viable, and ability of solar cookers to achieve high temperature even with low solar resources was pointed out. And the complexities in parabolic solar cooker design were greatly reduced. A comprehensive mathematical code has been developed for analyzing the performance of designed parabolic solar cooker. The code considers all the heat energy balance equations and heat transfer mechanism including convection heat transfer inside the absorber. The presented code is implemented in MATLAB software, and it has ability to estimate the amount of heat converted by the collector, heat loss, thermal efficiency, and outlet temperature of the system. The system achieved utilization efficiency of up to 79.6 as shown in table.

The parabolic solar cooker designed in this study was also found to be more effective than many other solar cookers in existence. This was due to the reduced heat loss around its cavity receiver, which was achieved as a result of adding thermal insulation on cooking section and optimized entrance aperture. The design also eliminated the need for the user to be exposed to direct sun radiation, because the heat generated in the solar collection subsystem was channeled into the storage tank, which can be placed at any convenient spot in shed or cloudy conditions.

And with the implementation of this design as alternative to the fossil fuels, people will stop using more charcoal and firewood. Therefore, will be a reduction in the problems of deforestation, climate change, global warming, and some major health problems.

7.1. Recommendations.

The manufacturing cost of the designed parabolic solar cooker with all its parts is MK 60,000, despite the various innovative and improvisation ideas to reduce the cost. This because the design cost for a single system, and only one unit of some parts is needed. These individual units will be cheaper if they fabricated in bulk, therefore the manufacturing of this solar cookers on large scale will automatically reduce the production cost (due to mass production).

A comprehensive exergy analysis of the system should also be performed, as this can be stratified and done at various points in the system and can be used to know exactly where the energy quality is lost. The overall exergy efficiency loss point then can determined and necessary improvements can be made.

8. REFERENCE LIST.

Anon. n.d. “Solar Cooker Project of ADES.” 1–5.

Bigalow, Contributeurs Alan, Martha Port, and Jennifer Gasser. n.d. “Table of Contents.” 1–110.

Murray, By Ryan, Michael Byars, Cameron Coggburn, Chris Gochis, Parker Smith, Jakob Glidden, and Brett Stevens. 2014. “A Solar Energy Proposal for the University of Kansas.” 1–27.

Otte, Pia Piroschka. 2009. “Cooking with the Sun.” (May).

Patil, Rajendra. 2018. “An Overview of Solar Cookers.” (December).

Schäffler, Jason, and Jason Schäffler. n.d. “UNDP / GEF South African Solar Cooker Project (SOLCO) Final Evaluation Table of Contents List of Tables List of Figures.” (March 2006).

Gong, Guangjie, et al. "An optimized model and test of the China’s first high temperature parabolic trough receiver." Solar Energy 84 (2010): 2230-2245.

9. APPENDICES.

MATLAB CODE OF DESIGNED PARABOLIC SOLAR COOKER.

```
d=[1.5;2;2.5;3;3.5;4;4.5;5;5.5;6;6.5;7;7.5;8;8.5;9;9.5;10;10.5;11;17]; % (d(m)) input aparture
h=[0.2;0.25;0.3;0.35;0.4;0.45;0.5;0.55;0.6;0.65;0.7;0.75;0.8;0.85;0.9;0.95;1;1.05;1.1;1.15;2]; % (h(m)) input depth
f=[0.703125;1;1.302083333;1.607142857;1.9140625;2.2222222;2.53125;2.840909091;3.151041667;3.461538462;3.772321429;4.08333333;4.39453125;4.705882353;5.017361111;5.328947368;5.640625;5.952380952;6.26420454;6.576086957;9.03125]; % output focal length.
k=d.^2;
j=16.*h;
w=(f)./(d);
L=2*(f./d).^2;
G=(L)-1/8;
H=w./G;
SO=(pi.*(d).^2)./(4); % output surface of opening of paraboloid.
c=(8*pi.*(f).^2)./3;
M=(d./4.*f).^2;
N=((1.+M).^1.5)-1;
r=[0.75;1;1.25;1.5;1.75;2;2.25;2.5;2.75;3;3.25;3.5;3.75;4;4.25;4.5;4.75;5;5.25;5.5;5.75]; % input radius
%h=[0.02;0.25;0.25;0.3;0.3;1;0.07;0.19]; %input
Sa=(pi.*r.^2).*h;
C=(SO)./(Sa);
ar=[1;1]; % input
psm=[1;1]; % (ps-m) input
Tg=[1;1]; % input
aar=[0.99;0.9]; % (ar) % input
```

```
s=[1;1]; % input
Aa=[10.507;3.14]; % input
La=[1064;800]; % input
Qw=ar.*psm.*Tg.*aar.*s.*Aa.*La; % (Q opt W) % input
Qk= Qw./1000; % (Q opt W) OUTPUT
Dinner=[0.17;0.17;0.17;0.17;0.17;0.17]; % (Inner diameter in m) input
Douter=[0.173;0.173;0.173;0.173;0.173;0.173];
Lm=[0.2;0.2;0.2;0.2;0.2;0.2]; % (L m) input
Tinner=[330;313;343;353;363;373]; % (T inner in K)
Touter=[313;333;343;353;363;373];% (T outer in K)
Tair=[300;300;300;300;300;300]; % (T air in K) input
Tfilm=0.5.*(Tair + Touter); % (T film in K) input
V=[0.5;0.5;0.5;0.5;0.5;0.5]; % wind speed
v=[5.15E-05;5.15E-05;5.15E-05;5.15E-05;5.15E-05;5.15E-05]; % viscosity
Re=(V.*Douter)./v; % Reynolds n
NU=0.3.*(Re).^0.6; % Nusselt n
Kair=[0.0456;0.0456;0.0456;0.0456;0.0456;0.0456];
hw=((Kair)./(Douter)).*NU;
e=[0.5;0.5;0.5;0.5;0.5;0.5]; % ?
E=4.*((0.0000000567041).*e);
P=Tair.^3;
hr=E.*P;
UL=1./(hw + hr).^-1; % radiation coefficient
T=(Touter + Tair)./2;
Tr=T-Tair;
Ar=(2.*pi.*(Douter./2).^2)+(2.*pi.*(Douter./2).*Lm); % Receiver
Qloss=Ar.*UL.*Tr; % QLOSS
psm=[1;0.8;0.8;0.8;0.8;0.8]; % (ps-m) input
Tg1=[1;1;1;1;1;1]; % input
aar1=[0.8;0.8;0.8;0.8;0.8;0.95]; % ar input
```

```
S=[1;1;1;1;1;1]; % input
Aa=[3.14;3.14;3.14;3.14;3.14;3.14]; % input
La=[550;600;650;700;800;850]; % input
Qw=psm.*Tg1.*aar1.*S.*Aa.*La; % (Q opt W) output
Qk=Qw./1000; % (Q opt K w) output
fprintf('the out = %4f\n',Qk);
Qout=Qw-Qloss; % (Qout) output
Ycollector=(Qout)./(Aa.*La); % (? collector) efficiency output
fprintf('the efficiency = %4f\n',Ycollector);
plot(La,Ycollector)
```